SOUTHERN CALIFORNIA EDISON®

An *EDISON INTERNATIONAL*® Company

(U 338-E)

Application of SCE Requesting Approval of its Grid Safety and Resiliency Program and Associated Ratemaking Mechanisms
A.18-09-002

Workpapers

SCE-01 Grid Safety and Resiliency

September 2018

Testimony Volume	Section	Work Paper Title	Line and Page	FN
One	(IV)(B)(e)(1)	Mitigation Effectiveness Comparison	7, 48	83
One	(IV)(B)(e)(1)	An Engineering Analysis on Impacts of Contact from Objects (CFO) on Bare vs. Covered Conductor	9, 58	93
One	(IV)(B)(e)(1)	NEETRAC Final Report and SCE Summary of Covered Conductor Touch Current - NEETRAC Report	16, 58	95
One	(IV)(B)(e)(1)	Circuit Deployment Prioritization	1, 61	99
One	(IV)(B)(1)(e)(2)(a)	Pole Replacement Rate	1, 64	101
One	(IV)(B)(3)(a)	IEEE Fusing Support	3, 82	118

Mitigation Effectiveness Comparison
Supporting Section IV(B)(1)(c)

Objective Summary:

The detailed risk mitigation analysis as described at Section IV(B)(1)(c) in support of the Wildfire Covered Conductor Program (WCCP) followed three sequential steps: fault-to-fire mapping; mitigation-to-fault mapping; and the calculation of mitigation effectiveness factors and mitigation-cost ratios to determine the mitigation measure that provides the most overall value to customers in terms of addressing increasing wildfire risk.

Figure 1 – Risk Mitigation Analysis[1]

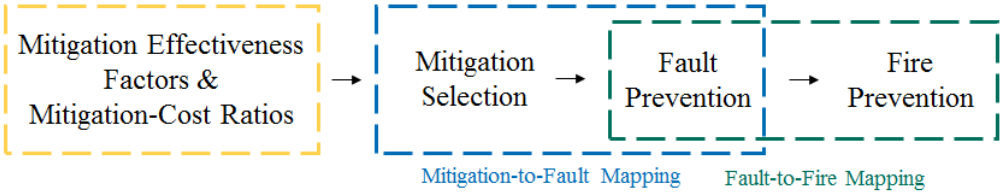

This document provides a summary of the methodology and results of this analysis.

Dataset Description – Fault Data

The fault history was provided by SCE's Outage Database & Reliability Metrics (ODRM). The ODRM fault history was filtered for events observed in 2015-2017 on distribution circuits for portions of distribution circuits traversing SCE's high fire risk areas (HFRA), as defined in SCE's supporting testimony. This resulted in a total of 15,615 fault events on these circuits in 2015-2017 with all fault causes included. Next, the fault list was further filtered to fault code causes as identified in the CPUC reportable Fire Data.[2] This included specific overhead cause codes such as contact from object and equipment/facility failure causes, but excluded other cause codes such as underground-related cause codes and cause codes like "unknown."

The resulting filtered ODRM data produced records of 8,458 such distribution fault events in years 2015-2017. Based on these results, an expected average of 2,819 faults per year was utilized within SCE's WCCP detailed risk mitigation analysis. Table 1 below provides the ODRM fault data details, and Figure 2 below provides a high-level pie chart summary of the percentage distribution of total faults into the three major categories, i.e., Contact From Object, Equipment/Facility Failure, and Other.

[1] Shown as Figure IV-6 in SCE's prepared testimony.
[2] Data was provided to Commission in accordance with Decision (D.) 14-12-015.

Table 1 – ODRM Fault Data, Fire-Related Causes, 2015-2017

Suspected Initiating Event	Faults Observed Over 3 Years	Average Annual Faults
Contact From Object	**2,684**	**895**
Animal	750	250
Balloon	457	152
Other	144	48
Vegetation	713	238
Vehicle Hit	620	207
Equipment/Facility Failure	**4,061**	**1,354**
Capacitor Bank	25	8
Conductor/Wire	436	145
Crossarm	118	39
Fuse/BLF/Cutout	294	98
Insulator	71	24
Other - Equipment	332	111
Splice/Connector/Tap	413	138
Transformer	2,372	791
Other	**1,713**	**571**
Total	**8,458**	**2,819**

Figure 2 – ODRM Fault Data, Fire-Related Causes, 2015-2017

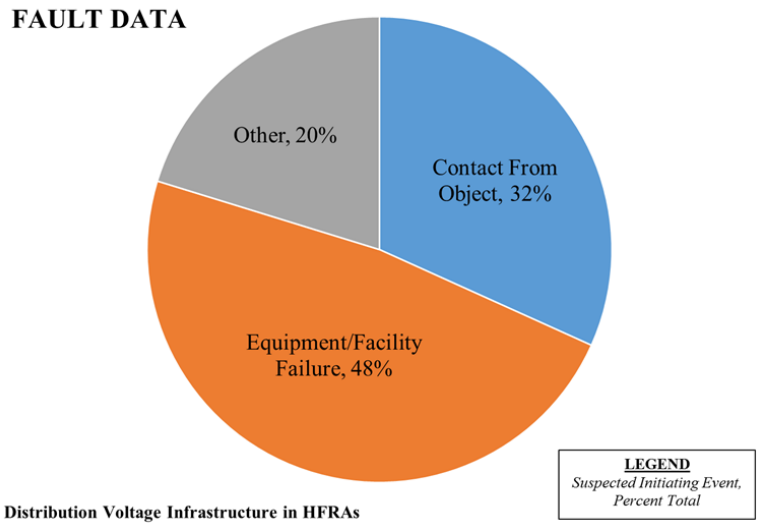

Dataset Description – Fire Data

The underlying fire data used for this analysis was previously provided to the CPUC in accordance with Decision (D.) 14-12-015. Similar to the fault data above, the fire data were filtered to include only fires that occurred in HFRA. In addition, only fires associated with distribution voltages (≤ 33kV) were used in the analysis.

The fire data included records of 132 such fire ignition events in years 2015-2017. Based on these results, an expected annual average of 44 fire ignition events per year was used for this analysis. Table 2 below provides the fire data details, and Figure 3 below provides a high-level pie chart summary of the percentage distribution of total fires into the three major categories, i.e. Contact From Object, Equipment/Facility Failure, and Other (grouped together as 'Other, Unknown, Wire-Wire Contact').[3]

Table 2 – CPUC Fire Data, Distribution Voltages, 2015-2017

Suspected Initiating Event	Fires Observed Over 3 Years	Average Annual Fires
Contact From Object	**70**	**23.3**
Animal	15	5.0
Balloon	14	4.7
Other	10	3.3
Vegetation	22	7.3
Vehicle Hit	9	3.0
Equipment/Facility Failure	**40**	**13.3**
Capacitor Bank	2	0.7
Conductor/Wire	12	4.0
Crossarm	1	0.3
Fuse/BLF/Cutout	1	0.3
Insulator	5	1.7
Other - Equipment	8	2.7
Splice/Connector/Tap	8	2.7
Transformer	3	1.0
Other, Unknown, Wire-Wire Contact	**22**	**7.3**
Total	**132**	**44.0**

[3] The majority of these "Other" ignition events were identified as "Unknown" in the data set.

Figure 3 – CPUC Fire Data, Distribution Voltages, 2015-2017

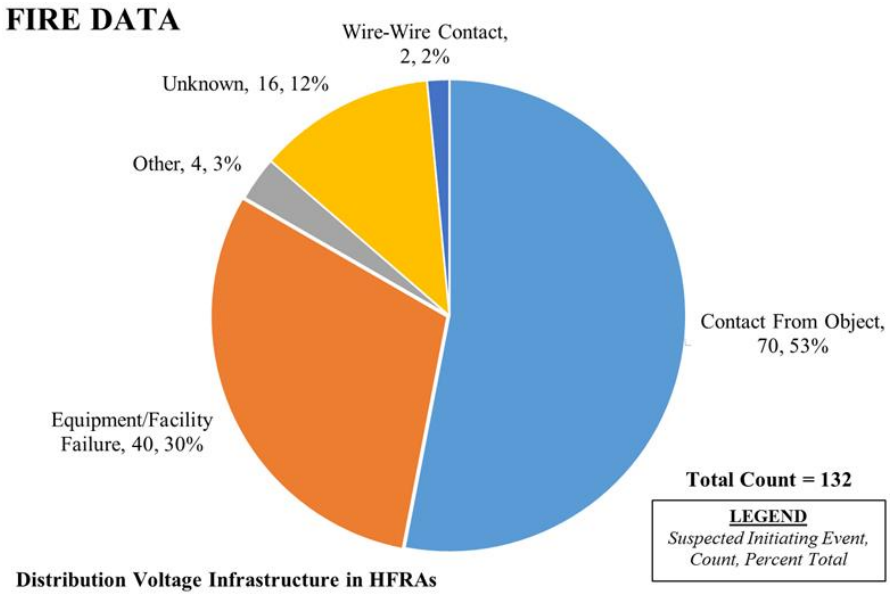

Fault-to-Fire Mapping Analysis

Utilizing the fault data and fire data shown above, a fault-to-fire mapping analysis was performed. This analysis aligned the 2,819 faults per year with the 44 fires per year, which provided a method to calculate the *relative potential likelihood that a specific type of fault would be associated with a fire ignition event.*

For example, 250 annual animal-related Contact From Object (CFO) faults were mapped to 5 animal-related CFO fires per year. This suggests that animal-related CFO faults have a 2% likelihood in being associated with a fire ignition event (since 5 fires per year / 250 faults per year = 0.02). Similar calculations were repeated for all fault and fire categories included in the data tables above.

The full results of this fault-to-fire mapping analysis are provided below in Table 3.

Table 3 – Fault-to-Fire Mapping Analysis

	Column A	Column B	Column C	Column D
Suspected Initiating Event	Annual Fires (Count)	Annual Fires (Percent)	Annual Frequency of Fault	Likelihood of being associated with a Fire
Contact From Object	**23.3**	**53%**	**895**	**2.6%**
Animal	5.0	11%	250	2.0%
Balloon	4.7	11%	152	3.1%
Other	3.3	8%	48	6.9%
Vegetation	7.3	17%	238	3.1%
Vehicle Hit	3.0	7%	207	1.5%
Equipment/Facility Failure	**13.3**	**30%**	**1,354**	**1.0%**
Capacitor Bank	0.7	2%	8	8.0%
Conductor/Wire	4.0	9%	145	2.8%
Crossarm	0.3	1%	39	0.8%
Fuse/BLF/Cutout	0.3	1%	98	0.3%
Insulator	1.7	4%	24	7.0%
Other	2.7	6%	111	2.4%
Splice/Connector/Tap	2.7	6%	138	1.9%
Transformer	1.0	2%	791	0.1%
Other	**7.3**	**17%**	**571**	**1.3%**
Total	**44.0**	**100%**	**2,819**	

In Table 3 above, 'Column A' shows the annualized total of each type of fire as reported to the CPUC, with 'Column B' representing the percentage of each type as a percentage of the annual total. 'Column C' is the annualized total of ODRM fire-related faults. The value in 'Column D' is a derived value determined by dividing the associated value in 'Column A' by 'Column C' to estimate the historical likelihood that a certain fault type was associated with a fire ignition event.

Mitigation-to-Fault Mapping

Next, SCE conducted a comprehensive review of mitigation alternatives and their effectiveness at reducing or eliminating faults. This analysis relied on engineering subject matter expertise to identify how much of each general fault type—contact from object, equipment/facility failure, and other—could be mitigated by a specific mitigation measure.

During this review, the question analyzed was whether a mitigation alternative would be effective at avoiding each identified type of fault. As a simplifying assumption, mitigations were assumed to be either completely effective or ineffective against a specific ODRM cause code.[4]

[4] 'Foreign Material' and 'Ice/Snow' cause codes are included within the 'Other' category shown in Table 4. For purposes of the analysis, covered conductor was assumed to be completely effective against 'Foreign Material' cause codes, and assumed to be completely ineffective against 'Ice/Snow'.

The results of this mitigation-to-fault mapping are presented in Table 4 below.

Table 4 – Mitigation to Fault Mapping Analysis

	ODRM Cause Code	Covered Conductor Effective?	Bare Conductor Effective?	Undergrounding Effective?
Contact From Object	Animal	**Yes**	No	**Yes**
	Balloon	**Yes**	No	**Yes**
	Other	**Partial (Yes for 'Foreign Material')**	No	**Yes**
	Vegetation Blown; Vegetation Overgrown	**Yes**	No	**Yes**
	Vehicle Hit	No	No	**Yes**
Equipment / Facility Failure	Transformer	No	No	**Yes**
	Conductor / Wire	**Yes**	**Yes**	**Yes**
	Splice / Connector / Tap	**Yes**	**Yes**	**Yes**
	Fuse / BLF / Cutout	No	No	**Yes**
	Lightning Arrestor	No	No	**Yes**
	Crossarm	No	No	**Yes**
	Pothead	No	No	**Yes**
	Insulator	No	No	**Yes**
	Switch / Disconnect AR	No	No	**Yes**

Mitigation Effectiveness Factors

Next, SCE combined the results of the fault-to-fire mapping and the mitigation-to-fault mapping in order to calculate mitigation effectiveness factors for each mitigation alternative.

For example, an annual total of 250 animal-related CFO faults were identified as being associated with 11% of the total wildfire risk (see Table 3). Furthermore, animal-related CFO faults were identified as being effectively mitigated by covered conductor in the mitigation-to-fault mapping. Therefore, animal-related CFO fires were identified as able to be mitigated through full deployment of covered conductor.

As another example, an annual total of 207 vehicle-related CFO faults were identified as being associated with 7% of the total wildfire risk (see Table 3). However, vehicle-related CFO faults were identified as not being effectively mitigated by covered conductor in the mitigation-to-fault mapping. Therefore, vehicle-related CFO fires were characterized as unmitigated by covered conductor deployment.

The resulting mitigation effectiveness factors for the covered conductor mitigation alternative are provided in Table 5 below.

Table 5 – Covered Conductor Effectiveness Analysis

	Covered Conductor	
Suspected Initiating Event	**Mitigated Events**	**Equivalent Fires**
Contact From Object	**677**	**19.5**
Animal	250	5.0
Balloon	152	4.7
Other	37	2.5
Vegetation	238	7.3
Vehicle Hit	0	0.0
Equipment/Facility Failure	**283**	**6.7**
Capacitor Bank	0	0.0
Conductor/Wire	145	4.0
Crossarm	0	0.0
Fuse/BLF/Cutout	0	0.0
Insulator	0	0.0
Other	0	0.0
Splice/Connector/Tap	138	2.7
Transformer	0	0.0
Other	**0**	**0.0**
Mitigated Total	**960**	**26.2**
Total Fires		**44.0**
Mitigation Effectiveness		**60%**

In Table 5 above, "mitigated events" column shows the number of annual faults for those categories identified as "yes" in Table 4 or zero for those categories identified as "no" in Table 4. Likewise, the "equivalent fires" column shows the number of annual ignition events for categories identified as "yes" in Table 4 or zero for categories identified as "no" in Table 4.

Dividing the "mitigated total" of "equivalent fires" by "total fires" yields the mitigation effectiveness factor. In this case, 26.2 equivalent fires that could be mitigated with covered conductor represents approximately 60% of the 44 annual fires (26.2 equivalent fires / 44 annual fires = 0.60).

As shown below, this methodology was repeated for the bare conductor and underground conversion mitigation alternatives. Based on the results, an overall 15% mitigation effectiveness factor was calculated for bare conductor. See the Table 6 below.

Table 6 – Bare Conductor Effectiveness Analysis

	Bare Conductor	
Suspected Initiating Event	**Mitigated Events**	**Equivalent Fires**
Contact From Object	**0**	**0.0**
Animal	0	0.0
Balloon	0	0.0
Other	0	0.0
Vegetation	0	0.0
Vehicle Hit	0	0.0
Equipment/Facility Failure	**283**	**6.7**
Capacitor Bank	0	0.0
Conductor/Wire	145	4.0
Crossarm	0	0.0
Fuse/BLF/Cutout	0	0.0
Insulator	0	0.0
Other	0	0.0
Splice/Connector/Tap	138	2.7
Transformer	0	0.0
Other	**0**	**0.0**
Mitigated Total	**283**	**6.7**
Total Fires		**44.0**
Mitigation Effectiveness		**15%**

Since underground conversion was used as the reference baseline for mitigation effectiveness (because it removes all exposures related to overhead power lines), SCE used a 100% mitigation effectiveness factor. See Table 7 below.

Table 7 – Undergrounding Effectiveness Analysis

	Undergrounding	
Suspected Initiating Event	**Mitigated Events**	**Equivalent Fires**
Contact From Object	**895**	**23.3**
Animal	250	5.0
Balloon	152	4.7
Other	48	3.3
Vegetation	238	7.3
Vehicle Hit	207	3.0
Equipment/Facility Failure	**1,354**	**13.3**
Capacitor Bank	8	0.7
Conductor/Wire	145	4.0
Crossarm	39	0.3
Fuse/BLF/Cutout	98	0.3
Insulator	24	1.7
Other	111	2.7
Splice/Connector/Tap	138	2.7
Transformer	791	1.0
Other	**571**	**7.3**
Mitigated Total	**2,819**	**44.0**
Total Fires		**44.0**
Mitigation Effectiveness		**100%**

Mitigation-Cost Ratios and Customer Value

Finally, these mitigation effectiveness factors were used in combination with unit costs to estimate mitigation-cost ratios. A mitigation-cost ratio is calculated by dividing the mitigation effectiveness factor (as calculated above and expressed as a decimal) by the mitigation unit cost (expressed in millions of dollars and on a per-mile basis).

The results of this analysis are summarized below.

Table 8 – Mitigation-Cost Ratio Analysis

Mitigation Option	Relative Mitigation Effectiveness Factor	Cost per Mile ($ million)	Mitigation-Cost Ratio
Re-conductor – Bare	0.15	0.30	0.50
Re-conductor – Covered	0.60	0.43	1.40
Underground Conversion	1.00	3.00	0.33

A mitigation-cost ratio is not the same as a typical cost-benefit ratio, since mitigation-cost ratios are not dimensionless (i.e., the numerators and denominators have different units). However, comparing the mitigation-cost ratios provides a meaningful indicator of the relative value of each

mitigation (as compared to the alternatives considered). For example, a comparatively higher mitigation-cost ratio indicates greater overall mitigation value, i.e. greater overall customer benefit per dollar spent, and a comparatively lower mitigation-cost ratio indicates lower overall mitigation value for customers, i.e. less benefit per dollar spent. Comparing the mitigation-cost ratio of covered conductor results in covered conductor providing 2.8 times the value as bare re-conductoring (1.40 / 0.50 = 2.8) and 4.2 times the value as underground conversion (1.40 / 0.33 = 4.2).

Engineering Analysis on the Impacts of Contact from Objects on Bare vs. Covered Conductors –Workpaper Supporting Section (IV)(B)(e)(1)

Prepared by: Southern California Edison Apparatus and Standards Engineering

Engineering Analysis on the Impacts of Contact from Objects (CFO) on Bare vs. Covered Conductors

Table of Contents

Engineering Analysis on the Impacts of Contact from Objects (CFO) on Bare vs. Covered Conductors

Engineering Analysis on the Impacts of Contact from Objects (CFO) on Bare vs. Covered Conductors

1.0 Executive Summary

SCE performed an engineering analysis and supporting testing on covered conductor to evaluate its effectiveness for mitigating incidental contact with a variety of objects as reflected by review of the fault potential. Objects include vegetation (tree branch/limb, palm frond), wildlife, metallic balloons, and conductors contacting one another. These studies support testimony representations made within **Section (IV)(B)(1)(e) at page 57** related to the proposition that low energy is produced from covered conductor contact with objects as reflected within the test studies discussed within this report. Furthermore, computerized engineering simulations and empirical tests demonstrated that covered conductor reduced the occurrence of faults caused by contact with objects, a potential source of fire ignition.

Three methods were used to evaluate the fault potential impact of covered conductors when in contact with objects:

1. **Currents were estimated by inputting calculations of circuit parameters into Power Systems Computer Aided Design (PSCAD).** An electrical circuit was built in the software package PSCAD for bare and covered conductors. The capacitance[1] between the branch and the covered conductor was approximated as parallel plate capacitors[2] with similar dimensions to the branch. The resistance[3] of the branch and the insulation were calculated based on dimensions and resistivity of the respective materials.
2. **Currents were estimated using the Current Distribution Electromagnetic Fields Grounding and Soil Structure Analysis (CDEGS) software simulation tool.** The CDEGS simulation tool models the geometry and material properties of the circuit. Contacts from objects on bare conductors were modeled as references for fault current and energy comparison with the same contact scenarios on covered conductors. A general case was first modeled in CDEGS assuming average tree branch dimensions and a 16 kV phase-to-phase voltage circuit. Specific cases were then modeled in CDEGS as a basis for empirical testing.
3. **System Voltage Testing was performed on a 12 kV phase-phase circuit at SCE's Equipment Demonstration and Evaluation Facility (EDEF) connected to SCE's 12 kV distribution system**. This test was performed using only covered conductor, not bare conductor as information exists for bare conductor due to its industry use.

SCE first performed the PSCAD simulation and then subsequently performed the CDEGS simulation and conducted the tests at SCE's EDEF. All three methods generally showed similar results. SCE presented the PSCAD simulation figures (summarized in Table 1) in testimony because PSCAD is the most conservative of the three methods (i.e., it is the least likely to overestimate the fault mitigation benefits of covered conductor), producing the highest estimates of current and energy levels. All three methods demonstrated that charging currents on the outer cover, when in contact with various objects, are below 1 mA. This magnitude of current is well below values corresponding to perceptible tingling upon contact (National Institute for Occupational Safety

[1] Capacitance is the ability of a system to store an electric charge.
[2] A capacitor is a device used to store an electric charge, consisting of one or more pairs of conductors separated by an insulator.
[3] Resistance is a measure of the difficulty to pass an electric current through an object

and Health)[4]. Currents below 1 mA equate to low energy values, reducing the chance of fault and potential ignition risk. By comparison, a cell phone charges at 3 to 4 watts while an outlet charger left disconnected from a phone consumes 1 to 2 watts (Heikkinen & Nurminen, 2012). Comparatively, covered conductor empirical testing yielded energy values ranging from 0.00000007 watts (Metallic Balloon) to 0.0048 watts (Brown Branch), significantly lower than the energy of a charger disconnected from a phone. Table 1 and Table 2 illustrate the low energy and current results from the simulation and testing. Overall, the computer analysis, empirical testing, and observations reaffirmed that the energy values when compared to bare conductors were significantly lower as shown in the results below.

Table 1 shows a comparison of current and energy values of a branch on bare conductor versus covered conductor that were simulated in PSCAD and CDEGS. Both simulation methods illustrate that the currents are significantly below 1 mA, resulting in low energy values that is unlikely to result in arcing.

Table 1: Summary of Covered Conductor vs. Bare Conductor General Case Simulation Results

Simulation Method	Conductor Type	Current in Branch	Resistance of Branch	Power into Branch
PSCAD	Bare Conductor	2800 mA	5800 Ω	45,472 W
	Covered Conductor	**0.18 mA**	5800 Ω	0.00019 W
CDEGS	Bare Conductor	2730 mA	5800 Ω	43,227 W
	Covered Conductor	0.04 mA	5800 Ω	0.00001 W

Table 2 summarizes the current and energy results from the computer simulations (CDEGS) and empirical testing (EDEF). Both methods illustrate that the currents are significantly below 1 mA, resulting in low energy values that is unlikely to result in arcing.

Table 2: Summary of Simulated and Tested Results for Specific Gases

Simulated/Test Subject	Current		Energy	
	Simulation Current with Test Subject (mA)	Empirical Current with Test Subject (mA)	Power -Simulation (Watts)	Power –Empirical Testing (Watts)
Palm Frond	0.005	0.001	0.00525	0.00021
Brown Branch[1]	0.00	-0.001	0.17	0.0048
Green Branch	0.003	0.001	0.000012	0.0000014
728 Ohm Resistor Ph-Ph	0.004	0.044	0.000000012	0.0000015
Metallic Balloon	0.009	0.128	0.00000000030	0.000000066

[1] The negative value of the current in the Brown Branch is the result of being at the bottom range for the measuring devices used for testing and signifies the small magnitude of current.

[4] See Section 11.8 for the effects of current on the human body as published by National Institute for Occupational Safety and Health

2.0 Scope and Purpose

The purpose of the study was to calculate and compare the expected short circuit current, energy, and arcing when various objects such as tree branches come into contact with bare and covered conductors.

2.1 Hypothesis

When a tree branch makes contact with two energized bare distribution electric conductors, the voltage between the two phases can be great enough to push electric current through the branch. A phase-to-phase fault occurs when a carbon ionization path is established through the branch, which allows electrons to move freely and create an electric short. Falling embers from this phase-to-phase arcing could have the potential to serve as a fire ignition source (Russell).

The hypothesis is that covered conductors, due to the layers of insulation, will reduce the energy transferred to the tree branch which in turn reduces the potential for arcing. This study was performed to quantify the effectiveness of this insulation.

The voltage on the conductor induces a charge on the outer layer. This charge, however, results in an insignificant amount of current present on that layer of the covered conductor. Therefore, contact with any given point on the undamaged outer cover is inadequate to produce arcing. In addition, the outer layer of the covered conductors is designed with track-resistant properties. This means that the covering materials prevent small charging current along the conductor from collecting and forming a conductive ionized path.

3.0 Covered Conductor Design

This study used covered conductors comprised of four components as shown below (Southwire, 2018) (Hendrix Aerial Cable Systems) (Hendrix Aerial Cable Systems, 2018):

1. Aluminum Conductor Steel Reinforced (ACSR) or Hard Drawn Copper (HDCU)
2. Conductor Shield (15 MILS)
3. Inner Insulation layer (75 MILS)
4. Outer Insulation layer (75 MILS)

Figure 1 shows a telescopic illustration of the covered conductor, allowing the four components of the covered conductor to be displayed.

Figure 1: Covered Conductor Design

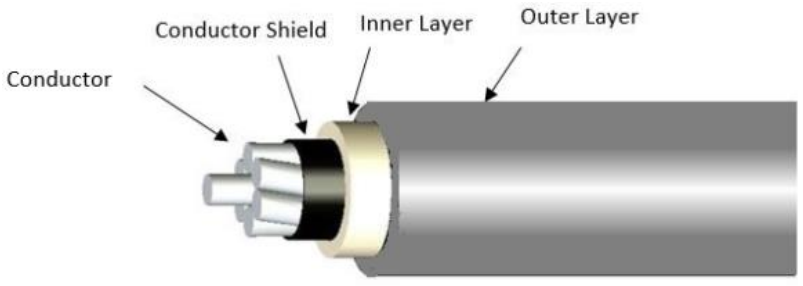

Engineering Analysis on the Impacts of Contact from Objects (CFO) on Bare vs. Covered Conductors

3.1 Conductor Shield

The conductor shield is made of a semiconducting thermoset polymer. Its purpose is to reduce stress concentrations caused by flux lines from the individual conductor strands. By encircling the strands, it effectively transforms the strands into a single uniform conducting "cylinder" as the images below illustrates. The reduction of electrical stress, especially if the covered conductor is in contact with another object, will help preserve the integrity of the insulation and increase the service life of the covered conductor.

Figure 2 illustrates the electrical field on a conductor without a conductor shield. The overlap in the fields, as the arrows in the figure shows, results in electrical stress.

Figure 2: Flux Lines without Conductor Shield (Southwire)

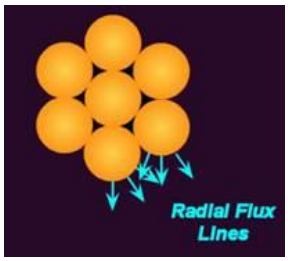

Figure 3 illustrates the electrical field on a conductor with a conductor shield. The conductor shield prevents the electrical fields from overlapping, allowing for uniformity around the entire conductor and a reduction in electrical stress.

Figure 3: Flux Lines with Conductor Shield (Southwire)

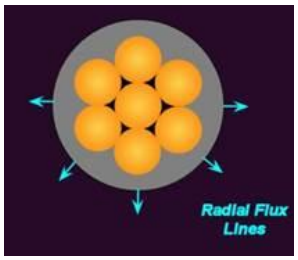

As illustrated above, the conductor shield helps to reduce electrical stress, especially when in contact with the ground. For example, it is possible for a tree branch to make long-term make phase-ground contact with the covered conductor. The conductor shield minimizes the voltage stress on the contact area, provided that the tree branch weight does not exceed the line and pole strength. An industry test result has shown that covered conductor with a conductor shield prolongs the time to failure by up to four times in an accelerated test protocol (wet wood contact and 2.5 times normal voltage). For the non-accelerated test protocol (wet wood contact and normal voltage), the covered conductor did not fail after 142 days, and the test ended (Ladinger).

3.2 Inner Layer

The inner layer is a crosslinked Low Density Polyethylene (XL-LDPE), which is an insulating material. The insulation contributes to the high impulse strength of the cover, protecting from phase-to-phase and phase-to-ground contact.

3.3 Outer Layer

The outer layer is a crosslinked High Density Polyethylene (XL-HDPE). It has the same insulating function as the inner layer. However, due to being high density, it is also a "tougher" layer, making it abrasion and impact resistant. The outer layer is also track resistant, which limits the charging current flowing on its surface. This track resistant property will help maintain the integrity of the insulation surface over time by significantly reducing electrical tracking that could lead to erosion of the insulation. Additionally, the XL-HDPE is specified for UV stability, making it less susceptible to UV degradation.

4.0 Calculation Methodology

Two methods were used to calculate the expected short circuit current when a foreign object contacts a bare or covered conductor. One method uses the software package Power Systems Computer Aided Design (PSCAD) while the other method uses the software package Current Distribution Electromagnetic Fields Grounding and Soil Structure Analysis (CDEGS). In both cases, electrical properties were calculated for the foreign object based on typical material properties. PSCAD uses a circuit analysis approach, while CDEGS computes electric and magnetic fields. Section 5.0 presents the PSCAD simulations. Section 6.0 presents the CDEGS simulations. Refer to section 4.3 for parameters used in both simulation methods. Section 8.0 present specific cases that were also modeled in CDEGS as a basis for empirical testing performed.

4.1: PSCAD Modeling

An electrical circuit was built in PSCAD for bare and covered conductors. The capacitance between the branch and the covered conductor was approximated as parallel plate capacitors with similar dimensions to the branch. The resistance of the branch and the insulation were calculated based on dimensions and resistivity of the respective materials. Conservative values were input as circuit parameters and based on the assumptions made, the PSCAD simulation should provide the highest estimates of current and energy.

4.2: CDEGS Modeling

The HIFREQ module of the software package CDEGS is able to directly calculate electric and magnetic fields, currents, and voltages from the geometry and material properties of the system. This removes the requirement to approximate the circuit parameters as simple resistors and capacitors. Therefore, this method is more aligned with field conditions.

4.3 Parameters Used for Models

4.3.1 PSCAD Parameters

Table 3 illustrates the parameters used in the PSCAD modeling. PSCAD involves modeling an electrical circuit. The parameters above were used for the capacitance and resistance values.

Table 3: PSCAD Modeling Parameters

Parameter	Value
Insulation Capacitance	60 pF
Insulation Resistance	5.95×10^{11} Ω
Tree Limb Length[5]	0.91 m
Tree Limb Resistance	5,800 Ω

Refer to Section 11.7 for the parameter calculations.

4.3.2 CDEGS Parameters

Table 4 illustrates the parameters used in the CDEGS modeling. CDEGS uses the geometry and material properties of the circuit. Therefore, capacitance values and resistance values are automatically calculated in the simulation.

Table 4: CDEGS Modeling Parameters

Parameter	Value
Tree Limb Length[6]	2.74 m
Tree Limb Resistance	5,800 Ω

Refer to Section 11.7 for the parameter calculations.

[5] The length of a tree branch should surpass the phase spacing to truly simulate a practical scenario. However, PSCAD simulations restrict the branch from surpassing the phase spacing. Therefore, a tree branch length and phase spacing of 0.91 m (3 ft) was used in the simulation to meet SCE phase spacing requirements. The length of the branch will not affect the simulation results because current and energy are a function of the branch's resistance and not its length.

[6] The CDEGS model used a tree branch length of 2.74 m (9 ft) to reflect a real world scenario where the limb length may exceed the phase spacing. A length of 9 ft was used to closely model a palm frond.

5.0 PSCAD Generic Case Models

5.1: Bare Conductors

Based on the values shown in Section 4.3.1, the following model in PSCAD was formed for the case in which a tree branch makes contact with bare conductors. The results show that an initial current of 2.8 A is produced when a tree branch falls on bare conductors. This current will quickly increase as the resistance of the branch decreases due to the formation of a carbon ionization pathway, eventually leading to a phase-to-phase fault.

Figure 4 illustrates the circuit created in PSCAD simulating a 3 foot branch across two phases of bare conductor. A resistance of 5,800 Ω was used to model the tree branch.

Figure 4: PSCAD Bare Conductor Model

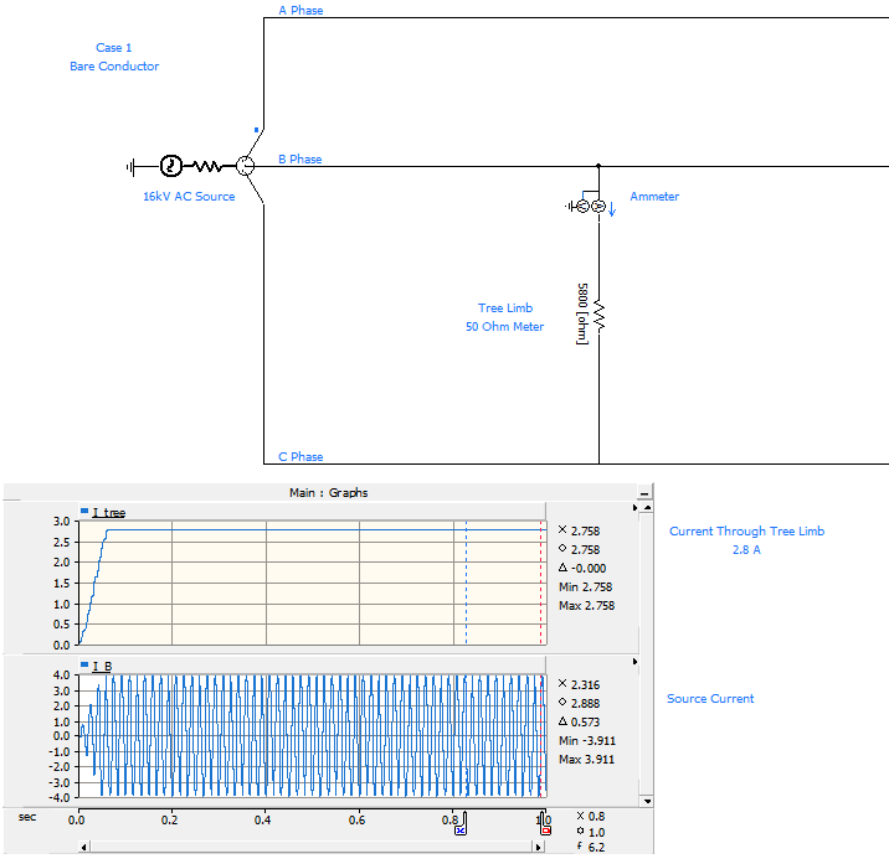

5.2: Covered Conductors

The following model in PSCAD was used for the case where a tree branch falls on covered conductors, based on the parameters in Section 4.3.1. The results show a current of 0.18 mA when the tree branch falls on covered conductors. This current magnitude is not sufficient to produce the energy required for arcing.

Engineering Analysis on the Impacts of Contact from Objects (CFO) on Bare vs. Covered Conductors

Figure 5 illustrates the circuit created in PSCAD simulating a 3 foot branch across two phases of covered conductor. A resistance of 5,800 Ω was used to model the tree branch. Capacitors were used to model the current transferred from the conductor to the branch with the covering in between.

Figure 5: PSCAD Covered Conductor Model

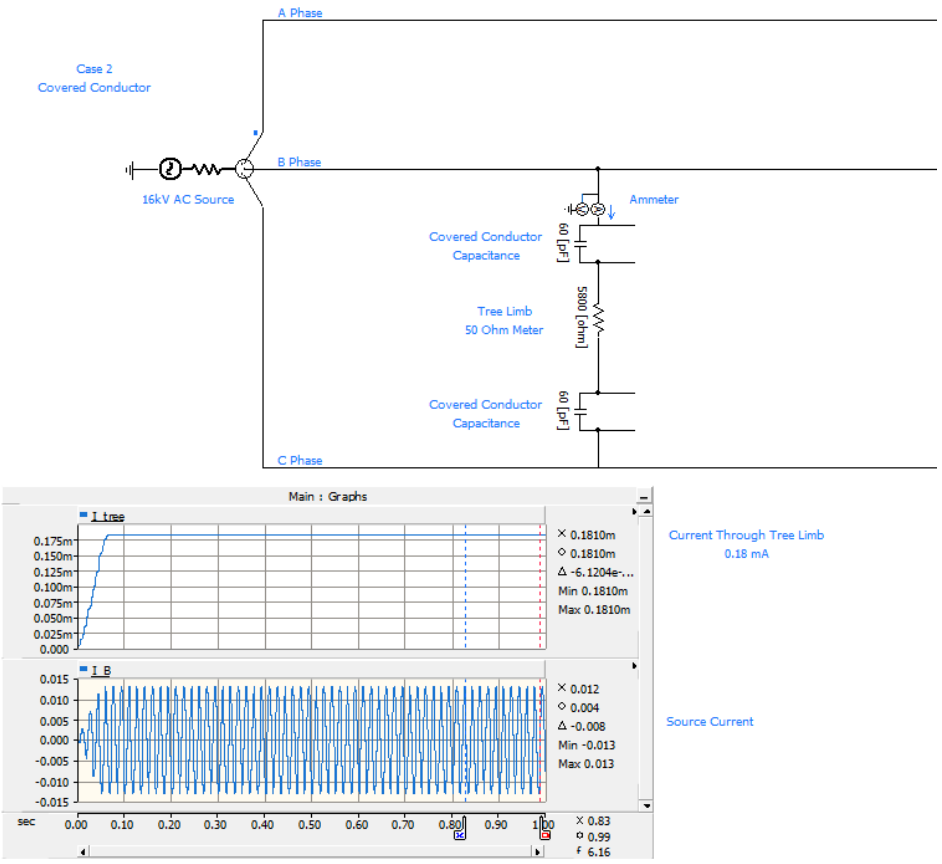

Engineering Analysis on the Impacts of Contact from Objects (CFO) on Bare vs. Covered Conductors

6.0 CDEGS Generic Case Models

Currents and voltages were calculated using the CDEGS software simulation tool. The CDEGS simulation tool models the geometry and material properties of the circuit. Contacts from objects on bare conductors were modeled as references for fault current and energy comparison with the same contact scenarios on covered conductors. A general case was first modeled in CDEGS assuming average tree branch dimensions and a 16 kV phase-to-phase voltage circuit.

Section 6.1, through computer simulation, models tree branch contact on bare conductors. Section 6.2 illustrates the model for tree branch contact on covered conductors.

6.1 Bare Conductors

The following simulated model was used for the case where a tree branch falls on bare conductors, based on the parameters in Section 4.3.2. Approximately 2.73 A is flowing through the shorting contact, as shown in Figure 6 below. This model was for a general case, assuming average tree branch dimensions and a 16 kV phase-to-phase voltage circuit.

Figure 6 shows the simulated model of a 9 foot tree limb across parallel bare conductors. The colors in the figure depict the values of the current in the system. Red equates to a current of 2.73 A (2730 mA) and green equates to 0.10 A (100 mA). This amount of current may lead to arcing.

Figure 6: Simulated Bare Conductor Longitudinal Current

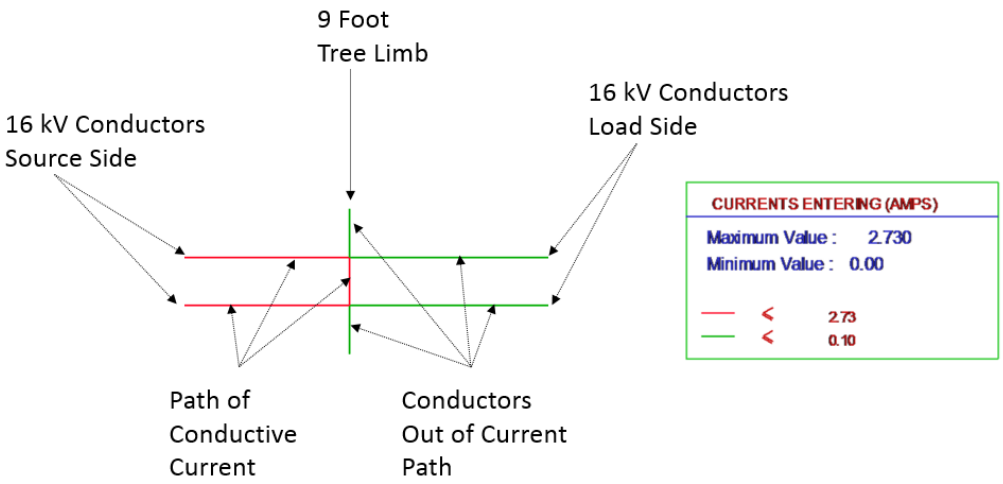

Current will always flow through the path of least resistance. The path of least resistance in this case is through the tree branch. The current on the branch could create a potential fire ignition event since the contact areas, which are points of high current concentrations, could be more likely to heat up quickly.

Engineering Analysis on the Impacts of Contact from Objects (CFO) on Bare vs. Covered Conductors

Figure 7 shows a representation of the flow of current between the bare conductors and the tree limb. The majority of the current enters and leaves the tree limb at discrete points or hot spots. These hot spots are points of high current density and could be more likely to heat up quickly.

Figure 7: Current Path for Tree Limb on Bare Conductor

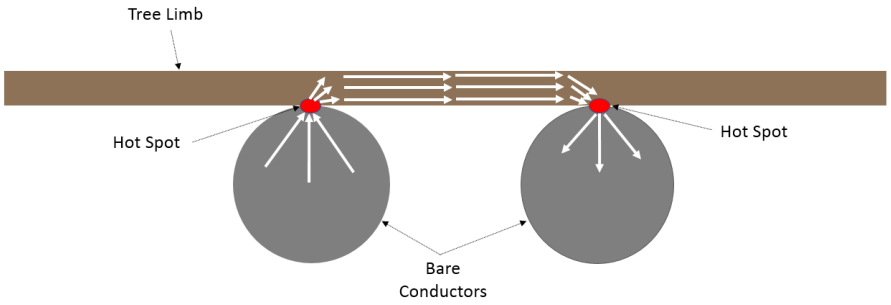

6.2 Covered Conductors

Simulation software models the electrical characteristics of the actual conductors and insulation. The results shown in Figure 8 and Figure 9 show a total of 0.04 mA of current flowing through the tree limb. This model was for a general case, assuming a 9 foot tree branch length and a 16 kV phase-to-phase voltage circuit.

Figure 8 shows the simulated model of a 9 foot tree limb across parallel covered conductors and the longitudinal current flowing through the branch. The colors in the figure depicts the values of the current in the system. The values in the table above are scaled to 1×10^{-3}. Therefore, the values shown on the table must be multiplied by 0.001 to obtain the true value. For example, the purple line, which corresponds to the maximum current density in the tree limb, equates to 0.00004 A (0.04 mA), indicating that the highest amount of current going through the branch is 0.04 mA. This current is extremely low and would be unlikely to cause arcing.

Figure 8: Simulated Covered Conductor Longitudinal Current

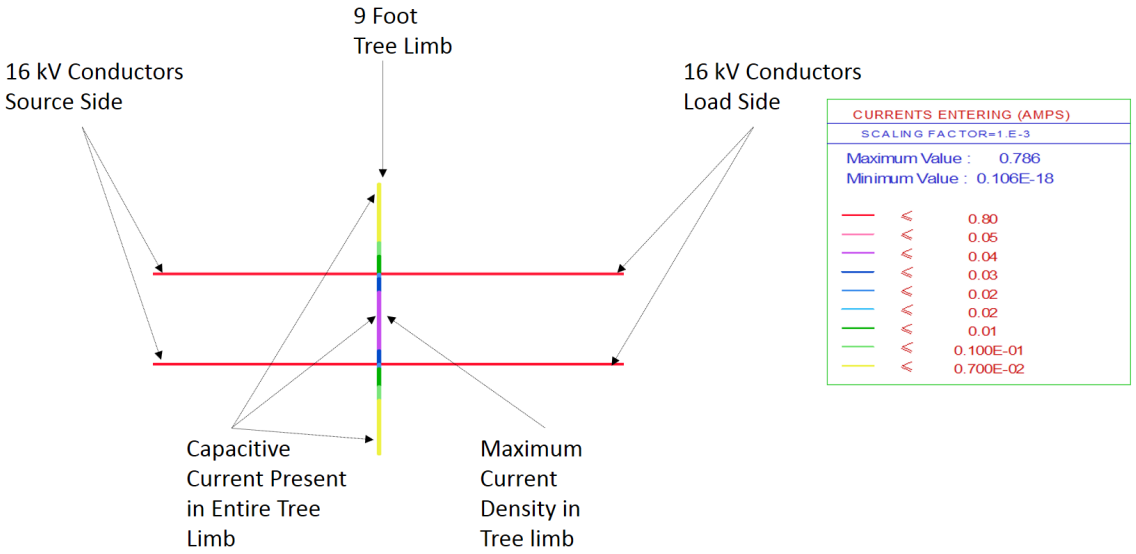

Engineering Analysis on the Impacts of Contact from Objects (CFO) on Bare vs. Covered Conductors

Figure 9 shows the simulated model of a 9 foot tree limb across parallel covered conductors and the point of current entry. The point of current entry is the area where the tree branch and covered conductor make contact. The colors in the figure depict the values of the current in the system. The values in the table above are scaled by 1×10^{-3}. Therefore, the values shown on the table must be multiplied by 0.001 to obtain the true value. For example, the red line, which corresponds to the capacitive current entering the tree limb, equates to 0.00004 A (0.04 mA), indicating that the highest amount of current entering the branch is 0.04 mA. This current is extremely low and is unlikely to cause arcing.

Figure 9: Simulated Covered Conductor Current Point of Entry

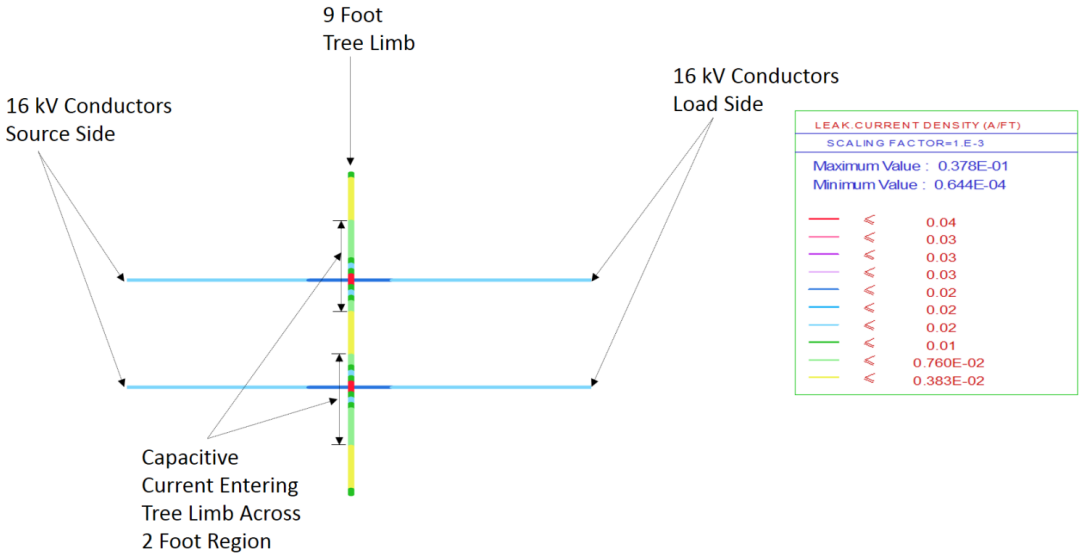

Unlike the bare conductor case, the path of current is spread across a wide area. There is current across the entire length of the tree limb, but the highest current occurs in the center as shown in Figure 8. Figure 9 shows the majority of the current enters the tree limb across an approximately two foot long region instead of at a discrete point. This is a consequence of the multiple parallel paths for current as shown in Figure 10. The points of high current density needed to spark a fire do not exist.

Figure 10 shows a representation of the multiple parallel paths for capacitive current between the covered conductors and the tree limb. This leads to the majority of the current entering the tree limb across an approximately two foot long region instead of at a discrete point.

Figure 10: Capacitance between Covered Conductors and Tree Limb

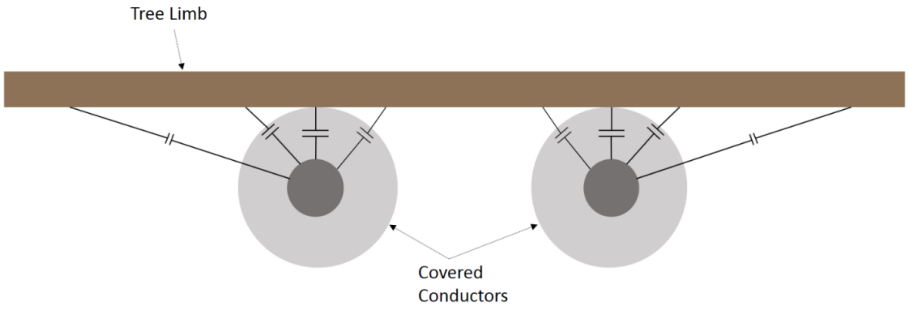

7.0 Generic Case: Current and Energy of Bare vs. Covered Conductors

Both simulation models (PSCAD in Section 5.0 and CDEGS in Section 6.0) illustrate an approximate current of 2.8 A (2800 mA) on the tree branch when it is in contact with bare conductors. Comparatively, a tree branch on covered conductors results in a current values of 0.00018 A (0.18 mA) and less than 0.00001 A (0.01 mA) through the branch in PSCAD and CDEGS, respectively. The simulated current values and the calculated resistance values of a tree branch (Section 4.3) can be used to calculate energy into the branch using the following equation:

$$P = I^2R \qquad \textit{Equation 1}$$

Where
P is the power (energy)
I is the current
R is the resistance

When calculating power, the difference between covered conductor and bare is more apparent because power is proportional to the magnitude of current squared.

Table 5 summarizes the results of both simulation methods and translates the current into energy. Energy was calculated using current squared multiplied by the resistance ($P = I^2R$). The PSCAD values are comparable to CDEGS values when modeling a tree branch on bare conductor. In the covered conductor simulation, the PSCAD current results are greater than the CDEGS results. Conservative modeling was used in PSCAD to obtain the maximum possible current through the branch, leading to higher current value in the simulation. Both simulation methods show by using covered conductors, the rate of energy into the branch is reduced by a factor of more than a hundred thousand. This reduction will significantly reduce the probability of arcing and potential for fire ignition.

Engineering Analysis on the Impacts of Contact from Objects (CFO) on Bare vs. Covered Conductors

Table 5: Current and Energy General Case

Simulation Method	Conductor Type	Current in Branch	Resistance of Branch	Power into Branch
PSCAD	Bare Conductor	2800 mA	5800 Ω	45,472 W
	Covered Conductor	0.18 mA	5800 Ω	0.00019 W
CDEGS	Bare Conductor	2730 mA	5800 Ω	43,227 W
	Covered Conductor	0.04 mA	5800 Ω	0.00001 W

8.0 SCE Distribution System Voltage Testing - EDEF

System Voltage Testing was performed on a 12 kV phase-phase circuit at SCE's Equipment Demonstration and Evaluation Facility (EDEF) powered by the SCE distribution system. No contacts on bare conductors were tested because these faults are well understood in the industry. Only contacts from objects on covered conductors were performed.

8.1 Simulation

Simulations modeled a 12 kV phase-phase circuit with various foreign objects laid across the phase conductors. Conductor-Conductor contact was also modeled. These simulations served as the basis for testing performed at SCE's EDEF. Current values in the simulations, models are compared at the same point measured at EDEF testing. Results for these simulations are presented in the following sections and the results can be seen in Section 11.7 3 of the Appendix.3 of the Appendix.

8.2 Test Set Up

This test was used to validate the current values modeled in the simulation and physically demonstrate that short term phase-phase contact on covered conductors (CC) will not cause faults or arcing.

Figure 11 shows the actual test set up and a schematic of the test set up. Two phases of covered conductors were isolated from a 3 phase, 4-wire system. The circuit was energized at 12 kV phase-phase. The covered conductors were spaced 36 inches apart and supported by 25 kV Polymer Pin-Type Vice Top Line Insulators with Nylon Inserts. The insulators were connected to an 8 foot composite crossarm. Current transformers were used to monitor the current on the covered conductors. Objects used included a palm frond, a brown branch, a green branch, metallic balloons, and conductor-conductor contact. Refer to Section 11.5 for circuit map. 1/0 AWG covered conductor was used for all test cases.

During testing, the current in the covered conductor was recorded without the test subject making contact (Tare Current without Test Subject). The Tare Current without Test Subject is considered as the reference current since this current is considered as noise for the purposes of this test. An object was then placed on both phases and the current was recorded again (Current with Test Subject). The difference between the Tare Current without Test Subject and the Current with Test Subject was calculated to obtain the effect of the object on the system with the tare removed. The Change in Current with Test Subject is considered to be the current observed on the conductor for purposes of this report.

The same methods were applied to the simulations of the test cases to produce the data below.

Engineering Analysis on the Impacts of Contact from Objects (CFO) on Bare vs. Covered Conductors

Figure 11: Empirical Test Set Up

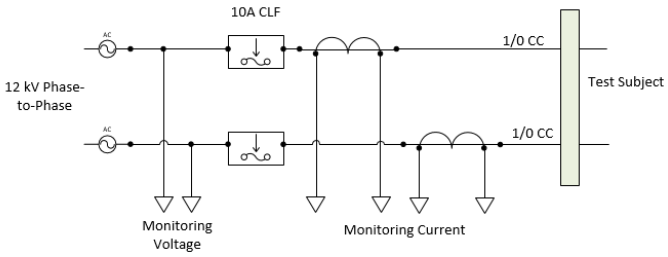

8.2.1 Palm Frond

A palm frond was placed mid-span of the covered conductor set-up, as shown on Figure 12. The palm frond rested on the covered conductor for 5 minutes while the circuit was energized at 12 kV phase-phase. For the duration of the test, two current transformers monitored the leakage current on the covered conductors. No arcing was observed when the circuit was energized. No damage on the covered conductors and palm frond was observed after the test, refer to Appendix Section 11.4 for a microscopic cutaway view of the post-test covered conductor**.**

Table 6 summarizes and compares the empirical results with the simulated results. Overall, the current observed when the palm frond made phase-phase contact was 0.001 mA

Figure 12: Palm Frond Test Set-Up

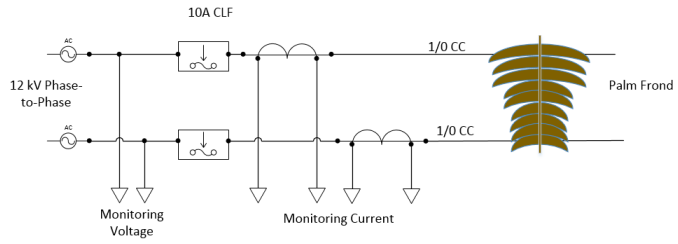

Table 6: Simulated and Empirical Palm Frond Results

Test Subject	Moisture Content (%)	Test Subject Resistance @ 5kVDC	Length of Subject (in.)	Diameter of Subject (in.)	CDEGS Tare Current w/out Test Subject (mA)	CDEGS Current with Test Subject (mA)	CDEGS Change in Current with Test Subject (mA)	Tare Current w/out Test Subject (mA)	Current with Test Subject (mA)	Change in Current with Test Subject (mA)
Palm Frond	4.60%	210 MΩ	45 in.	0.822 in.	0.110	0.115	0.005	0.016	0.017	0.001

8.2.2 Branch

A brown branch (3.60% moisture) was placed mid-span of the covered conductor set-up, as shown in Figure 13. The branch rested on the covered conductor for 5 minutes and 59 seconds while the circuit was energized at 12 kV phase-phase. For the duration of the test, two current transformers monitored the leakage current on the covered conductor. No arcing was observed when the circuit was energized. No damage on the covered conductor and dry branch was observed after the test, refer to Appendix Section 11.4 for a microscopic cutaway view of the post-test covered conductor.

Figure 13: Brown Branch Test Set-Up

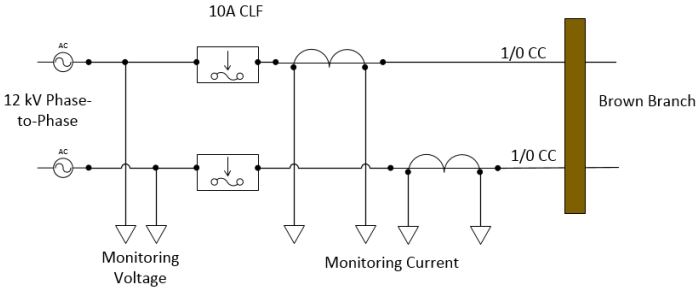

A green branch (12.20% moisture) was placed mid-span of the covered conductor set-up after testing the dry branch, as shown in Figure 14. The branch rested on the covered conductor for 5 minutes and 16 seconds while the circuit was energized at 12 kV phase-phase. For the duration of the test, two current transformers monitored the leakage current on the covered conductors. No arcing was observed when the circuit was energized. No damage on the covered conductors and green branch was observed after the test, refer to Appendix Section 11.4 for microscopic cutaway view of the post-test covered conductor**.**

Figure 14: Green Branch Test Set-Up

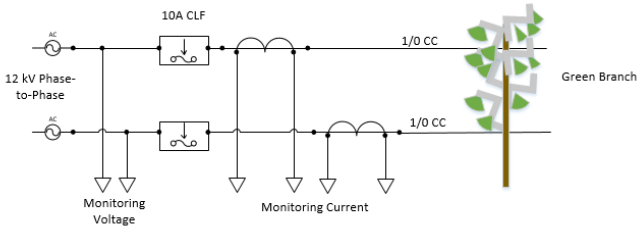

Table 7 summarizes and compares the empirical results with the simulated results. Overall, the current observed when the palm frond made phase-phase contact was – 0.001 mA for the brown branch and 0.001 mA for the

green branch. The negative value of the current in the brown branch is due to the current being at the low end of the measuring device's limit.

Table 7: Simulated and Empirical Branch Results

Test Subject	Moisture Content (%)	Test Subject Resistance @ 5kVDC	Length of Subject (in.)	Diameter of Subject (in.)	CDEGS Tare Current w/out Test Subject (mA)	CDEGS Current with Test Subject (mA)	CDEGS Change in Current with Test Subject (mA)	Tare Current w/out Test Subject (mA)	Current with Test Subject (mA)	Change in Current with Test Subject (mA)
Brown Branch	3.60%	4760 MΩ	49 in.	1.527 in.	0.110	0.116	0.006	0.016	0.015	-0.001
Green Branch	12.20%	1.35 MΩ	35.5 in.	0.493 in	0.110	0.113	0.003	0.016	0.017	0.001

8.2.3 728 Ω Resistor (Animal Contact)

A 728 Ohm (Ω) resistor was placed mid-span of the covered conductor set-up, as shown in Figure 15. The 728 Ω resistor represented wildlife contact. The resistor rested on the covered conductor for 4 minutes and 19 seconds while the circuit was energized at 12 kV phase-phase. For the duration of the test, two current transformers monitored the leakage current on the covered conductors. No arcing was observed when the circuit was energized. No damage on the covered conductors and the resistor was observed.

Figure 15: Animal Contact Test Set-Up

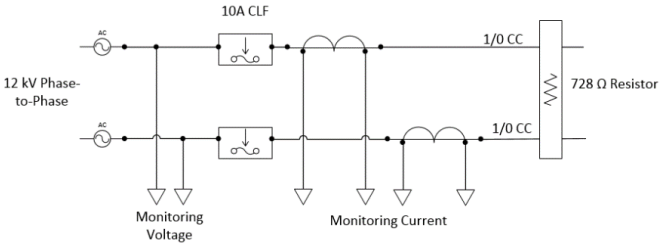

Table 8 summarizes and compares the empirical results with the simulated results. Overall, the current observed for phase-phase animal contact was 0.044 mA.

Engineering Analysis on the Impacts of Contact from Objects (CFO) on Bare vs. Covered Conductors

Table 8: Simulated and Empirical Animal Contact Results

Test Subject	Moisture Content (%)	Test Subject Resistance @ 5kVDC	Length of Subject (in.)	Diameter of Subject (in.)	CDEGS Tare Current w/out Test Subject (mA)	CDEGS Current with Test Subject (mA)	CDEGS Change in Current with Test Subject (mA)	Tare Current w/out Test Subject (mA)	Current with Test Subject (mA)	Change in Current with Test Subject (mA)
728 Ohm Resistor Ph-Ph	NA	728 Ω	36 in.	1 in.	0.110	0.114	0.004	0.016	0.06	0.044

8.2.4 Metallic Balloon

Two metallic balloons were placed mid-span of the covered conductor set-up, as shown in Figure 16. The metallic balloons rested on the covered conductors and one another to form a continuous bridge between the phases for 5 minutes and 5 seconds while the circuit was energized at 12 kV phase-phase. For the duration of the test, two current transformers monitored the leakage current on the covered conductors. No arcing was observed when the circuit was energized. No damage on the covered conductors and metallic balloons was observed after the test, refer to Appendix Section 11.4 for microscopic cutaway view of the post-test covered conductor**.**

Figure 16: Metallic Balloon Contact Test Set-Up

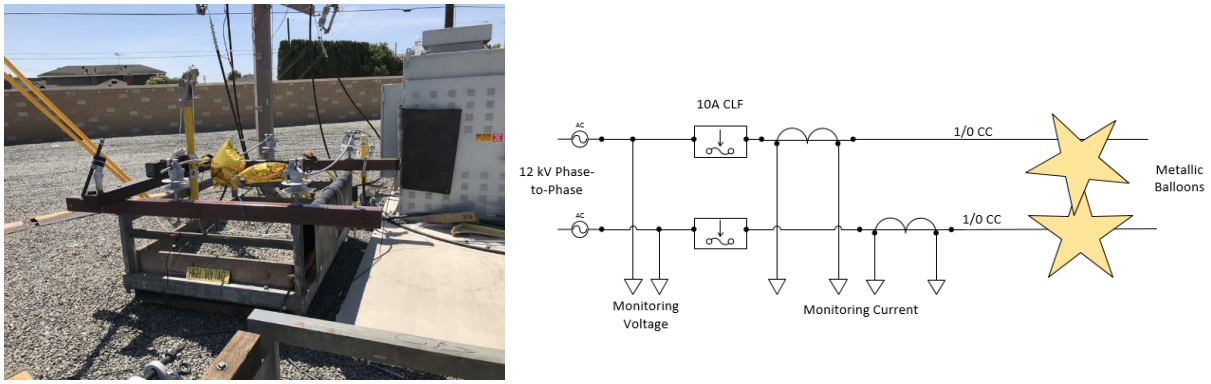

Table 9 summarizes and compares the empirical results with the simulated results. Overall, the current observed when the metallic balloon made phase-phase contact was 0.128 mA.

Table 9: Simulation and Empirical Metallic Balloon Results

Test Subject	Moisture Content (%)	Test Subject Resistance @ 5kVDC	Length of Subject (in.)	Diameter of Subject (in.)	CDEGS Tare Current w/out Test Subject (mA)	CDEGS Current with Test Subject (mA)	CDEGS Change in Current with Test Subject (mA)	Tare Current w/out Test Subject (mA)	Current with Test Subject (mA)	Change in Current with Test Subject (mA)
Metallic Balloon	NA	4 Ω	NA	18 in.	0.110	0.119	0.009	0.016	0.144	0.128

Engineering Analysis on the Impacts of Contact from Objects (CFO) on Bare vs. Covered Conductors

8.2.5 Conductor-to-conductor contact

A pulley system was used to simulate conductor-to-conductor contact, as shown in Figure 17. The two covered conductors made contact for 4 minutes and 17 seconds while the circuit was energized at 12 kV phase-phase. For the duration of the test, two current transformers monitored the leakage current of the covered conductors. No arcing was observed when the circuit was energized. No damage on both covered conductors were observed after the test, refer to Appendix Section 11.4 for microscopic cutaway view of the post tested covered conductor**.**

Figure 17: Conductor-to-Conductor Contact Test Set-Up

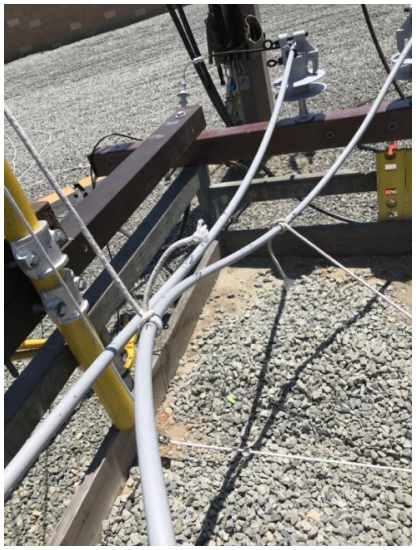

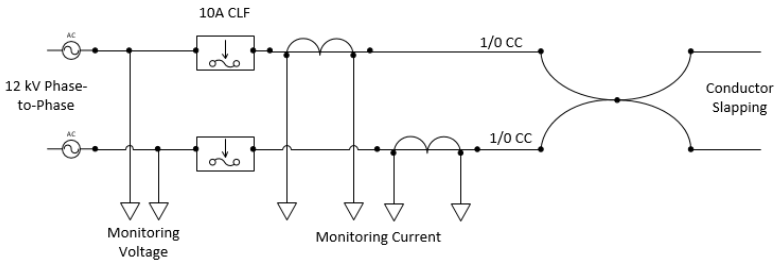

Table 10 summarizes and compares the empirical results with the simulated results. Overall, the current observed when the palm frond made phase-phase contact was 0.008 mA.

Table 10: Simulation and Empirical Conductor-to-conductor Test Results

Test Subject	Moisture Content (%)	Test Subject Resistance @ 5kVDC	Length of Subject (in.)	Diameter of Subject (in.)	CDEGS Tare Current w/out Test Subject (mA)	CDEGS Current with Test Subject (mA)	CDEGS Change in Current with Test Subject (mA)	Tare Current w/out Test Subject (mA)	Current with Test Subject (mA)	Change in Current with Test Subject (mA)
Conductor-to-conductor	NA	610 GΩ	102 in.	NA	0.110	0.152	0.042	0.016	0.024	0.008

8.3 EDEF Test Conclusion

The empirical testing demonstrated that real world scenarios such as tree branches and stray metallic balloons yield significantly different results when comparing bare to covered conductors. Empirical testing exhibited no sparking or current over 1 mA. This is important when considering that a 12 kA distribution substation is located 500 circuit feet from the test location, offering reduced impedance. The close proximity, as shown in Section 11.5 of the Appendix, to the source would allow a higher fault magnitude if catastrophic events were to occur. Evidence of covered conductor effectiveness was not only seen in the measured instantaneous observations but also in the post analysis. Post analysis of the covering as seen through cut insulation wafers exhibited in Appendix Section 11.4 displays no visible damage through any layer of the conductor's insulation. Infrared reference snap shots as shown in Section 11.6 were also taken at the point of contact between conductors and test subjects as well as conductor-to-conductor contact. The previous tests in combination with Table 5 through Table 9 exhibit a current magnitude less than 1 mA. All test current values were consistent with simulated results. Tests and analysis confirm the effectiveness of the conductor's covering as well as the significant benefits to grid resiliency.

Table 11 summarizes the computer simulated (CDEGS) and empirical (EDEF) current and energy results. All current values were below 1 mA, leading to energy values that are unlikely to cause arcing.

Table 11: Simulation and Empirical Test Results Summary

Simulated/Test Subject	Current		Energy	
	CDEGS Current with Test Subject (mA)	EDEF Current with Test Subject (mA)	Power -CDEGS (Watts)	Power -EDEF (Watts)
Palm Frond	0.005	0.001	0.00525	0.00021
Brown Branch	0.006	-0.001	0.17136	0.00476
Green Branch	0.003	0.001	0.000012	0.0000014
728 Ohm Resistor Ph-Ph	0.004	0.044	0.000000012	0.0000015
Metallic Balloon	0.009	0.128	0.00000000030	0.000000066

[1]*The negative value of the current in the Brown Branch is at the low end threshold of the measuring devices used for testing, signifying the small magnitude of current.*

9.0 Conclusion

The empirical testing performed at EDEF validated the ability of covered conductor to withstand contact from various objects without a high fault current or arcing. The low current thresholds shown by the model were confirmed by empirical data, demonstrating that the insulating capabilities of covered conductor limits the risk of arcing (and the associated potential for fire ignition). The empirical results show that using covered conductors eliminated sparking, limited energy to less than 1 watt and reduced current into an object to much less than 1 mA. Putting this into perspective, a typical cell phone charges at 3 to 4 watts, while a charger left unplugged without a phone consumes 1 to 2 watts (Heikkinen & Nurminen, 2012). In comparison, the highest power calculated is in the low end range of a cell phone charger unplugged from a phone. Also, considering the thresholds of the National Institute for Occupational Safety and Health (NIOSH) (National Institute for Occupational Safety and Health), the data gathered are well below the published values associated with perceptible tingling upon contact.

The minimal current in conjunction with the temperature change (≈+/-1.6°C) in the infrared snap shots shown in Section 11.6 indicates that contact has a minimal effect on either the conductor or test subject in the time duration of testing. The empirical testing enabled conductor to conductor contact without creating any phase-phase faults or even minor sparking. In addition, post analysis sample wafers of the covered conductor exhibited no visible signs of damage in either layer of insulation, further demonstrating the insulation's durability.

The analysis and empirical testing demonstrated that the use of covered conductors can prevent phase-to-phase and phase-to-ground faults and the associated risk sparking and arcing, potential fire ignition sources.

10.0 References

1. CAL FIRE. (2015-2016). *Historical Wildfire Activity Statistics*. Retrieved from CalFire Redbook: http://www.fire.ca.gov/fire_protection/fire_protection_fire_info_redbooks
2. Defandorf, F. M. (1956, July). Electrical Resistance to Earth of a Tree. Washington, D.C., United States of America.
3. Heikkinen, M., & Nurminen, J. (2012, January 1). *Measuring and modeling mobile phone charger energy consumption and environmental impact.* Espoo, Finland. Retrieved from Tech Radar: https://www.techradar.com/news/phone-and-communications/mobile-phones/should-we-unplug-our-chargers-each-night-1280918
4. Hendrix Aerial Cable Systems. (2018, April 27). Hendrix Tree Wire Specification for SCE. Milford, New Hampshire, United States of America: Marmon Utility LLC.
5. Hendrix Aerial Cable Systems. (n.d.). Covered Conductors - Tree Wire Systems. Milford, New Hampshire, Unites States of America: A Marmon/Berkshire Hathaway Company.
6. Ladinger, C. (n.d.). *Spacer Cable Systems for Rural Electric Cooperatives.*
7. Lee, R. H. (1982). The Other Electrical Hazard: Electric Arc Blast Burns. *IEEE Transactions on Industry Applications, Vol. IA-18, NO. 3*, May.
8. Minnesota Rural Electric Association. (2016, December). Cow Resistance: 500 Ohms in the Minnesota Stray Voltage Guide. Maple Grove, Minnesota, Unites States of America.
9. National Institute for Occupational Safety and Health. (2009). *Electrical Safety Safety and Health for Electrical Trades.*
10. Russell, D. (n.d.). Causes of Wildfire Ignition by Powerlines - Good Science vs. Bad Science. *Wildland Fire Litigation Conference.*
11. Southwire. (2018, March 30). 15kV 3-Layer Tree Wire.
12. Southwire. (n.d.). Underground Distribution Training Primary and Secondary Cables.

11.0 Appendix

11.1 Covered Conductor Deterioration

The analysis presented in this report applies only to undamaged covered conductor. If the insulation has entirely stripped off, then the results will be the same as for bare conductor. If the insulation has slight deterioration, the values are assumed to be nearly identical to those for undamaged covered conductor. If the covered conductor deteriorates to the point where the dielectric strength of the insulation material is less than the applied voltage, arcing can occur and currents may be similar to the case of bare conductor.

11.2 Summary of Results for General Case

Table 12: Summary Table of Contact From Object Using Computer Simulation

Summary Table of Contact From Object Using Computer Simulation							
Contact from Object (CFO)	**Object Resistance[1]**	**Bare Conductor**			**Covered Conductor**		
		Contact Current	**P-P Voltage**	**Power**	**Contact Current**	**P-P Voltage**	**Power**
Tree/Vegetation	7,100 Ω	2.3 A	16 kV	40,000 W	0.0002 A	16 kV	<< 0.001 W
Metallic Balloon	0.003 Ω[3]	29,000 A[5]	16 kV	2,523,000 W	0.0002 A	16 kV	<< 0.001 W
Animal	500 Ω[4]	32 A	16 kV	512 kW	0.0002 A	16 kV	<< 0.001 W
Conductor-Conductor[2]	0.003 Ω[3]	29,000 A[5]	16 kV	2,523,000 W	0.0002 A	16 kV	<< 0.001 W

1. Object Resistance values are to be assumed and validated in lab tests.
2. Conductor-Conductor is bare-to-bare and covered-to-covered. Bare and Covered conductor mixed scenario is not considered.
3. Arc resistance is calculated using contact current and Reference 7 (Lee, 1982).
4. The most commonly studied animal is cattle which are typically around 500 Ω (Minnesota Rural Electric Association, 2016). Smaller animals have higher resistances.
5. The current will be decided by the system fault current at the point of contact. For comparison, the highest fault current 12 kV substation on the SCE system is 28,826 A and the highest fault current 16 kV substation on the SCE system is 14,737 A.

Engineering Analysis on the Impacts of Contact from Objects (CFO) on Bare vs. Covered Conductors

11.3 Simulated Plots for Empirical Test Cases

Note the different scaling factors indicated in the legend for each plot.

Figure 18 shows the simulated model of the palm fond used during empirical testing across parallel covered conductors. The longitudinal current is the current flowing through the palm frond. The colors in the figure depicts the values of the current in the system. The values in the table above are scaled by 1×10^{-3}. Therefore, the values shown on the table must be multiplied by 0.001 to obtain the true value.

Figure 18: Simulated Palm Frond on Covered Conductor Longitudinal Current

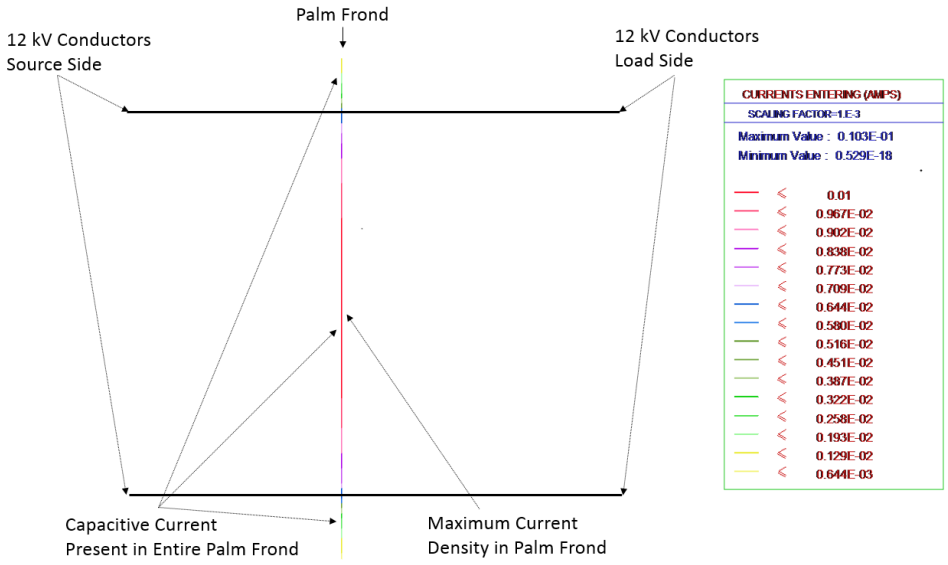

Engineering Analysis on the Impacts of Contact from Objects (CFO) on Bare vs. Covered Conductors

Figure 19 shows the simulated model of the brown branch used during EDEF testing across parallel covered conductors. The longitudinal current is the current flowing through the dry branch. The colors in the figure depicts the values of the current in the system. The values in the table above are scaled by 1×10^{-4}. Therefore, the values shown on the table must be multiplied by 0.0001 to obtain the true value.

Figure 19: Simulated Brown Branch on Covered Conductor Longitudinal Current

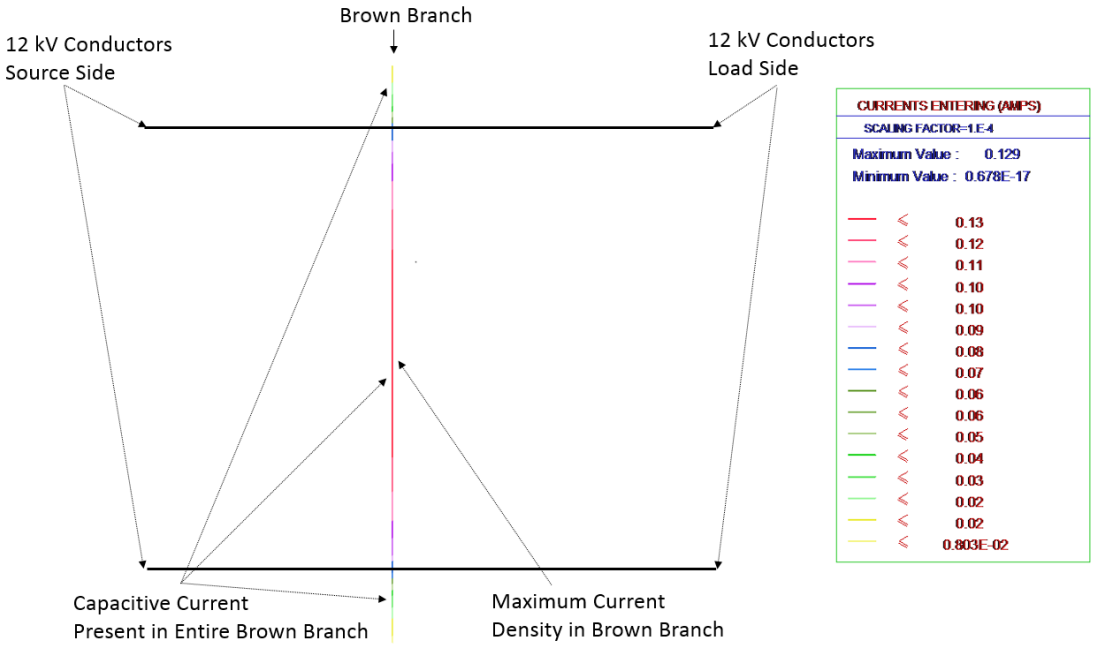

Figure 20 shows the simulated model of the green branch used during empirical testing across parallel covered conductors. The longitudinal current is the current flowing through the green branch. The colors in the figure depicts the values of the current in the system. The values in the table above are scaled by 1 × 10^{-6}. Therefore, the values shown on the table must be multiplied by 0.000001 to obtain the true value.

Figure 20: Simulated Green Branch on Covered Conductor Longitudinal Current

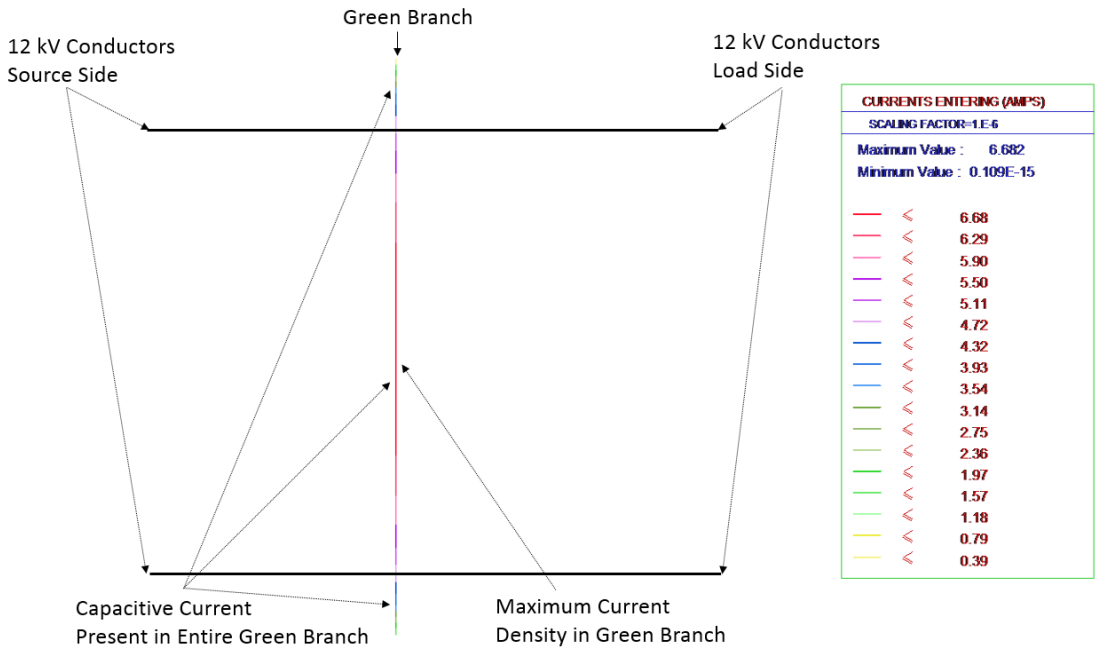

Figure 21 shows the simulated model of the 728 ohm resistor simulating animal contact used during empirical testing across parallel covered conductors. The longitudinal current is the current flowing through the resistor. The colors in the figure depicts the values of the current in the system. The values in the table above are scaled by 1×10^{-6}. Therefore, the values shown on the table must be multiplied by 0.000001 to obtain the true value.

Figure 21: Simulated 728 Ohm Resistor on Covered Conductor Longitudinal Current

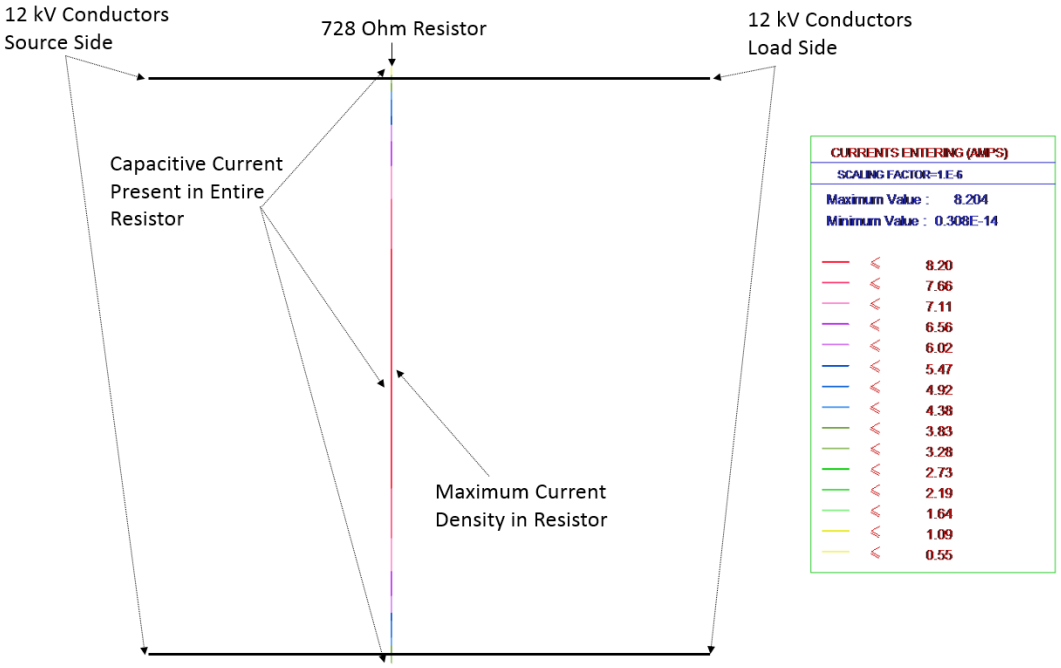

Figure 22 shows the simulated model of the metallic balloon used during empirical testing across parallel covered conductors. The longitudinal current is the current flowing through the metallic balloon. The colors in the figure depicts the values of the current in the system. The values in the table above are scaled by 1×10^{-6}. Therefore, the values shown on the table must be multiplied by 0.000001 to obtain the true value.

Figure 22: Simulated Metallic Balloon on Covered Conductor Longitudinal Current

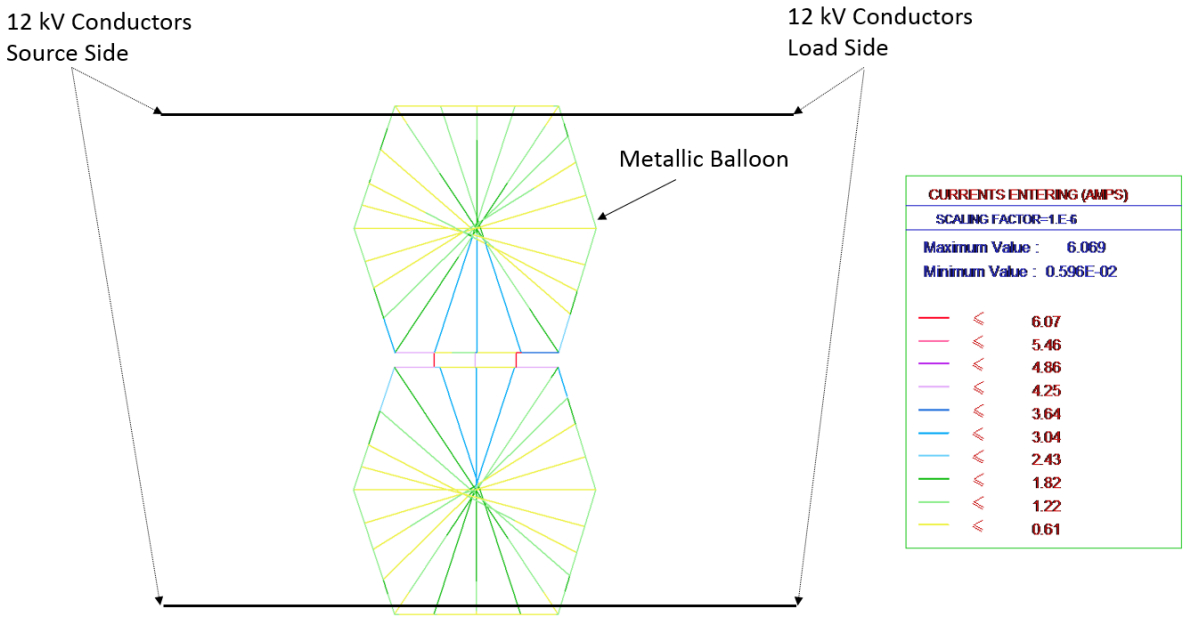

Engineering Analysis on the Impacts of Contact from Objects (CFO) on Bare vs. Covered Conductors

Figure 23 shows the simulated model of the covered conductor-conductor empirical test. The longitudinal current is the current flowing on the covering of the covered conductors. The colors in the figure depicts the values of the current in the system. The values in the table above are scaled by 1×10^{-3}. Therefore, the values shown on the table must be multiplied by 0.001 to obtain the true value.

Figure 23: Simulated Covered Conductor-Conductor Longitudinal Current

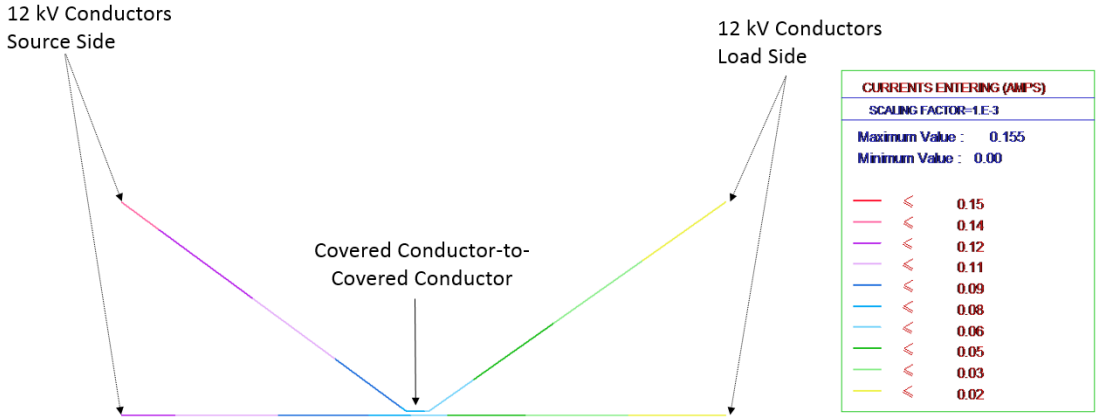

Engineering Analysis on the Impacts of Contact from Objects (CFO) on Bare vs. Covered Conductors

11.4 Microscopic view of Covered Conductor Wafers

During the EDEF tests, palm frond, branch, and slap test sample areas on the conductor were marked at each spot where the test subject came in contact with the covered conductor. At the conclusion of the test both conductors were taken to the Root Cause and Equipment Performance Group. The group cut the conductors at the point of contact as marked by field personnel and analyzed comparing to a non-tested specimen.

Samples analyzed did not show any visible characteristics of partial discharge or abnormality. The red arrows as indicated in the following pictures are at the point where the test subject touched the covered conductor. It is important to note that the vertical cut as shown in the microscopic slides are part of the analysis process and not representative of a conductor issue.

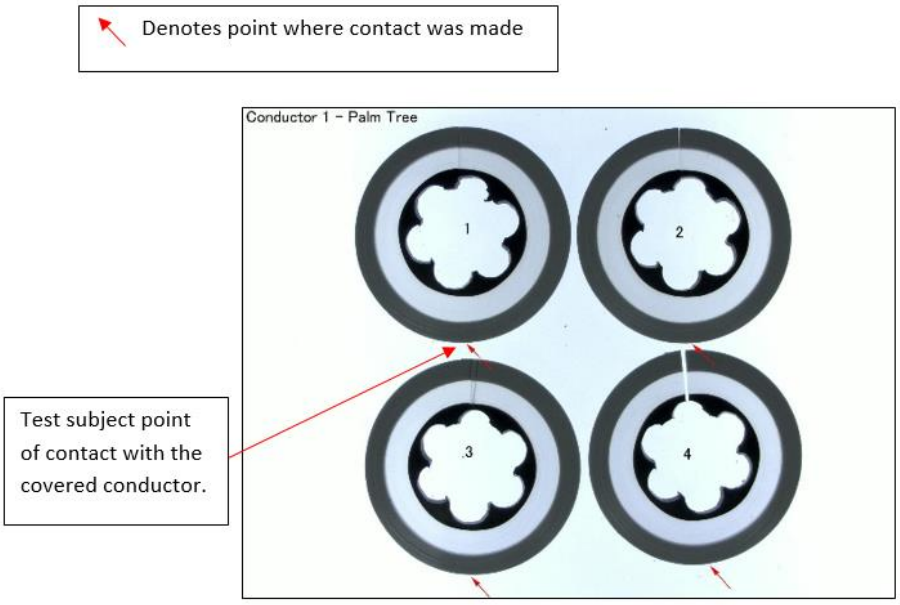

Reference of Wafer Sample

Engineering Analysis on the Impacts of Contact from Objects (CFO) on Bare vs. Covered Conductors

Brown Palm Frond Conductor

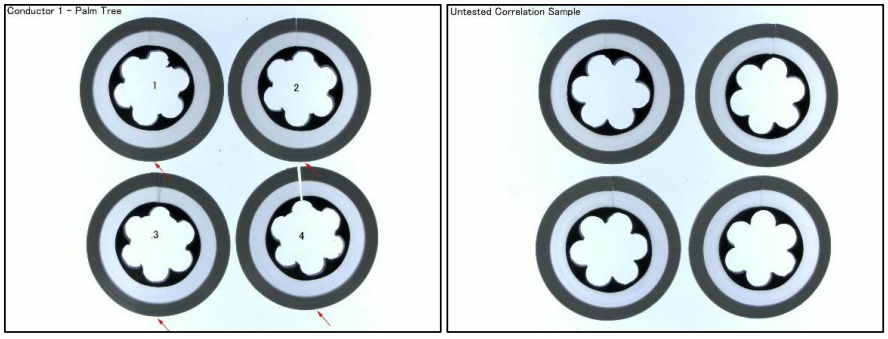

Palm Frond – Conductor 1 Reference-Non-Tested Sample

Green Palm Frond Conductor

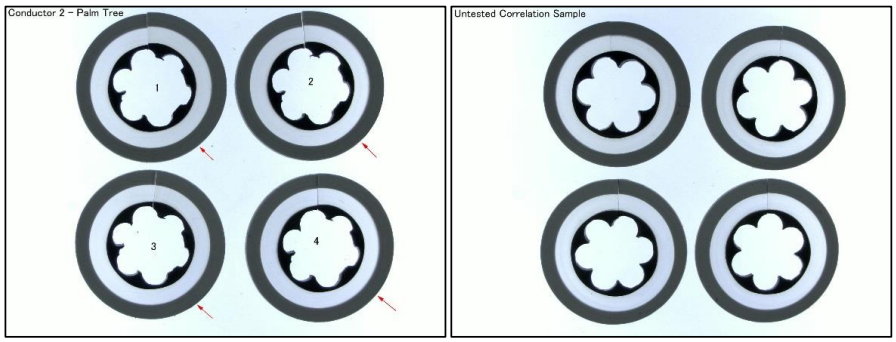

Palm Frond – Conductor 2 Reference-Non-Tested Sample

Engineering Analysis on the Impacts of Contact from Objects (CFO) on Bare vs. Covered Conductors

Brown Branch Conductor

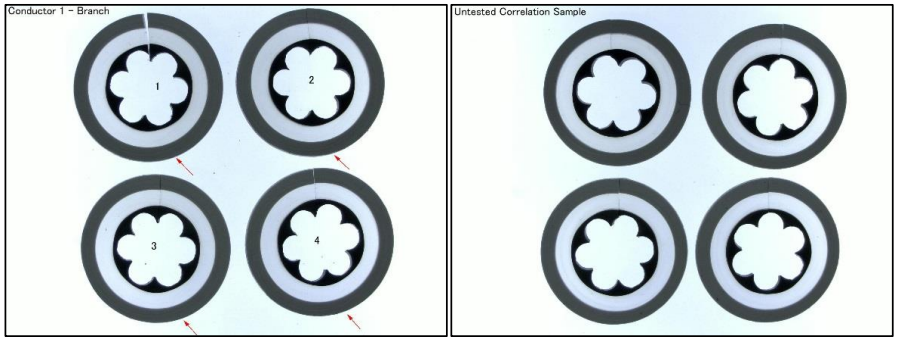

Branch – Conductor 1 Reference-Non-Tested Sample

Green Branch Conductor

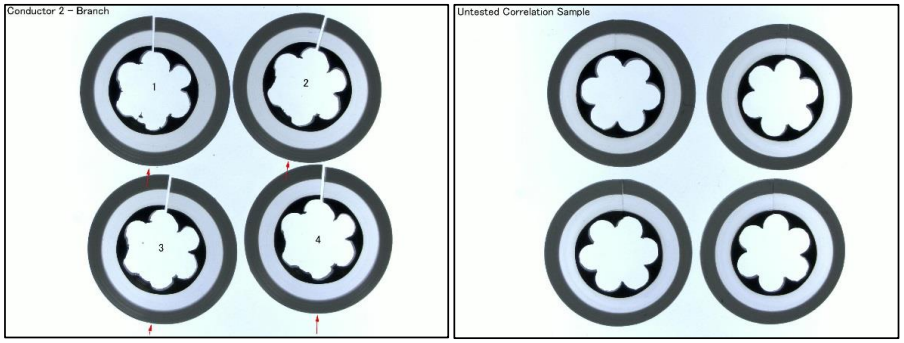

Branch – Conductor 2 Reference-Non-Tested Sample

Engineering Analysis on the Impacts of Contact from Objects (CFO) on Bare vs. Covered Conductors

Conductor-Conductor

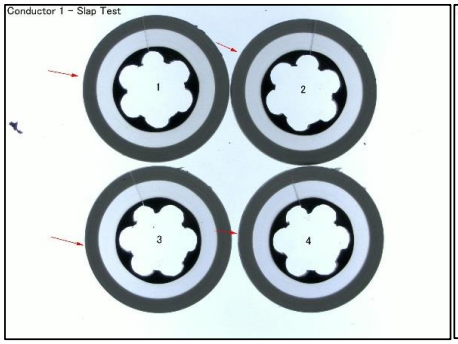

Slapping Conductor – Conductor 1

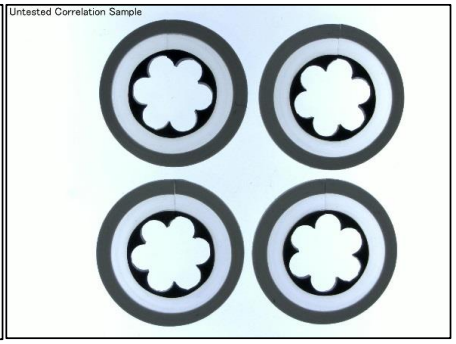

Reference-Non-Tested Sample

Conductor-Conductor -2

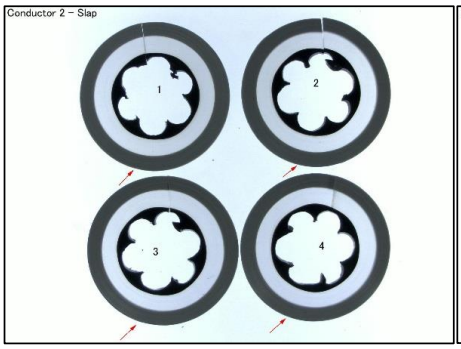

Slapping Conductor – Conductor 2

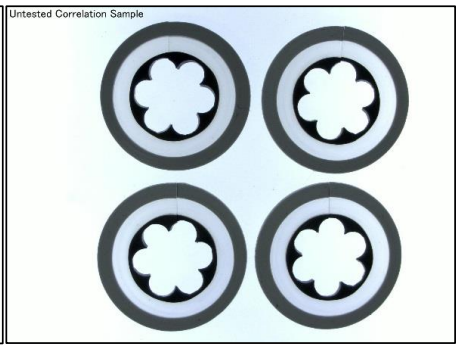

Reference-Non-Tested Sample

Engineering Analysis on the Impacts of Contact from Objects (CFO) on Bare vs. Covered Conductors

11.5 EDEF Circuit Map

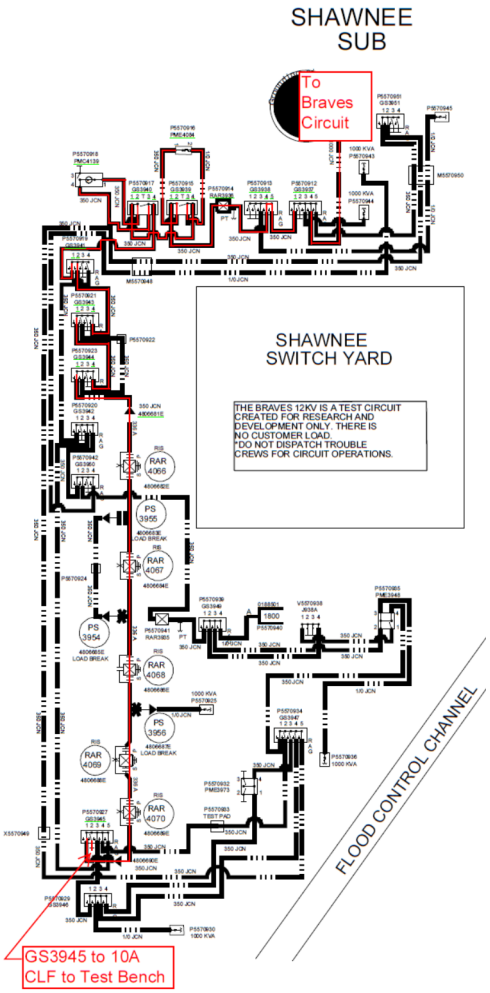

Engineering Analysis on the Impacts of Contact from Objects (CFO) on Bare vs. Covered Conductors

11.6 Infrared Observation of Test Subjects

An infrared observation was performed during the testing of the covered conductor. The purpose of the observation was to visually detect any heat that may occur at the contact point between the conductor and test subject. The camera used was a FLIR Infrared Camera T1030SC with an emistivity set at 0.95. The temperature cross hairs were focused on the contact point between the test subject and the covered conductor. Throughout the tests, no significant heat increase was observed at the contact point between test subject and conductor. The below figure is a descriptive example of the data detailed in the picture.

Description of Details in the Infrared Picture

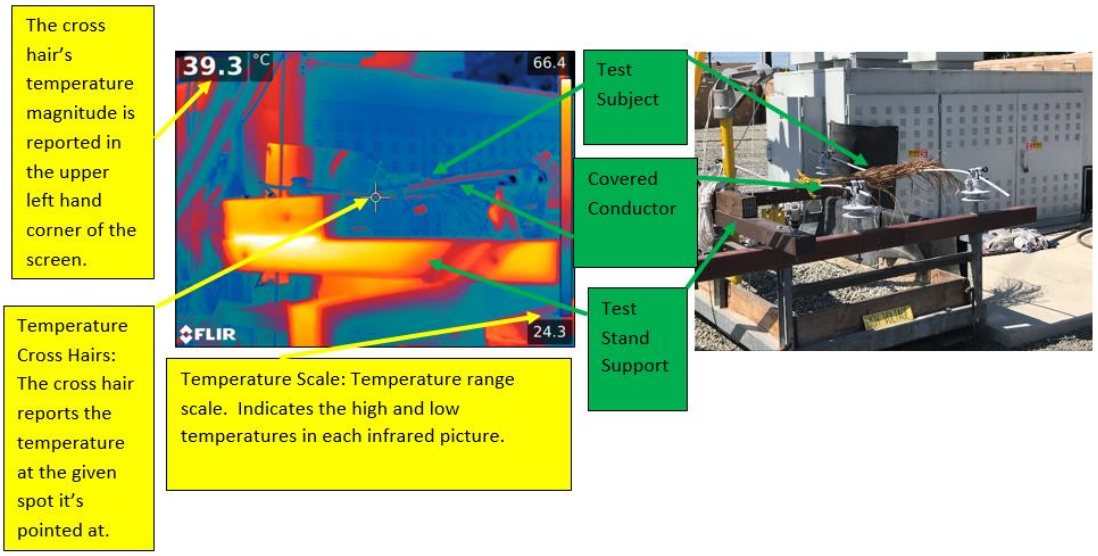

Engineering Analysis on the Impacts of Contact from Objects (CFO) on Bare vs. Covered Conductors

11.6.1 Infrared – Palm Frond on Covered Conductor

Average Reference Temp of Conductor without test subject: 39.3°C

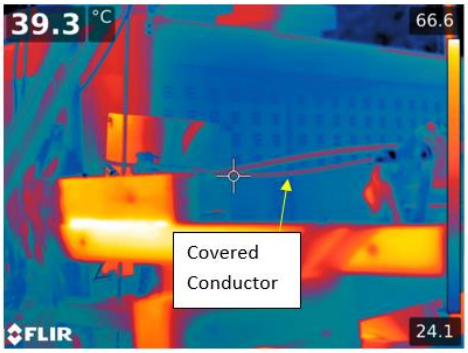

10:07:33 AM De-Energized – Test Subject Temp: 39.3°C

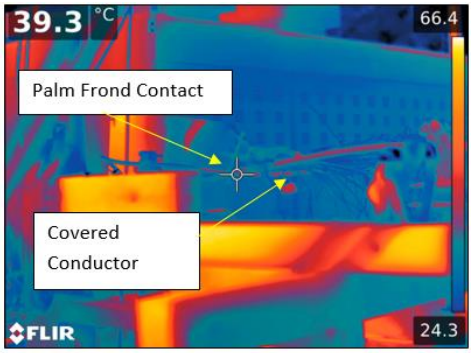

10:09:15 AM Energized – Test Subject Temp: 39.3°C

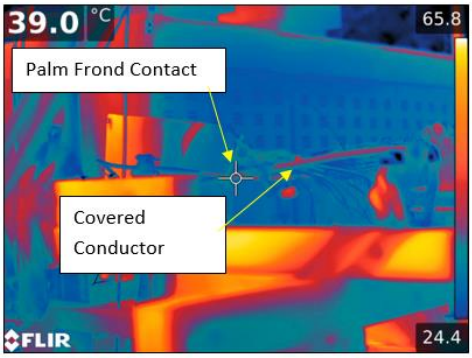

10:12 AM Energized – Test Subject Temp: 39.0°C

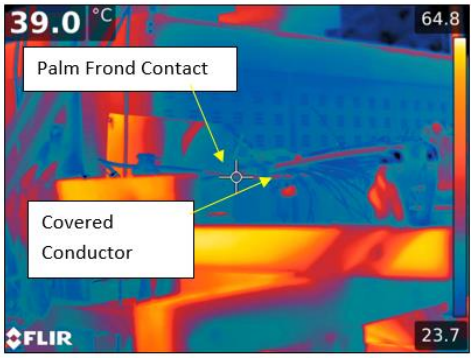

10:14 AM De-Energized –Test Subject Temp: 39.0°C

Engineering Analysis on the Impacts of Contact from Objects (CFO) on Bare vs. Covered Conductors

11.6.2 Infrared – Branch on Covered Conductor

Average Reference Temp of Conductor without test subject: 39.5°C

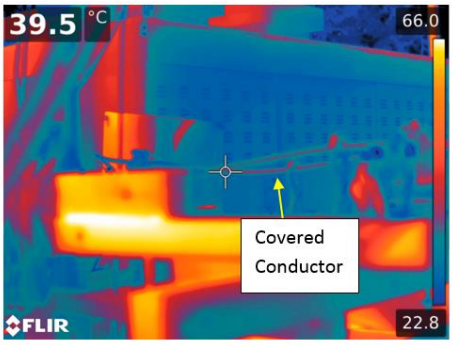

10:25 AM De-Energized – Conductor Temp.: 39.5°C

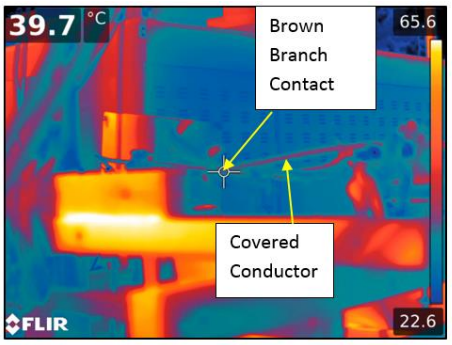

10:28:15 AM Energized – Test Subject Temp.: 39.7°C

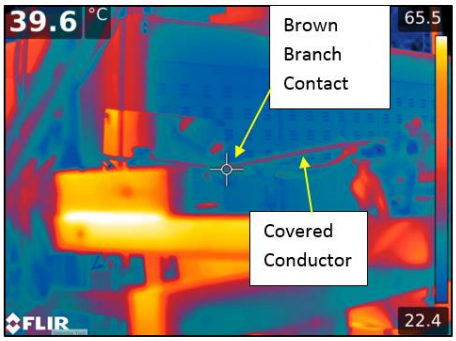

10:30:05 AM Energized – Test Subject Temp.: 39.6°C

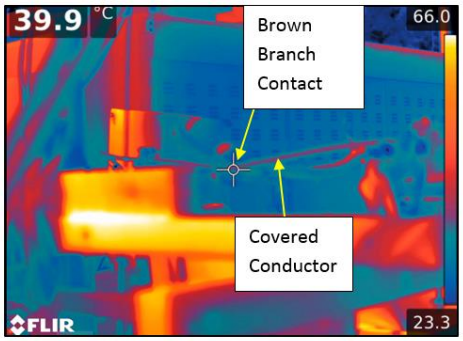

10:31:45 AM Energized – Test Subject Temp.: 39.9°C

Engineering Analysis on the Impacts of Contact from Objects (CFO) on Bare vs. Covered Conductors

11.6.3 Infrared – Green Branch on Covered Conductor

Average Reference Temp of Conductor without test subject: 39.7°C

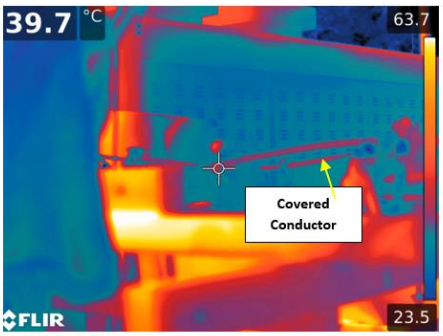

10:31 AM De-Energized – Conductor Temp.: 39.7°C

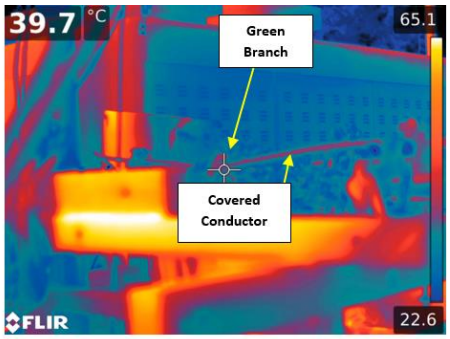

10:37 AM Energized –Test Subject Temp.: 40°C

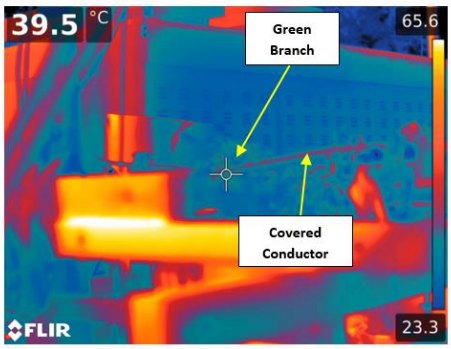

10:39 AM Energized –Test Subject Temp.: 39.5°C

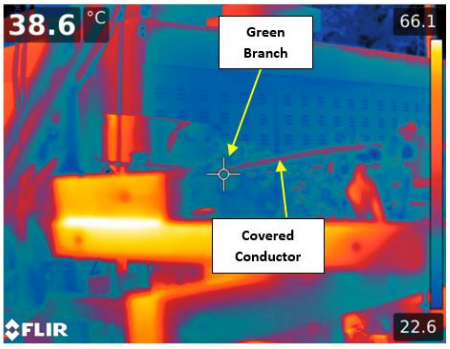

10:43 AM Energized –Test Subject Temp.: 38.6°C

Engineering Analysis on the Impacts of Contact from Objects (CFO) on Bare vs. Covered Conductors

11.6.4 Infrared – 728Ω Resistor Phase-Phase on Covered Conductor

Average Reference Temp of Conductor without test subject: 42.6°C

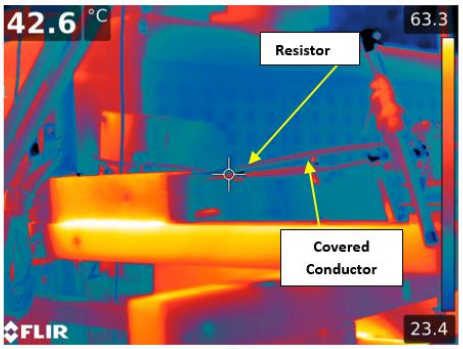

11:13 AM De-Energized –Conductor Temp.: 42.6°C

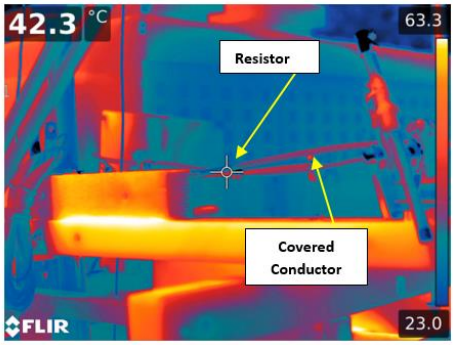

11:14 AM Energized –Test Subject Temp.: 42.3°C

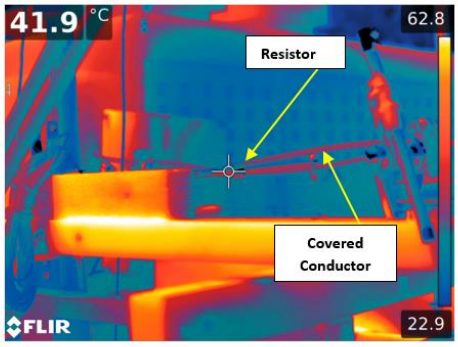

11:15 AM Energized –Test Subject Temp.: 41.9°C

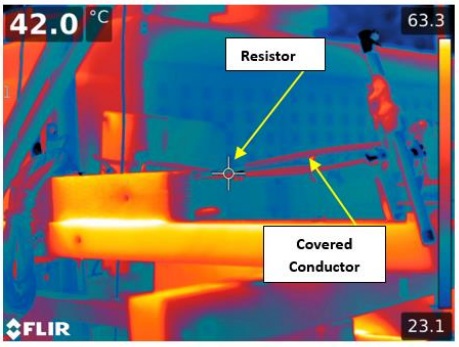

11:18 AM Energized –Test Subject Temp.: 42.0°C

Engineering Analysis on the Impacts of Contact from Objects (CFO) on Bare vs. Covered Conductors

11.6.5 Infrared – Metallic Balloon on Covered Conductor

Average Reference Temp of Conductor without test subject: 37.9°C

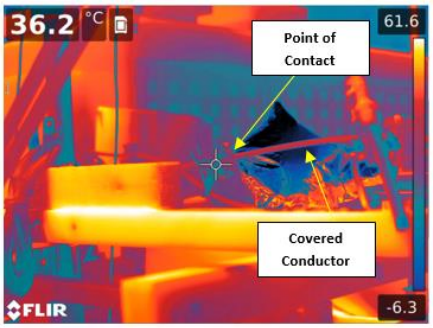

11:24 AM De-Energized –Conductor Temp: 36.2°C

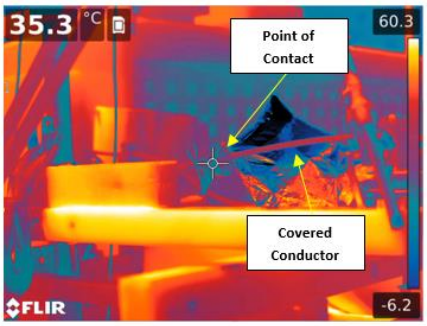

11:25:20 AM Energized –Test Subject Temp: 35.3°C

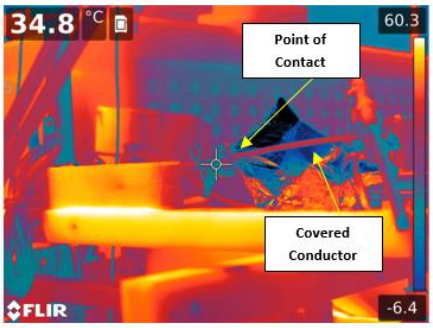

11:26.30 AM Energized –Test Subject Temp: 34.8°C

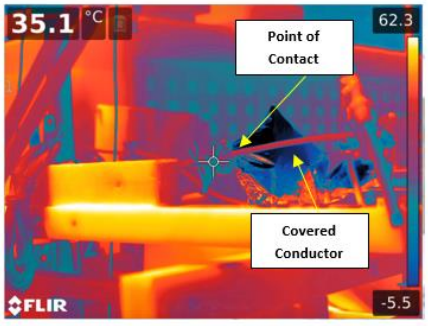

11:29:00 AM Energized –Test Subject Temp: 35.1°C

*Note: The metallic balloon infrared pictures are for visual temperature reference. The temperature cross-hairs were slightly off of the point of contact.

11.7 Simulation Parameters Calculation

11.7.1 Covered Conductor Parameters

11.7.1.1 Insulation Capacitance

The capacitance from the branch to the conductor is approximated as a parallel plate capacitor with the same area as the branch.

$$C = \frac{\varepsilon_0 \varepsilon_r A}{d} \qquad \textbf{Equation 2}$$

Where
C is capacitance [Farads]
ε_0 is the permittivity of free space = 8.85 x 10^{-12} [Farads/meter]
ε_r is the relative permittivity of the material
A is the area of the capacitor [m^2]
d is the separation between the two plates [m]

The radius of a tree branch is assumed to be 4.5 cm for the purpose of this generic analysis. The area of the capacitor is approximated as the cross sectional area of the tree branch.

$$A = \pi r^2$$

$$A = \pi(0.045\ m)^2 = 0.0064\ m^2$$

The distance between the plates is approximated as the thickness of the covered conductor insulation.

d = 150 mil = 0.00381 m

The relative permittivity of the insulation material, $\in_r$, is 4.1.

From the above parameters and Equation 2, the capacitance between the branch and the covered conductor is approximately 60 pico-Farads (pF).

11.7.1.2 XLPE Insulation Resistance Calculation

The resistance across the XLPE insulation was approximated as having the same cross sectional area as the branch and the same thickness as the insulation on the conductor.

$$\mathrm{R} = \frac{\rho \mathrm{l}}{A} \qquad \textbf{Equation 3}$$

Where
l is the length of the object [meters]
A is the cross sectional area of the object [m^2]
ρ is the resistivity of the material [ohm meters]

The length is equal to the insulation thickness.

l = 150 mil = 0.00381 m

Engineering Analysis on the Impacts of Contact from Objects (CFO) on Bare vs. Covered Conductors

The area is equal to the cross sectional area of the branch

$$A_{PSCAD}=0.0078\ m^2$$

$$A_{CDEGS}=0.0064\ m^2$$

The resistivity is equal to the resistivity of the insulation material

$$\rho=10^{12}\ \text{ohm m}$$

From the above parameters and Equation 3, the resistance between the branch and the covered conductor is approximately $5.95x10^{11}$ ohms (Ω).

Since the resistance value of the insulation is much greater than the capacitive reactance value of the insulation, the resistance in parallel with the capacitance can be excluded from the model. Resistive current through the insulation is negligible.

11.7.2 Tree Limb Parameters

The following tree limb parameters were used to model the general case:

1. The length is approximated to 3 feet for PSCAD and 9 feet for CDEGS

$$L_{PSCAD} = 3\ \text{feet} = 0.91\ \text{m}$$

$$L_{CDEGS} = 9\ \text{feet} = 2.74\ \text{m}$$

2. The radius of a tree branch is assumed to be 5 cm for PSCAD and 4.5 cm for CDEGS modeling

3. The resistivity is equal to the resistivity of the wood.

ρ=50 ohm-m (Defandorf, Electrical Resistance to Earth of a Tree, 1956)

The resistance of the tree limb can be calculated based on the above parameters and Equation 4.

$$R = \frac{\rho L}{A} \qquad \textbf{\textit{Equation 4}}$$

Where
L is the length of the object [meters]
A is the cross sectional area of the object [meters^2]
ρ is the resistivity of the material [ohm meters]

From the above parameters and Equation 4, the resistance between the branch and the covered conductor is approximately 5,800 Ω for both PSCAD and CDEGS models.

Engineering Analysis on the Impacts of Contact from Objects (CFO) on Bare vs. Covered Conductors

11.8 Effects of Electrical Current

Table 13: Effects of Electrical Current on the Human Body (National Institute for Occupational Safety and Health, 2009)

Current	Effect
Below 1 mA	Generally not Perceptible
1 mA	Faint Tingle
5 mA	Slight Shock; Not painful but disturbing. Average individual can let go
6-25 mA (women) 9-30 mA (men)	Painful shock, loss of muscular control. The freezing current or "let-go" range. Individual cannot let go, but can be thrown away from the circuit if extensor muscles are stimulated
50-150 mA	Extreme pain, respiratory arrest (breathing stops), severe muscular contractions. Death is possible

11.8 Summary of Results for EDEF

Table 14*: *Summary of Simulated and Empirical Testing Results

Equipment Demonstration Evaluation Facility (EDEF) Test											
						Simulated			Empirical Testing		
Cable Size (AWG)	Test Subject	Moisture Content (%)	Test Subject Resistance @ 5kVDC (MEGOHMS)	Length of Subject (in.)	Diameter of Subject (in.)	CDEGS Tare Current w/out Test Subject (mA)	CDEGS Current with Test Subject (mA)	CDEGS Change in Current with Test Subject (mA)	Tare Current w/out Test Subject (mA)	Current with Test Subject (mA)	Change in Current with Test Subject (mA)
1/ 0	Palm Frond	4.60%	210	45 in.	0.822 in.	0.110	0.115	0.005	0.016	0.017	0.001
1/ 0	Brown Branch	3.60%	4760	49 in.	1.527 in.	0.110	0.116	0.006	0.016	0.015	-0.001
1/ 0	Green Branch	12.20%	1.35	35.5 in.	0.493 in	0.110	0.113	0.003	0.016	0.017	0.001
1/ 0	Animal Contact (728 Ohm Resistor) Ph-Ph	NA	0.000728	36 in.	1 in.	0.110	0.114	0.004	0.016	0.06	0.044
1/ 0	Metallic Balloon	NA	0.000004	NA	18 in.	0.110	0.119	0.009	0.016	0.144	0.128
1/ 0	Conductor-Conductor	NA	NA	102 in.	NA	0.110	0.152	0.042	0.016	0.024	0.008

SCE Covered Conductor Touch Current

NEETRAC Project: 18-025

Test Data

April 23, 2018

Requested by: Mr. Robert Tucker
Southern California Edison

Principal Investigator:
Raymond C. Hill, PE
Lead Engineer – High Voltage Lab

Co-PI & Author:
Anil B. Poda
Research Engineer

Reviewed by:
Raymond C. Hill, PE

NOTICE

The information contained herein is, to our knowledge, accurate and reliable at the date of publication.

Neither GTRC nor The Georgia Institute of Technology nor NEETRAC shall be responsible for any injury to or death of persons or damage to or destruction of property or for any other loss, damage or injury of any kind whatsoever resulting from the use of the project results and/or data.

GTRC, GIT and NEETRAC disclaim any and all warranties, both express and implied, with respect to analysis or research or results contained in this report.

It is the user's responsibility to conduct the necessary assessments in order to satisfy themselves as to the suitability of the products or recommendations for the user's particular purpose.

No statement herein shall be construed as an endorsement of any product, process or provider.

Copyright of this report shall reside with GTRC.

Sponsor(s) are assigned the non transferrable rights listed below:

1. Sponsor has title to the evaluation data contained herein. If there is more than one sponsor, they have joint title to the evaluation data.

2. Sponsor(s) may conduct their own analysis of the data, while representing such analysis as their own.

3. Sponsor(s) may use Copyrighted material in its entirety within their organizations (listed below).

4. Sponsor(s) may provide Copyrighted material in its unabridged entirety without any transfer of rights to external entities for that entity's internal use only as indicated in the NOTE below.

5. Sponsor(s) may place Copyrighted material in its entirety in the public domain (literature packet, internet, etc.) provided that the context of such publication may not be construed as an endorsement of any product, process or provider by GTRC, GIT, or NEETRAC.

Sponsors may not distribute or publish abstracted or excerpted material from this document without the prior written permission of NEETRAC.

For the avoidance of doubt, sponsor(s), in the context of this assignment of rights, shall mean the entities listed below:

Southern California Edison

NOTE: This Copyrighted material is intended solely for the use of the project sponsor(s) in the manner listed above. If you are not an intended recipient you are hereby notified that any dissemination, distribution or copying of this Copyrighted material is prohibited. If you have received this Copyrighted material in error, please immediately notify the provider and permanently delete this Copyrighted material and any copies.

18-025: SCE Covered Conductor Test Cases

1.0 INTRODUCTION

Southern California Edison requested Georgia Tech / NEETRAC ((National Electric Energy Testing, Research & Application Center) to perform laboratory tests and simulation studies on a 12 kV distribution system with overhead insulation covered conductor using WinIGS simulation software.

The study cases performed in this project are described below:

I. Fault Current Analyses

II. SCE System Study Test Cases

III. Laboratory tests on covered conductor and verifying the Laboratory results using WinIGS software

A 20-foot insulated covered conductor sample was provided for testing by Southwire upon SCE's request. The initial measurement (capacitance and reactance) values of the cable were measured at NEETRAC using an LCR meter.

As part of the fault current analyses, a 2 mile long 12 kV distribution system was designed based on the circuit parameters provided by Mr. Robert Tucker of SCE and some assumptions were considered by NEETRAC as shown in Section 5.0. The possible fault currents under different conditions (LL, LLG and SLG) were generated (modeled) at 1 mile from the substation. The results and the measured cable values were reviewed by Mr. Robert Tucker before proceeding with other simulation test cases. The results were comparable with the SCE's system field conditions.

After the fault current analyses, the 12 kV distribution system model was used to simulate several possible field test cases considering bare conductor and insulated covered conductor designs as shown in Section 3.0. In each test case, with a person making bare hand contact, voltage and current were calculated by the software and the test results placed in Table 2.

The insulated covered conductor was tested in the laboratory for two test scenarios as stated in Section 4.0. The laboratory test results were verified using the WinIGS software. The laboratory test results and WinIGS simulated results are placed in Table 3.

Testing and evaluations were performed at the Georgia Tech / NEETRAC Medium Voltage Laboratory in Forest Park, Georgia, USA during the month of April 2018. The preparation and installation of the test setup was performed by NEETRAC personnel.

2.0 SCE SYSTEM FOR FAULT CURRENT ANALYSES

2.1 12 kV System

Phase B conductor is broken in between PWS1 and PWS2 poles.

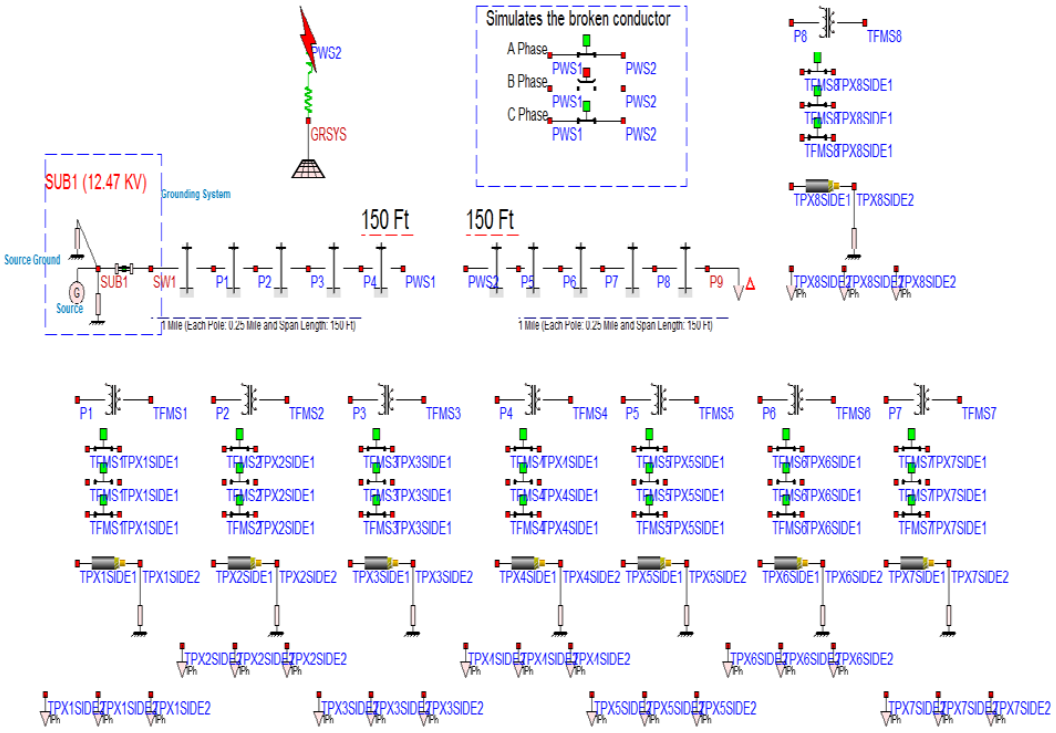

Figure 1: 12 kV System used for Fault Current Analyses

2.2 Fault Currents at 1 Mile from Sub

Table 1: Fault Currents Available at 1 Mile from Substation

Fault Type (W.r.to Phase B)	**LLG**	**LL**	**SLG**
Fault Current – Line Side (PWS1)	4.0854	3.7837	2.7639
Fault Current – Load Side (PWS2)	0.0018	0.0027	0.0105
Sequance Impedance	Positive/Negative	Positive/Negative	Zero

2.3 Zero Sequence - SLG Fault on Line Side: 2.76 KA

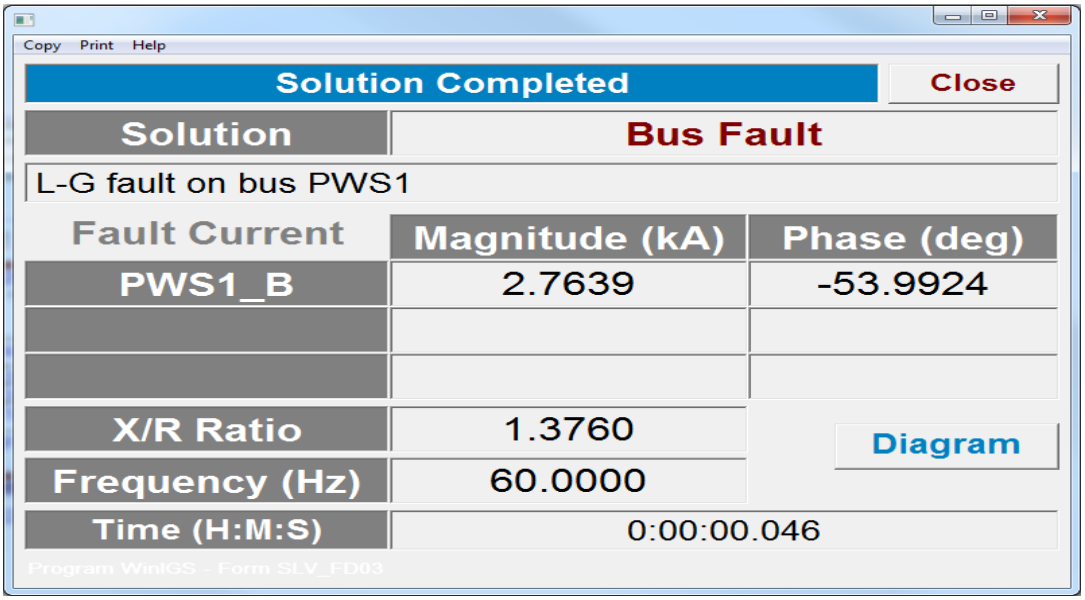

2.4 Zero Sequence - SLG Fault on Load Side: 0.0105 KA

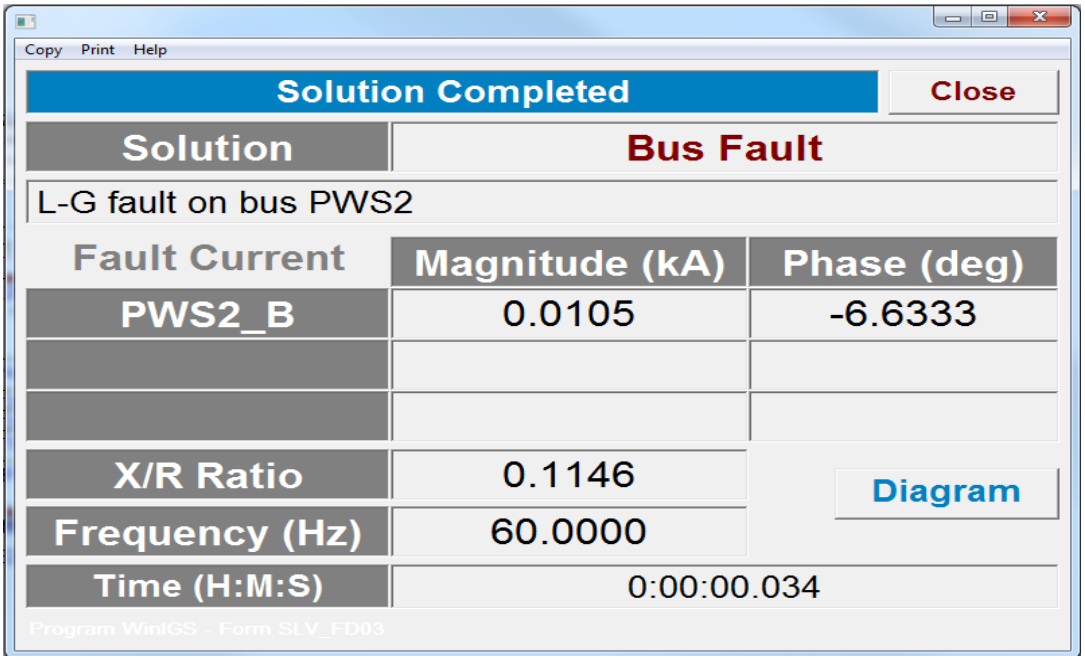

2.5 Positive/Negative Sequence – LL Fault on Line Side: 3.7837 kA

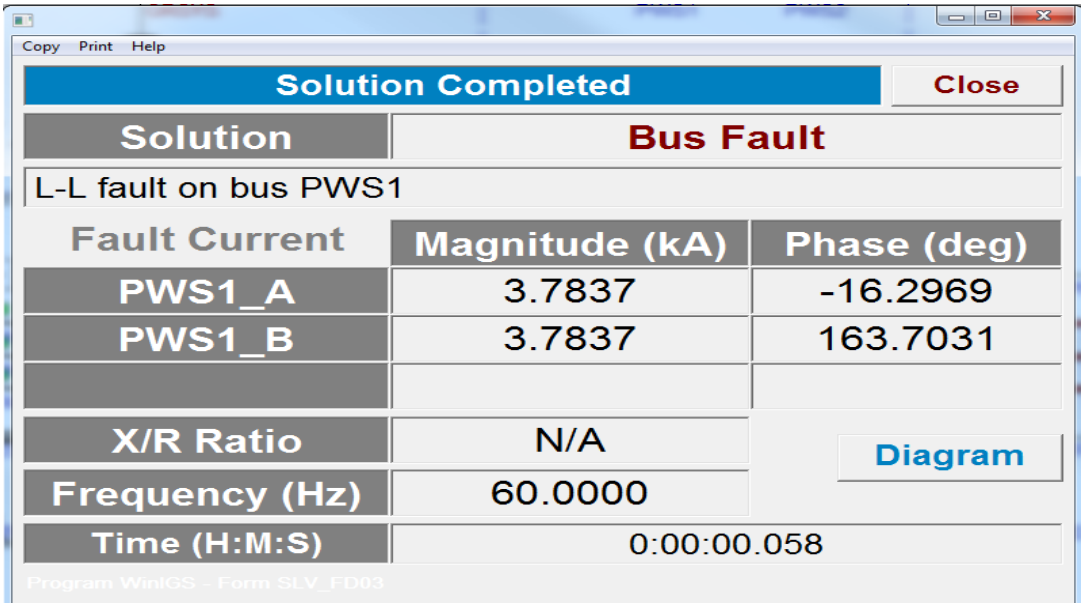

2.6 1.7 Positive/Negative Sequence – LL Fault on Load Side: 0.0027 kA

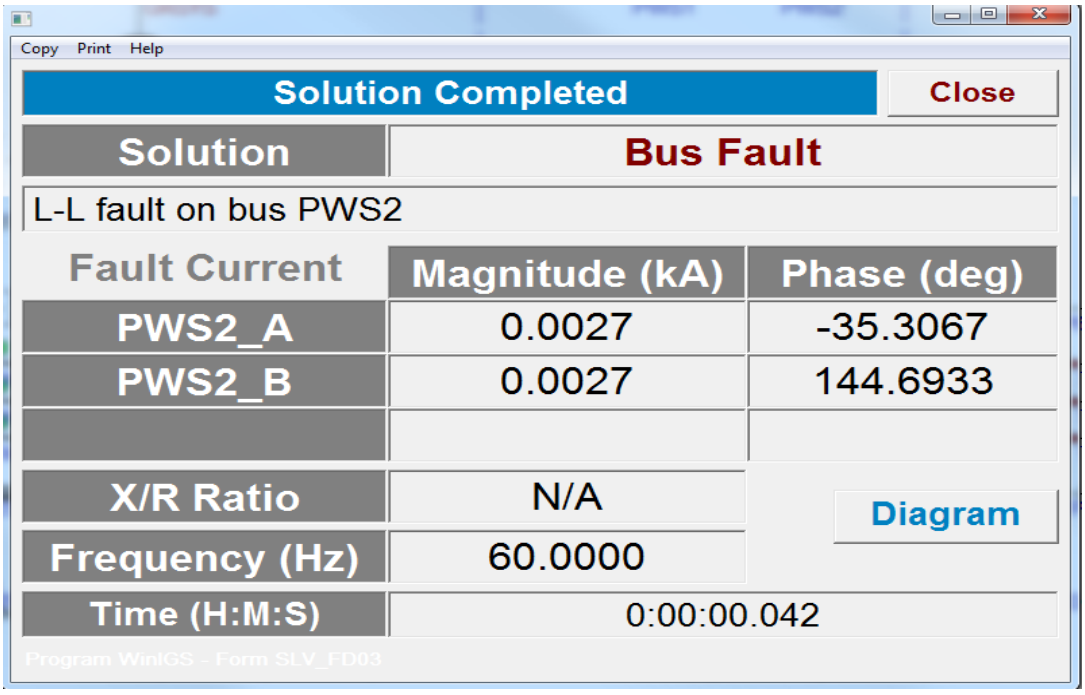

2.7 Positive/Negative Sequence – LLG Fault on Line Side: 4.0854 kA

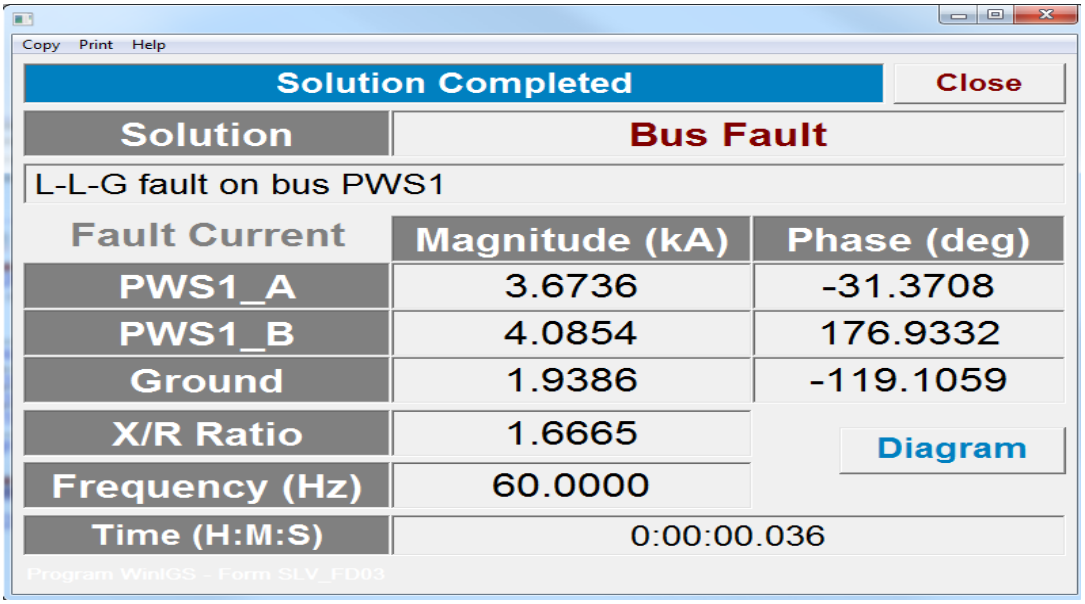

2.8 Positive/Negative Sequence – LLG Fault on Line Side: 0.0018 kA

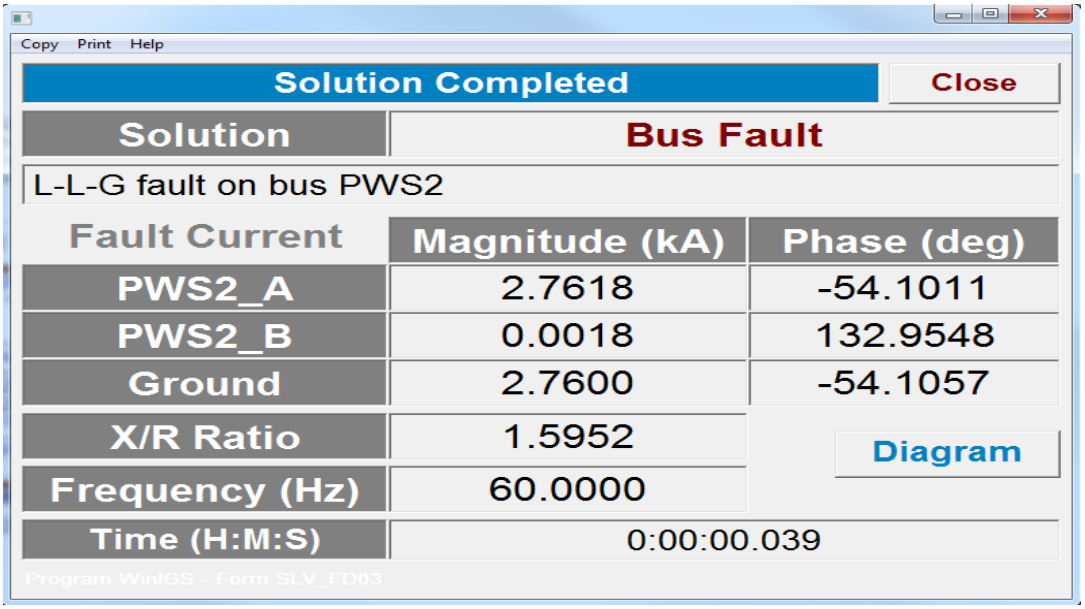

3.0 SCE SYSTEM TEST CASES

Test Case 1: Person holding *continuous bare* conductor under normal operating conditions (Figure 2)

Test Case 2: Person holding *continuous insulated* conductor under normal operating conditions (Figure 2)

Test Case 3: Person holding *broken bare* conductor on line side while the conductor is touching the ground (Figure 3)

Test Case 4: Person holding *broken bare* conductor on line side while the conductor is *not* touching the ground (Figure 4)

Test Case 5: Person holding *broken bare* conductor on load side while the conductor is touching the ground (Figure 5)

Test Case 6: Person holding *broken bare* conductor on load side while the conductor is *not* touching the ground (Figure 6)

Test Case 7: Person holding *broken insulated* conductor on line side while the conductor is touching the ground (Figure 3)

Test Case 8: Person holding *broken insulated* conductor on line side while the conductor is *not* touching the ground (Figure 4)

Test Case 9: Person holding *broken insulated* conductor on load side while the conductor is touching the ground (Figure 5)

Test Case 10: Person holding *broken insulated* conductor on load side while the conductor is *not* touching the ground (Figure 6)

Table 2: SCE System – Public Contact Test Case Results

Test Case (Reference)	Person contact W.r.to conductor Description	Person Contact Phase (1 mile from Sub)	Person Contact Voltage	Person Contact Current	Voltage across the Short Conductor[3] (50 Ohm)	Current Flowing through the Short Conductor[3] (50 Ohm)
Case 1 (Figure 2)	Holding continuous bare conductor	Phase A	7.17 kV	7.17 A	-	-
Case 2 (Figure 2)	Holding continuous covered conductor	Phase A	202.5 mV	202.4 µA	-	-
Case 3 (Figure 3)	Holding broken bare conductor touching ground	Phase B – Line Side	6.99 kV	6.99 A	6.99 kV	139.9 A
Case 4 (Figure 4)	Holding broken bare conductor hanging in air	Phase B – Line Side	7.17 kV	7.17 A	-	-
Case 5 (Figure 5)	Holding broken bare conductor touching ground	Phase B – Load Side	0.37 kV	0.37 A	0.37 kV	7.35 A
Case 6 (Figure 6)	Holding broken bare conductor hanging in air	Phase B – Load Side	3.16 kV	3.36 A	-	-
Case 7A (Figure 3)	Holding broken covered conductor while the insulation touching the ground	Phase B – Line Side	9.67 mV	9.67 µA	9.67 mV	193.5 µA
Case 7B (Figure 3)	Holding broken covered conductor while the conductor touching the ground	Phase B – Line Side	198.1 mV	198.1 µA	7.00 kV	140.1 A
Case 8 (Figure 4)	Holding broken covered conductor hanging in air	Phase B – Line Side	203.2 mV	203.2 µA	-	-
Case 9A (Figure 5)	Holding broken covered conductor while the insulation touching the ground	Phase B – Load Side	7.61 mV	7.61 µA	7.61 mV	152.3 µA
Case 9B (Figure 5)	Holding broken covered conductor while the conductor touching the ground	Phase B – Load Side	10.88 mV	10.88 µA	384.8 V	7.695 A
Case 10 (Figure 6)	Holding broken covered conductor hanging in air	Phase B – Load Side	159.9 mV	159.9 µA	-	-

Note: 1. Capacitance of the covered conductor with two hand contact: 75 pF

2. Calculated reactance value using the measured capacitance = $1/(2\pi fC) = 35.37\ M\Omega$

3. Short Conductor – Small portion of the conductor touching the ground in parallel with the person holding the conductor.

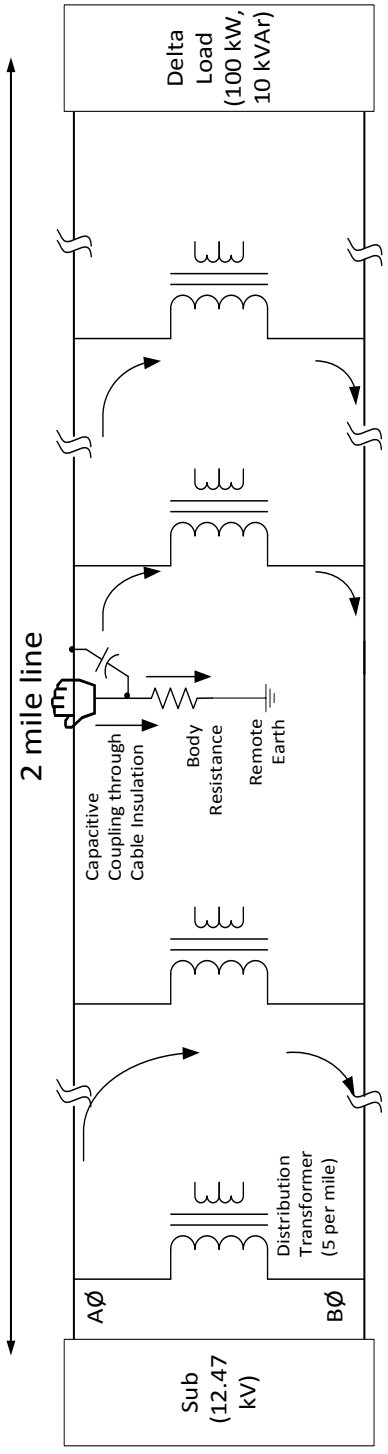

Figure 2: Simulation Scenario for Test Cases 1 & 2

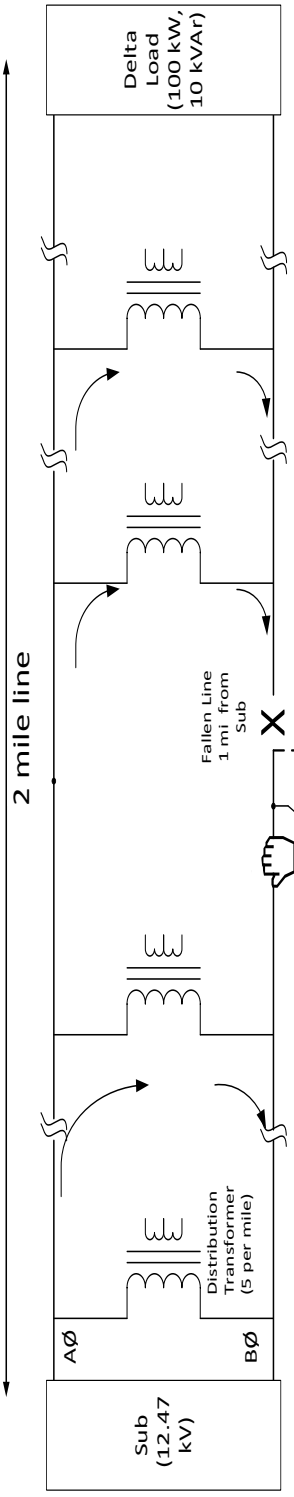

Figure 3: Simulation Scenario for Test Cases 3 & 7

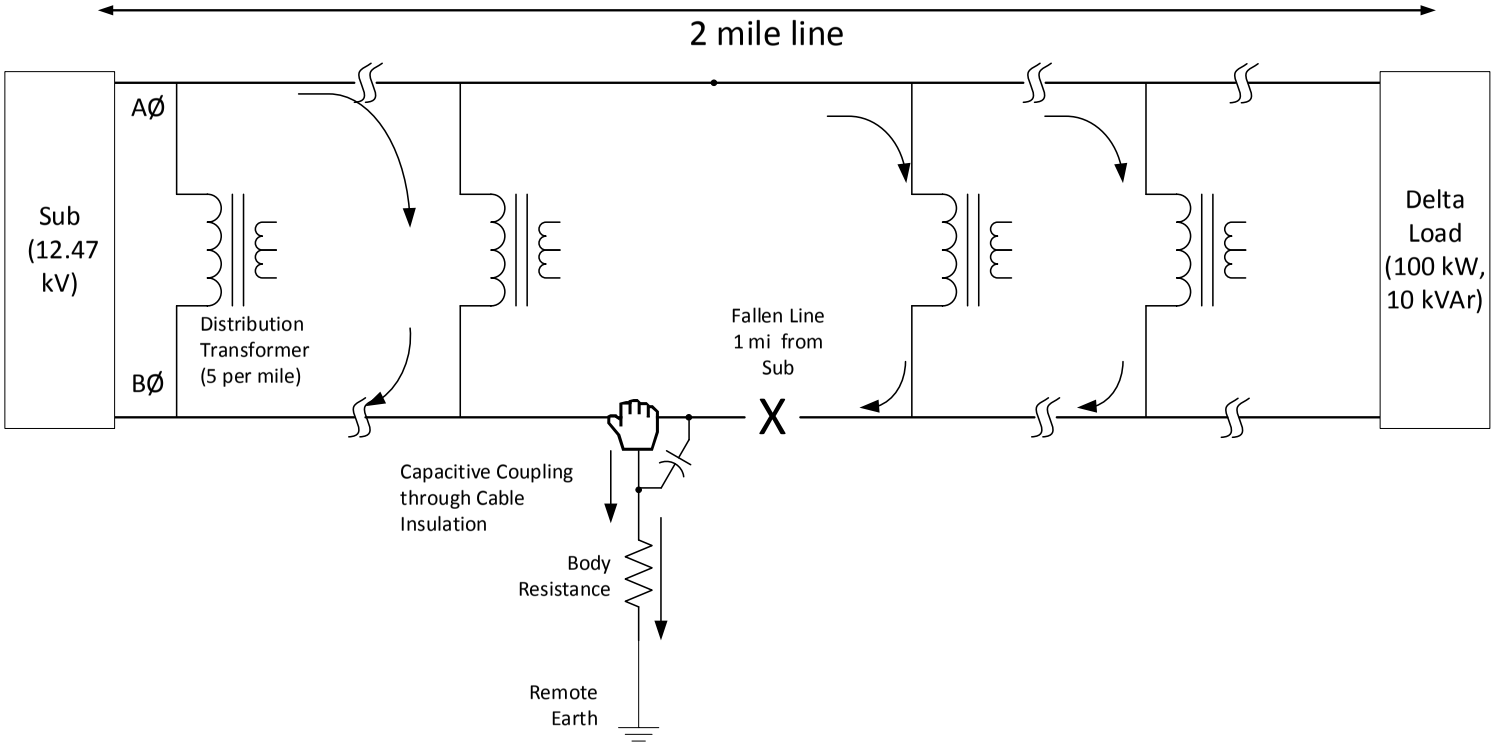

Figure 4: Simulation Scenario for Test Cases 4 & 8

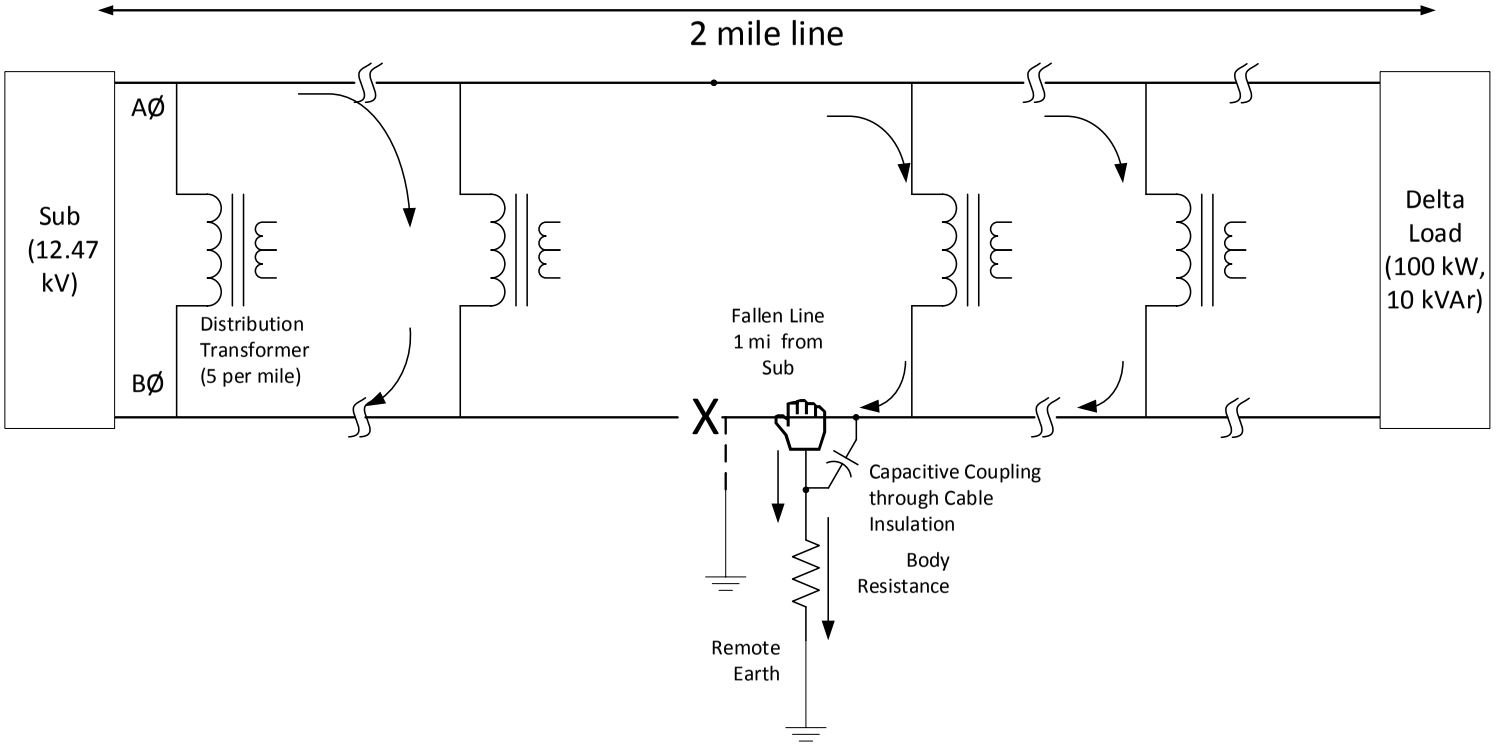

Figure 5: Simulation Scenario for Test Cases 5 & 9

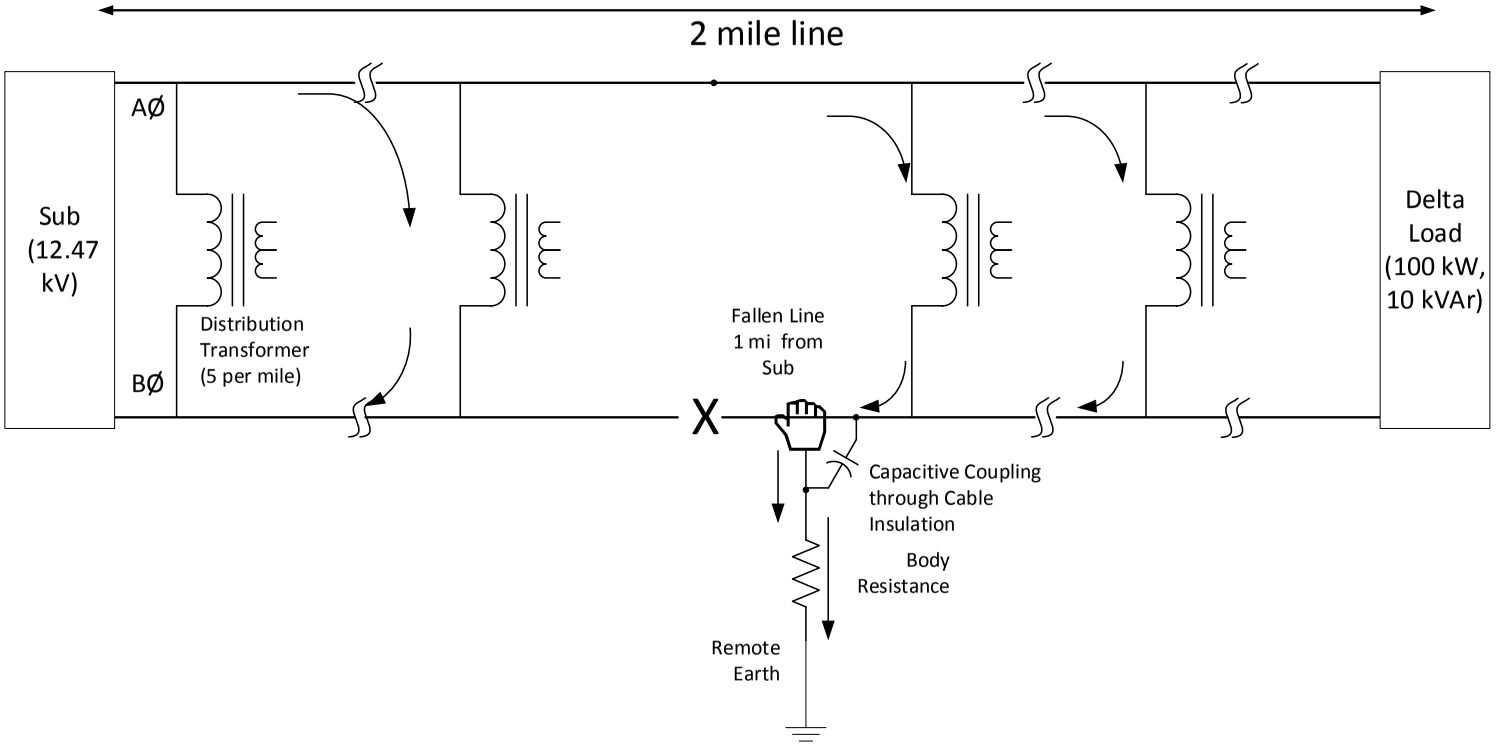

Figure 6: Simulation Scenario for Test Cases 6 & 10

4.0 LABORATORY SYSTEM TEST CASES

The below test cases were simulated in WinIGS software and the results are compared with actual laboratory test results.

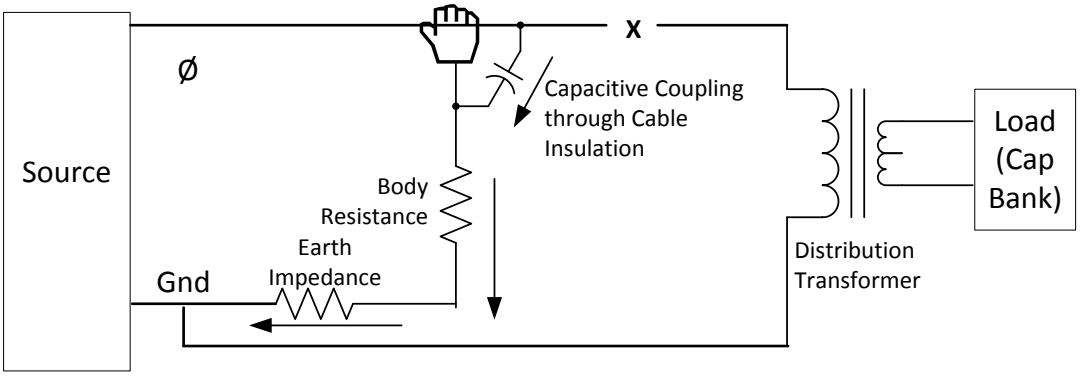

Figure 7: Simulation Scenario for Test Cases 11 & 12

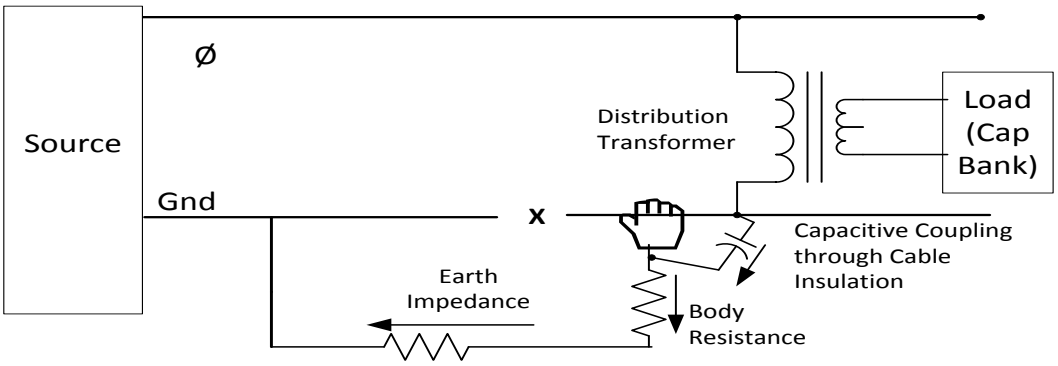

Figure 8: Simulation Scenario for Test Cases 13 & 14

Test Case 11: Person holding *broken bare* conductor on line side (Figure 7)

Test Case 12: Person holding *broken insulated* conductor on line side (Figure 7)

Test Case 13: Person holding *broken bare* ground wire on load side (Figure 8)

Test Case 14: Person holding *broken insulated* ground wire on load side (Figure 8)

*__Note:__ ground wire – return neutral conductor connected between the distribution transformer and source ground in air for the lab test case. In the field (SCE system), this would be another phase conductor since the line leaving the SCE substation is a delta.

Table 3: Person Contact Current measured using Laboratory test Setup

Test Case (Reference)	Person contact W.r.to conductor Description	Person Contact Phase (1 mile from Sub)	Person Contact Current measured in Lab	Person Contact Current measured through WinIGS Simulation Software
Case 11 (Figure 7)	Holding *broken bare* conductor	Line Side	-*	5.3 A
Case 12 (Figure 7)	Holding *broken covered* conductor	Line Side	227 µA	220 µA
Case 13 (Figure 8)	Holding *broken bare* ground wire connected through transformer primary	Load Side	-*	34.2 mA
Case 14 (Figure 8)	Holding *broken covered* ground wire connected through transformer primary	Load Side	227 µA	218 µA

Note: * - Bare conductor test cases were not performed in the Laboratory.

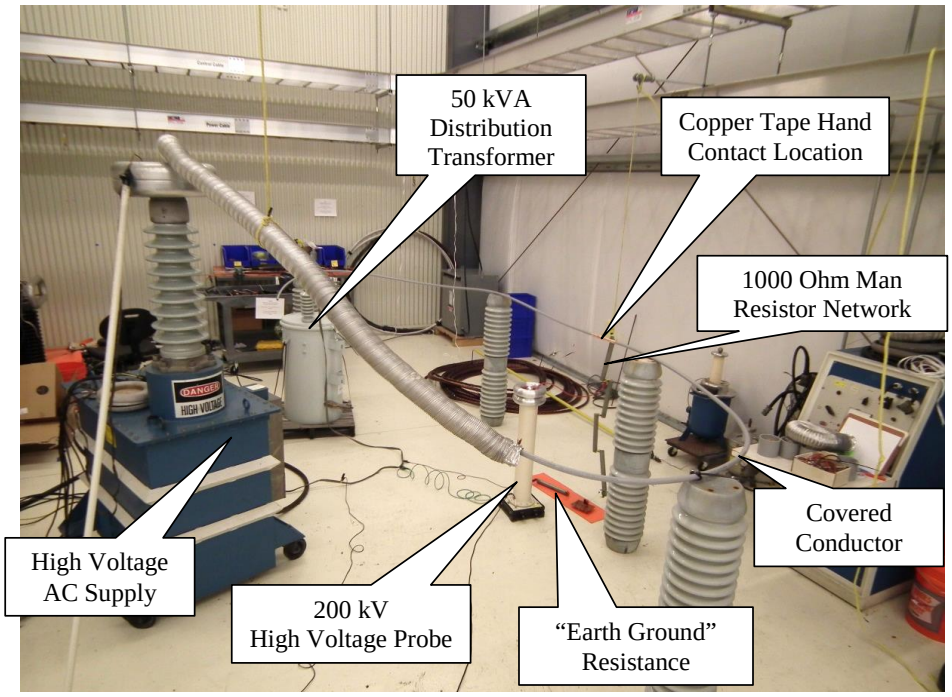

Figure 9: Laboratory Test Setup

5.0 ASSUMPTIONS

For the purpose of computer modeling, the following general assumptions are made. Additional assumptions or changes specific to individual simulations are as noted in the figures and tables.

- The 12.47 kV source substation is represented with positive sequence impedance - R1=0.018 pu & X1=0.311 pu, Negative sequence impedance - R1=0.008 pu & X1=0.221 pu, $R_{ground\ grid}$ = 1 Ω and $Z_{1TL+1feeder}$ = 0.15+j 0.65Ω.
- All of the line configurations and dimensions were used based SCE's suggestion of having a "Horizontal Cross-arm Distribution Pole without Neutral" configuration.
- Phase conductor sizes for the three phase circuit are AWG #1/0 ACSR.
- Approximately five transformers per mile are installed. The secondary side of the transformer is connected to three different housing loads (A-N @ 10 kW,1 kVAR, B-N @ 10kW, 1 kVAR and A-B @ 20 kW, 2 kVAR) through an insulated copper wire.
- Person Body Resistance = 1000 Ω (two hand grip)
- For laboratory test cases, earth impedance = 250 Ω.

6.0 EQUIPMENT

100 kV Biddle Transformer Set	CN-4022
Phenix 200 kV AC/DC KVM Probe	CQ-2251
Hewlett Packard LCR Meter	CQ-2195
Fluke Multi-meter	CQ-6806

SCE Summary of NEETRAC Test Report for Covered Conductor Touch Current – Support for Section (IV)(B)(1)(e)

This document summarizes the results of the Covered Conductor Touch Current NEETRAC Report.

Prepared by Southern California Edison, Apparatus and Standards Engineering

I. Introduction

This document was prepared by SCE to summarize a SCE commissioned test performed by the National Electric Energy Testing, Research and Applications Center (NEETRAC) on covered conductor touch current to validate that covered conductor reduces charging current. This summary supports representations made within Section (IV)(B)(1)(e) regarding human contact with covered conductors. In particular, the insulating cover on covered conductor reduces the charging current enough to be generally not perceptible during human contact with the cover of energized covered conductor; contact with energized bare conductor wire can result in electrocution.[1]

II. Effects of Electrical Current on the Human Body

The charging current test results can be compared to generally accepted benchmarks on the effects of human contact with different current levels:

Table 1: Effects of Electrical Current (Center for Disease Control, 2009)

Current	Effect
Below 1 mA	Generally not Perceptible
1 mA	Faint Tingle
5 mA	Slight Shock; Not painful but disturbing. Average individual can let go
6-25 mA (women) **9-30 mA (men)**	Painful shock, loss of muscular control. The freezing current or "let-go" range. Individual cannot let go, but can be thrown away from the circuit if extensor muscles are stimulated
50-150 mA	Extreme pain, respiratory arrest (breathing stops), severe muscular contractions. Death is possible

III. Covered Conductor vs. Bare Conductor Touch Currents

A. Test Cases

The following are covered conductor test cases that were simulated and laboratory tested by NEETRAC:

- Person holding broken covered conductor on **line side**[2]
- Person holding broken covered conductor on **load side**[3]

[1] See Table 2: NEETRAC Results
[2] Test Case 12 on NEETRAC Report
[3] Test Case 14 on NEETRAC Report

The following are bare conductor test cases that were simulated by NEETRAC:

- Person holding broken bare conductor on **line side**[4]
- Person holding broken bare conductor on **load side**[5]

Note that bare conductor test cases were not performed in the laboratory.

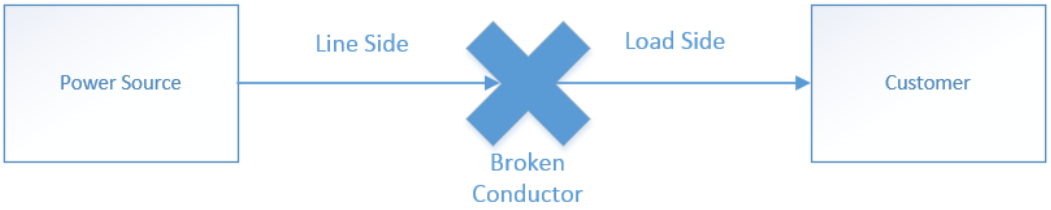

Figure 1: Line side and Load side Diagram

B. Test Results

Test Information:

- Conductor: 1/0 Covered Conductor
- Source: 12.447 kV
- Test Results: Human contact current measured

Table 2: NEETRAC Test Results (See NEETRAC Report, page 15)

	Covered Conductor		Bare Conductor
	Simulation Results (Theoretical Value)	Lab Test Results (Actual Values)	Simulation Results (Theoretical Value)
Line Side	0.220 mA	0.227 mA	5,300 mA
Load Side	0.218 mA	0.227 mA	34.2 mA

Table 2 summarizes the results for test cases 11 through 14 in the NEETRAC report. The small difference between the simulation and laboratory test values demonstrate the accuracy of the simulation. Although the bare conductor test cases were not laboratory tested, the results of the simulation are comparable to real-world values.

For additional details, refer to the appended NEETRAC Report. Note that covered conductor current values in the report are provided in microamps (µA). To convert microamps to milliamps (mA), the values must be multiplied by 0.001. Additionally, bare conductor current values may be denoted in Amps (A). To convert Amps to milliamps, the values must be multiplied by 1000.

[4] Test Case 11 on NEETRAC Report
[5] Test Case 13 on NEETRAC Report

IV. Summary

The data show that charging currents on covered conductors are below 1 mA as represented within Section (IV)(B)(1)(e) at page 58. Human contact with this current is generally not perceptible whereas human contact with the charging current of bare wire can result in electrocution.

V. References

Center for Disease Control. (2009). Electrical Safety, Safety and Health for Electrical Trades Student Manual. Retrieved from CDC: https://www.cdc.gov/niosh/docs/2009-113/pdfs/2009-113.pdf

NEETRAC. (2018). SCE Covered Conductor Touch Current. Georgia Tech Research Corporation.

Circuit Deployment Prioritization
Section (IV)(B)(e)(1)

Introduction

As discussed in Section (IV)(B)(e)(1), SCE developed a deployment prioritization methodology for its Wildfire Covered Conductor Program (WCCP) to guide the deployment of covered conductor in place of existing bare distribution primary conductor in high fire risk areas (HFRA). This methodology prioritizes deploying covered conductor on circuits posing the greatest wildfire risk, focusing on ignition consequence and ignition frequency. This methodology also took into consideration the mitigation effectiveness of covered conductor as deployed in specific areas of high fire risk. Within each factor category, individual attributes were selected and subsequently assigned a weighting, as shown below.

Category	Total Category Weighting	Attribute	Individual Attribute Weighting
Ignition Consequence Factors	50%	Circuit Length in Tier 3	25%
		Circuit Length in Tier 2	15%
		Circuit Length in High Wind within HFRA	10%
Ignition Frequency Factors	30%	Historic Vegetation Faults in HFRA	15%
		Historic Wire Down Events	10%
		Circuit Length of Vintage Small Conductor	5%
Mitigation Effectiveness Factor	20%	Estimated number of mitigated faults in proportion to circuit length in HFRA	20%

Development of Methodology

SCE conducted a comprehensive process to determine how best to prioritize covered conductor deployment within the HFRA. SCE initially considered deploying covered conductor on any circuit located in CPUC Tier 3 HFRA. This approach was rejected, however, in favor of a more nuanced analysis that took into account other contributing factors to wildfire risk in order to provide for a more effective and efficient deployment strategy.

Given the variety of circumstances that could lead to a fire, SCE considered how best to leverage additional datasets to develop a more sophisticated approach to its prioritization methodology. For this effort, SCE formed a cross-function team to assess attributes best representing the potential for wildfire risk. These internal stakeholders included representatives from SCE's Transmission and Distribution Engineering, Business Resiliency and Risk Management organizations. Three general categories were determined to best inform SCE's prioritization methodology: ignition consequence, ignition frequency and mitigation effectiveness.

In order to determine the relative value between each category, SCE used a comparative approach. When considering ignition consequence and ignition frequency, SCE recognized that not all ignitions result in catastrophic wildfires. Therefore, placing greater priority on high consequence areas of our system would likely address greater risk. As such, the ignition consequence attributes, in aggregate, were given greater value than ignition frequency attributes.

Similarly, in determining the relative value of mitigation effectiveness compared to the other two general categories, SCE recognized that this factor—while valuable—would place greater emphasis on deploying covered conductor in areas where it is likely to be most effective and efficient, as opposed to areas where there is the greatest fire risk. SCE therefore gave this category a lower value than the other two, in order to maintain appropriate emphasis on deploying covered conductor in high fire risk areas and recognizing that covered conductor provides overall substantial benefits for mitigating fire risk, as discussed in testimony.

Ultimately, an aggregate 50% weighting was assigned to ignition consequence, an aggregate 30% weighting was assigned to ignition frequency, and an aggregate 20% weighting was assigned to mitigation effectiveness.

Ignition Consequence Factors

In sum, the ignition consequence factors account for 50% of the total prioritization weighting. As noted in the table above, this category has three attributes. In determining how to divide this 50% among the three attributes, SCE relied on subject matter input to best inform the weightings of the individual attributes, with validating analyses to further confirm the relative weightings where possible.

Circuit length in Tier 2 and Tier 3: SCE has approximately 4,500 distribution circuits in its service area. Approximately 1,300 of these circuits have at least some portion located within HFRA, which includes CPUC Tier 2 and Tier 3 areas.[1] In prioritizing these circuits for the WCCP, SCE placed a weight of 25% to the circuit length in a Tier 3 area and a weight of 15% to the circuit length in a Tier 2 area to reflect the greater risk associated with Tier 3 areas relative to Tier 2. This means that circuits with the longest length in Tier 3 are generally given priority over circuits of comparable length in Tier 2. Under certain circumstances, however, circuits with considerable length in Tier 2 could be prioritized over circuits with a short length in Tier 3.

In order to further validate these relative weightings, SCE reviewed the 2015-2017 fire history as reported to the CPUC. A majority of fires at distribution voltages up to 33kV were determined to occur within the Tier 3 area, providing further justification for Tier 3 receiving a greater weighting than Tier 2.

Wind Load Considerations in HFRA: Wind plays an important role in many contact-related faults, including contact with tree limbs and palm fronds. In addition, high wind speeds are a known contributor to larger fires. SCE understands that wind loading is considered as part of the CPUC's Tier 2 and Tier 3 designations; however, SCE decided to undertake an additional review of wind conditions on its system to further inform its deployment of covered conductor. For this effort, SCE utilized GIS data mapping and existing data from its Pole Loading program to map the estimated wind load on the portions of its circuits in HFRA and has also used this data in prioritizing circuits for WCCP.

[1] As explained in SCE's supporting testimony, HFRA refers to areas designated as Tier 2 or Tier 3 in recent CPUC mapping proceedings or SCE HFRA not in CPUC Tiers.

This factor (wind load) was assigned a weight of 10% as part of SCE's WCCP circuit prioritization methodology. This means that circuits with greater exposure to high wind conditions within the HFRA are generally given priority over circuits with minimal high wind exposure. Because wind loading is also taken into account as part of the CPUC's Tier 2 and Tier 3 designations, SCE assigned this factor a lower relative value, comparatively, within this category of attributes.

Ignition Frequency Factors

In sum, the ignition frequency factors account for 30% of the total prioritization weighting. As noted in the table above, this category has three attributes. In determining how to divide this 30% among the three attributes, SCE relied on subject matter input to best inform the weightings of the individual attributes, with validating analyses to further confirm the relative weightings where possible.

Number of historic vegetation faults in HFRA: Vegetation is a known contributor to ignition events associated with SCE distribution equipment. During the 2015 to 2017 time period, approximately 8% of annual faults associated with HFRA circuits were related to vegetation, yet these faults were associated with approximately 17% of the annual fire events within the HFRA.[2] Since vegetation-related faults pose a heightened fire risk as compared to other fault types and covered conductor is an effective mitigation tool for vegetation driven faults, this attribute was assigned a weight of 15% as part SCE's WCCP circuit prioritization methodology. This means that circuits with a history of vegetation faults within the HFRA are generally given priority over circuits with other historical fault types.

Furthermore, from 2015 to 2017, vegetation represented the leading cause of ignitions associated with SCE distribution equipment within HFRA.[3] This provides further justification for this attribute receiving the highest individual attribute weighting within this category.

Number of historic wire down events: Wire down events in HFRA also pose an ignition frequency risk. Therefore, circuits with a history of wire down events are likely to indicate an area of outsized ignition risk. This attribute was assigned a weight of 10% as part SCE's WCCP circuit prioritization methodology. This means that circuits with a history of wire down events are generally given priority over circuits without a history of wire down events.

Similar to the above, from 2015 to 2017, conductor-related fires represented one of the leading cause of ignitions associated with SCE distribution equipment within the HFRA.[4] Historical wire down events are considered to be a proxy for conductor-related ignitions. This provides further justification for this attribute being included, albeit at a lower attribute weighting compared to vegetation.

[2] This analysis is described in detail within the Mitigation Effectiveness Comparison Workpaper. It refers only to ignition events recorded at voltage levels up to 33kV.
[3] This analysis refers only to those ignition events recorded at voltage levels up to 33kV.
[4] This analysis refers only to those ignition events recorded at voltage levels up to 33kV.

Circuit length of vintage small conductor: Vintage small conductor could be subject to damage under fault conditions and is at risk of a wire down event and posing an ignition risk. In addition, smaller conductor is likely to be older than other parts of our system, and potentially exposed to corrosive conditions and degradation for a longer period. Under normal operating conditions, however, vintage small conductor is considered to be of limited risk of leading to an ignition event. Consequently, this attribute was assigned a weight of 5% as part of SCE's WCCP circuit prioritization methodology. This means that circuits with longer lengths of vintage small conductor are generally given priority over circuits with less vintage small conductor.

Mitigation Effectiveness Factor

Mitigation effectiveness accounts for 20% of the total prioritization weighting. SCE relied on subject matter input to determine this weighting value, and whether additional attributes were necessary. No other attributes were determined to further assist in determining which areas covered conductor would provide the greatest benefits when deployed.

Estimated number of faults mitigated in proportion to circuit length in HFRA: In conjunction with the analysis of the 2015-2017 fault history in ODRM, SCE utilized the data on each circuit's fault history to estimate the relative mitigation effectiveness of installing covered conductor. More specifically, a comparative value was calculated by dividing the number of historical faults within the HFRA potentially mitigated by covered conductor by the circuit's length within the HFRA. This factor was assigned a weight of 20% as part of SCE's WCCP circuit prioritization methodology. This weighting, all else equal, prioritizes circuits with a greater recorded rate of potentially mitigated faults per circuit length, compared to circuits with faults not expected to be addressed by covered conductor.

Results and Review

This methodology resulted in a prioritized listing of approximately 1,300 HFRA circuits with overhead conductor exposure. Circuits intended to be remediated within the 2018-2020 time period generally have greater Tier 3 and Tier 2 exposure, indicators of potential concerns with overall asset health, such as the historical number of wire down events, and a history of faults that are likely to be mitigated by covered conductor.

The final prioritized results also underwent a review by stakeholders to ensure the areas selected for initial deployment of covered conductor were indicative of areas of highest risk. In particular, the reviews focused on ensuring areas historically affected by wildfires were highly prioritized relative to other areas, and yet recognizing that future wildfires may not occur in the same areas as the past.

Workpaper for Pole Replacement Rates

Supporting Section (IV)(B)(1)(e)(2)(a)

Objective

The purpose of this work paper is to estimate pole replacement rates as discussed within Section (IV)(B)(1)(e)(2)(a) resulting from deployment of covered conductor for the Wildfire Covered Conductor Program (WCCP).

Software Used for Analysis
SPIDACalc version 6.3

Source Data for Analysis
Two sets of random pole samples were used for the analysis:

1. Pole Sample Set 1 – 605 random pole selection pulled from the existing 6,122 system sample set utilized for SPIDA software validation. The 6,122 system sample set contains 1,783 HFRA poles in high fire risk areas (HFRA), the 605 are a random selection of HFRA poles filtered for small and large wire only poles. For this study, small wire is generally considered conductor smaller than 1/0 ACSR and large wire to be 1/0 ACSR and larger. Service poles and communication only poles have been filtered from this analysis as they would not be candidate for the WCCP. This data set will be used to represent poles within HFRA that have not been replaced in recent years via other existing programs.

2. Pole Sample Set 2 – 241 random pole selection pulled from pole loading database of poles that have been recently replaced in HFRAs (within the past 4 years). This data set will be used to represent poles within HFRA that have been replaced in recent years.

Assumptions and Limitations

Assumptions

Recognizing that it is not possible to analyze every possible combination of pole, conductor, and loading condition, SCE used its existing pole database for SPIDA software validation. This sample set consists of a random sampling of poles within the SCE service territory and is representative of the SCE system overhead in general. The following is a list of underlying assumptions associated to the analysis performed:

- Sample sets adequately represent HFRAs
- Wind load distribution for sample set is representative of HFRAs for Heavy Loading and High Wind Conditions

- Existing Spida models are accurate
- Any conductor smaller than 1/0 ACSR, will be replaced with either 1/0 ACSR bare or covered (most likely case)
- For dual loading conditions (i.e. 6 lb and 12 lb or 6 lb and 18 lb), only higher loading condition will be considered
- Any new equipment (e.g. fuses) being installed do not require loading analysis; not required for equipment so long as load increase to pole is not greater than 5% (Reference G.O. 95 Rule 44.2)
- No conductor changes to secondary, service, or communication poles

Limitations

- This analysis was limited to direct mechanical loading impacts resulting from installing covered conductor on existing poles. There may be circumstances where site specific field conditions may warrant additional pole replacements. The following are most likely additional circumstances where pole replacement may be warranted:
- Electrical clearance issues – existing clearance issues or due to increase in sag of covered conductor
- Guy poles that support dead-end or line angle poles, where additional loading resulting from covered conductor exceeds the guy pole capacity
- Miscellaneous relocations associated with resolving potential conflicts due to proximity to structures or traffic

Existing electrical clearance issues would be resolved as a result of existing programmatic work. Potential electrical clearance issues relating to the increase in sag of covered conductor is anticipated to be minimal considering the sag difference between bare wire 1/0 ACSR on typical spans of 140-ft and 200-ft are 0.41 ft. and 0.78 ft. respectively. Replacement may be warranted on heavily congested poles that are tight on attachment spacing, however these poles would likely require replacement due to loading issues as well. Similarly, dead-end or line angle poles would likely require replacement due to loading requirements. Increasing the size of these poles could mitigate the need to replace the guy pole, but there may be limited circumstances where that would not be possible.

Method of Analysis

Pole loading analysis was performed on the two sample sets using SPIDACalc version 6.3. Sample Set 1 was checked for overload conditions in the "as-is" state with existing bare wire[1], a "to be" state with 1/0 ACSR bare wire, and a "to be" state with 1/0 ACSR covered conductor. If

[1] Existing bare wire may consist of #8 copper, #6 copper, #4 copper, #2 copper, 2/0 copper, 4/0 copper, #8 ACSR, #6 ACSR, #4 ACSR, #2 ACSR, 1/0 ACSR, 336 ACSR, or 653 ACSR conductor.

existing conductor was larger than 1/0 ASCR an equivalent size covered conductor was checked for in the "to be" state. Sample Set 2 was checked for overload conditions in the as-is state (already sized for a minimum wire size of 1/0 ACSR bare), and a "to be" state of 1/0 ACSR covered conductor. If existing as-is wire was larger than 1/0 ACSR, an equivalent larger size covered conductor was utilized.

Pole sample sets are statistically valid with a 95% confidence and reasonable margin of error. The margin of error calculated for Sample Set 1 is ±3.4% and the margin of error calculated for Sample Set 2 is -1.24% and +1.40% (bound by 0% on the low end).

Results of Analysis

Results of Sample Set 1 (poles that have not been replaced in recent years) are summarized in the table below. They indicate that 9.59% of SCE's poles located in HFRAs are overloaded in their existing condition and would require replacement to meet current safety factor requirements (column F). When wire smaller than 1/0 ACSR is replaced with 1/0 ACSR, the pole replacement rate increases to 13.06% (column H). When wires are changed to covered conductor, the pole replacement rate increases to 23.80% (column J). The anticipated increase in pole replacements when changing from SCE's current standard of 1/0 ACSR bare wire to 1/0 ACSR covered conductor would be 10.74%, the difference between column J and column H. 10.74% was used in calculating the unit cost for covered conductor.[2]

Sample Set 1 Summary Table – Poles that have not been replaced within the past 4 years.

	B	C	D	E	F	G	H
2	**Load Case**	**# of Poles in Analysis**	**% of Poles (C / C8)**	**# of Overloaded Poles As Is**	**% of As Is Overloaded Poles (F / C8)**	**# of Poles Overloaded Changing Conductor to 1/0 ACSR Bare**	**% of Poles Overloaded Changing Conductor to 1/0 ACSR Bare (H / C8)**
3	Light, 8 lb	107	17.69%	2	0.33%	8	1.32%
4	Heavy, 6 lb	208	34.38%	32	5.29%	36	5.95%
5	12 lb	212	35.04%	10	1.65%	15	2.48%
6	18 lb	74	12.23%	13	2.15%	19	3.14%
7	24 lb	4	0.66%	1	0.17%	1	0.17%
8	Total Poles	605	100.00%	58	**9.59%**	79	**13.06%**

[2] The total estimated pole replacement rate used to calculate the covered conductor unit cost is 33.24% (See work paper "Unit Cost – Covered Conductor"). This was derived by using the observed pole replacement rates of 34 circuits miles replaced with bare conductor under the Overhead Conductor Program (OCP) in 2017. These OCP projects had an observed pole replacement rate of 22.50%, 10.74% was added to the observed rate to equal 33.24%. It is important to use the observed rate as a baseline to account for limitations of the pole replacement study summarized in this document.

	B	I	J
2	**Load Case**	**# of Poles Overloaded Changing Conductor to CC**	**% of Poles Overloaded Changing Conductor to CC (J / C8)**
3	Light, 8 lb	17	2.81%
4	Heavy, 6 lb	53	8.76%
5	12 lb	38	6.28%
6	18 lb	32	5.29%
7	24 lb	4	0.66%
8	Total Poles	144	**23.80%**

Source file: Sample Set 1-Pole Study.xlsx

Results of Sample Set 2 (poles that have been replaced within the past 4 years) are summarized in the table below. As expected, there are no poles that would require replacement when existing small wire is replaced with 1/0 ACSR bare wire as these poles have been sized for a minimum conductor size of 1/0 ACSR bare wire (column D). If this subset of recently replaced poles were to be reconductored with 1/0 ACSR covered conductor, 1.24% of the poles could be anticipated to need replacement (column F). This subset of poles benefits from having been recently installed to meet current standards whereas Sample Set 1 above does not.

Sample Set 2 Summary Table– Recently Replaced Poles (poles that have been recently replaced in HFRAs (within the past 4 years)

	B	C	D	E	F
2	**Load Case**	**# of Poles**	**# of Overloaded Poles 1/0 ACSR Bare**	**# of Poles Overloaded Changing Conductor to CC**	**% Overloaded (F / C8)**
3	**Light, 8 lb**	14	0	0	0.00%
4	**Heavy, 6 lb**	69	0	2	0.83%
5	**12 lb**	106	0	0	0.00%
6	**18 lb**	51	0	1	0.41%
7	**24 lb**	1	0	0	0.00%
8	**Total Poles**	241	0	3	**1.24%**

Source file: Sample Set 2-Recently Replaced Poles Study.xlsx

Workpaper Support for Fusing Section (IV)(B)3)(a)

The enclosed IEEE report titled *Application of Current Limiting Fuses in Distribution Systems for Improved Power Quality and Protection*, was utilized in support of the representation regarding CLF energy reduction as compared to a conventional fuse. The direct support for the CLF energy reduction can be located at page 5 of the document and has been marked for reference.

96 WM 070-3 PWRD

APPLICATION OF CURRENT LIMITING FUSES IN DISTRIBUTION SYSTEMS FOR IMPROVED POWER QUALITY AND PROTECTION

Lj. Kojovic, Senior Member S. Hassler, Member
Cooper Power Systems
Franksville, WI

Abstract - This paper presents a comparative analysis of the effects of distribution system expulsion and current limiting fuse operations on power quality. To perform this analysis, digital fuse models were developed for use with the EMTP/ATP program. Expulsion fuses interrupt current at current zeros and are easily modeled. Current limiting fuses (CLFs) interrupt current by forcing a current zero and therefore, require a special modeling technique. CLFs were modeled by representing them as non-linear resistances. The non-linear resistances were calculated using laboratory test results of actual CLF operations. This technique is very convenient for simulating CLF operations and analyzing their interaction with the distribution system. This paper shows that CLFs improve power quality by supporting system voltage during faults and reducing voltage dip duration. Additionally, CLFs reduce the fault let-through I^2t.

Key words: Fuse, Current Limiting Fuse, Modeling, EMTP, ATP, Distribution Systems, Power Quality

INTRODUCTION

Current limiting fuses are used for overcurrent protection in electric distribution systems. They have many advantages over expulsion fuses. In addition to improving overcurrent protection, CLF fuses improve power quality by supporting the system voltage during faults and clearing high current faults much faster than expulsion fuses, reducing the duration of voltage dips. Electronic equipment in use today can be sensitive to even very short reductions in voltage which emphasizes importance of voltage support [1].

A number of papers have been written on current limiting fuses. Papers [2-10] present CLF operation theory, design criteria, and test methods. Mathematical analysis and analytical models are discussed in papers [11-16]. Reference [17] comprehensively covers electric fuses.

96 WM 070-3 PWRD A paper recommended and approved by the IEEE Transmission and Distribution Committee of the IEEE Power Engineering Society for presentation at the 1996 IEEE/PES Winter Meeting, January 21-25, 1996, Baltimore, MD. Manuscript submitted July 31, 1995; made available for printing November 30, 1995.

Today's computer programs and PC equipment are powerful tools for power system analysis. The Alternative Transients Program (ATP) and the Electromagnetic Transients Program (EMTP) are widely used for power system analyses. Both use similar algorithms and input data. Both can be used to simulate electro-magnetic, electro-mechanical, and control system transients on single or multiphase electric power systems. They can solve networks consisting of linear and/or non-linear elements and can be used for power system as well as for power electronic system analysis. To simulate and investigate CLF operations, digital models needed to be developed. Paper [18] presents a CLF model developed for use with EMTP/ATP. The model was used to determine which source voltage closing angle will produce the greatest I^2t value. However, this model cannot predict CLF overvoltages.

The CLF models presented in this paper were developed for the analysis of CLF operations in distribution systems using EMTP/ATP. The models can accurately simulate CLF currents and voltages, which is essential in the analysis of fuse operation. The first section of this paper presents CLF operation theory and discusses fuse resistance changes during current interruption. The modeling method is given in section two. Models were verified by comparing simulation results to the laboratory tests. CLF application considerations are discussed in section three. This section includes a comparative analysis of expulsion and current limiting fuse operations on distribution systems. Discussion of fuse operations and conclusions are given at the end of this paper.

1. THEORY OF OPERATION

This section presents a discussion of CLF operation theory based on laboratory tests.

Laboratory Tests

The laboratory test setup is shown in Figure 1. This circuit represents a simplified distribution system.

Test Parameters:
Current limiting fuse, 8.3 kV, 12 A
Line reactance, X_l=2.076 Ω
Line resistance, R_l=0.152 Ω

(Line resistance is much smaller than line reactance and was neglected in the analytical analysis, but was included in EMTP/ATP simulations.)
Available test current = 3500 Arms
Test voltage = 7200 Vrms
Fault incidence angle (α) was selected to be 10°

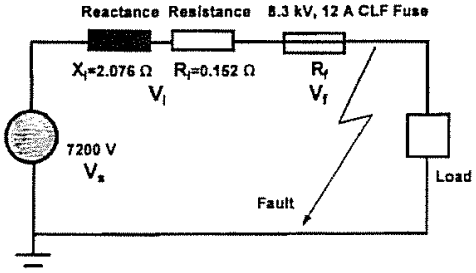

V_s - System voltage
V_l - Voltage across the line impedance
V_f - Fuse voltage

Figure 1. Laboratory Test Setup for CLF Testing

Laboratory test fuse current and voltage are shown in Figure 2. Figure 3 shows fuse current, voltage and resistance calculated from laboratory test data.

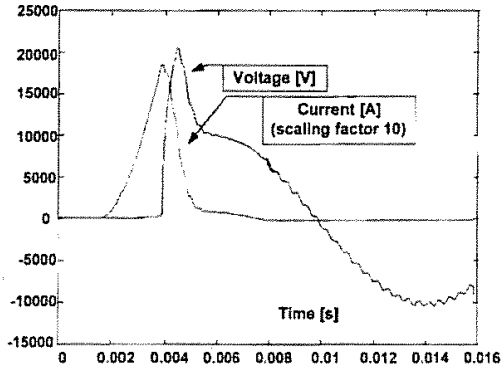

Figure 2. Fuse Current and Voltage (Laboratory Test)

Results Analysis

A. Melting Period

The voltage equation for the circuit shown in Figure 1 can be written as:

$$V_s = V_l + V_f \qquad (1)$$

or

$$V_0 \sin\omega t = L\frac{di}{dt} + iR_f \qquad (2)$$

When a fault occurs, the fuse element begins heating up to its melting temperature. The fuse resistance for a typical CLF increases to about R_f=0.2 Ω before melting. Therefore, the main voltage drop is across the line reactance (prior to the fuse melting open). The current slope just prior to the fuse melting can be determined from Figure 2 and Equation 3.

$$\frac{di}{dt} = 1360\frac{kA}{s} \qquad (3)$$

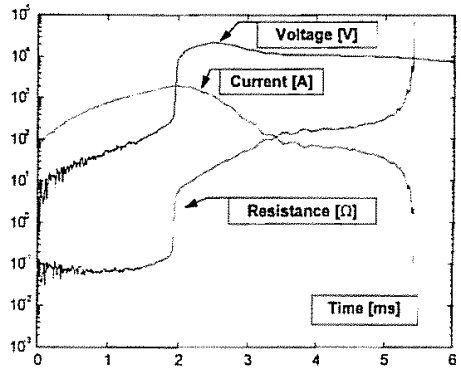

Figure 3. CLF Current, Voltage and Calculated Resistance

The voltage drop on the line reactance can be calculated as:

$$V_l = L\frac{di}{dt} = 5.5mH \times 1{,}360\frac{kA}{s} = 7480V \qquad (4)$$

The IR voltage drop across the fuse at the same time was measured to be 330V, such that:

$$L\frac{di}{dt} + iR = 7480 + 330 = 7810V \qquad (5)$$

This closely approximates the actual instantaneous laboratory test voltage of 7870 V, which verifies that equation (1) balances prior the fuse melting open.

B. Fuse Melted

When the fuse element melts, the fuse resistance increases. Test results show that in 25 μs, the fuse resistance increases to 1 Ω (with a slope of 100 kΩ/s). This causes the fuse voltage to increase to 3300 V. The system voltage at this moment was 7950 V. The current slope decreases, which is represented in Equation 6.

$$\frac{di}{dt} = \frac{V_s - V_f}{L} = \frac{7950V - 3300V}{5.5mH} = 845\frac{kA}{s} \Rightarrow 0 \quad (6)$$

When $V_s=V_f$, ***di/dt*** passes through zero. At this moment, the voltage across the line reactance is zero, the fault current is at its maximum, and the voltage drop across the fuse equals the system voltage. The measured fuse resistance at this instant in time was 4Ω.

The fuse resistance continues to rapidly increase, causing the current to decrease (negative ***di/dt***). The negative ***di/dt*** results in a voltage rise on the line reactance. The line reactance voltage now supports the system voltage and Equation 2 becomes:

$$V_0 \sin\omega t + L\frac{di}{dt} = iR_f \quad (7)$$

The fuse arc voltage at any instant equals the product of the instantaneous current times the instantaneous fuse resistance. The system overvoltage that will be created by the fuse operation depends on the rate at which the fuse resistance increases. With proper fuse design, the peak arc voltage occurs after the gradually increasing fuse resistance has reduced the system current. If the fuse resistance continued to increase with the initial slope of 100 kΩ/s, the overvoltage would be higher. However, Figure 4 shows that after 80 μs the fuse resistance decreases to 40 kΩ/s.

Here is an example of how the rate of current decrease (***-di/dt***) influences fuse arc voltage. It has been shown that before the fuse melts, the current slope (***di/dt***) is 1360 kA/s, which causes the voltage drop across the line reactance (V_l) to be approximately equal to the system voltage. After the fuse melts and the fuse resistance becomes high enough to reverse the rate of change of the current, V_l will support the system voltage as shown in Equation 7. If for example, the absolute value of the negative ***di/dt*** immediately after it changes polarity, is the same as it was before the fuse element melted (as positive ***di/dt***), the overvoltage created by the fuse will be close to 2 times the system voltage.

For higher magnitude negative ***di/dt*** values, which would be caused by a very fast rising fuse resistance, the fuse overvoltage would be higher and current would be interrupted sooner. For smaller ***di/dt*** values, which would be caused by the smaller rate of fuse resistance rise, the overvoltage would be smaller, and the current would be interrupted later. This shows that the rate at which the fuse resistance develops has a major influence on the fuse overvoltage and its operation.

This result can be demonstrated by using Equation 2, test results, and the following procedure:

- System voltage ⇒ $Vs=V_0 \sin(\omega t)$
- Calculated fuse current instantaneous value ⇒ $I_{n+1} = I_n + \frac{\Delta i}{\Delta t}\Delta t$
- fuse voltage ⇒ $I_{n+1}R$
- voltage on the line reactance ⇒ $V_l=Ldi/dt = V_s - V_f$

The fuse's resistance, shown in Figure 4, was calculated from the measured fuse current and voltage presented in Figure 2. This fuse resistance characteristic was than used to model the test circuit reaction to the fuse operation. Figure 5 shows system voltage and the calculated values for current, voltage across the line reactance, and voltage across the fuse. The fuse resistance changes from 0.2Ω to 4Ω within 56 μs, limiting the current peak. From this moment the current starts to decrease and the voltage begins rising above the system voltage. In the continuing process of fuse arcing, the fuse resistance further increases, forcing the current to zero. At this time $V_l=0$, fault current is interrupted, and the fuse voltage magnitude becomes equal to the system voltage.

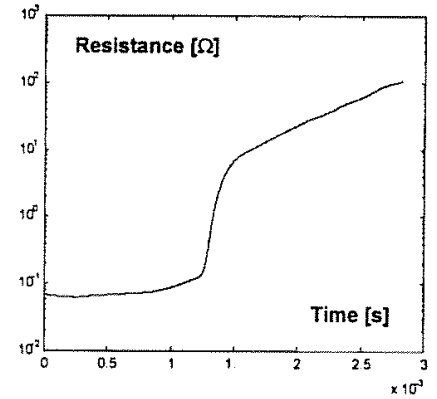

Figure 4. Fuse Resistance Calculated from Laboratory Tests

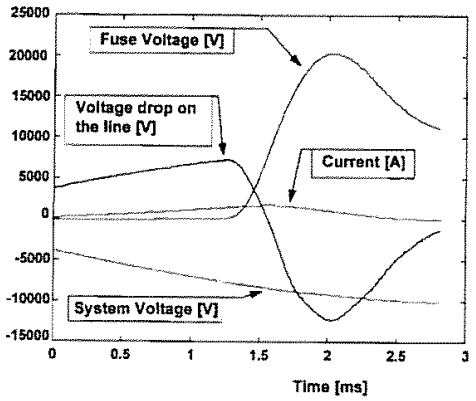

Figure 5. Fuse Voltage, System Voltage, Voltage Drop across the Line Reactance, and Current

2. MODELING METHOD

The main two parameters in the CLF operation model are the fuse's melt I^2t and the fuse's non-linear resistance characteristic after melting open. To investigate how these parameters vary with available fault current and fault incidence angles (for a typical 8.3 kV, 12 A CLF), tests were performed at 7.2 kV with 0°, 45° and 90° incidence angles at available fault currents of 3.5 kA, 7.0 kA and 26 kA. The melt I^2t and resistance characteristics were calculated from current and voltage measurements under each of these test conditions. The results are given in Table 1 and Figures 6 and 7. As expected the melt I^2t was independent of either the available fault current or the fault incidence angle. The dots in Figures 6 and 7 mark the instants at which peak arc voltages occurred. Note that the resistance characteristic of the fuse is common for all fault incidence angles on the 3.5 kA test circuit and for the 90° incidence angle on the 26 kA circuit through the time of peak arc voltage. The rate of increase of the resistance on the 7.0 kA circuit with a 90° incidence angle was slightly higher prior to reaching its peak arc voltage. Figures 8 and 9 compare EMTP/ATP simulations with laboratory tests for a 8.3 kV, 12 A CLF fuse in the 3.5 kA test circuit operating at 7.2 kV, with a 90° fault incidence angle.

Table 1. Melt I^2t for 8.3 kV, 12 A CLF. Tested at 7.2 kV

Fault Incidence angle		I^2t [A^2s]
0°	3.5 kA	1767
45°	3.5 kA	1782
90°	3.5 kA	1809
90°	7 kA	1859
90°	26 kA	1880

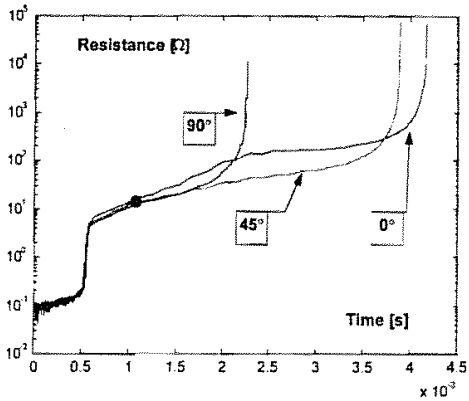

Figure 6. CLF Resistance Characteristic for 0°, 45° and 90° Incidence Angles for 3.5 kA Fault Current

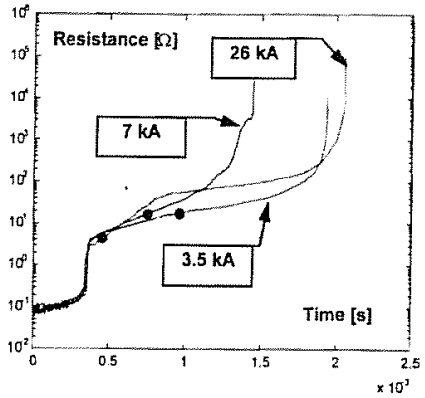

Figure 7. CLF Resistance Characteristic for 3.5 kA, 7.0 kA and 26 kA Available Currents with a 90° Fault Incidence Angle

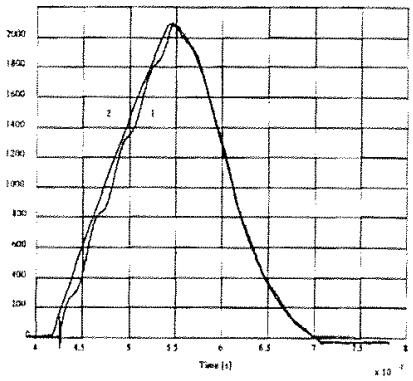

Figure 8. Comparison of Tested (1) and Simulated (2) Current Limiting Fuse Currents

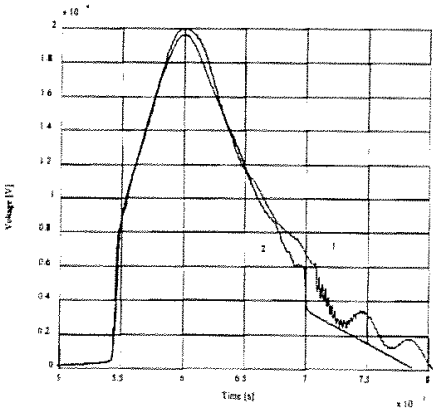

Figure 9. Comparison of Tested (1) and Simulated (2) CLF Voltages

3. APPLICATION CONSIDERATIONS

The response of electrical distribution systems to CLF operations can be accurately determined using the modeling technique previously described in this paper. One useful application of these models is to compare CLF and expulsion fuse operations with regard to their effects on power quality. This section compares the effect on power quality of using each type of fuse on a typical distribution system.

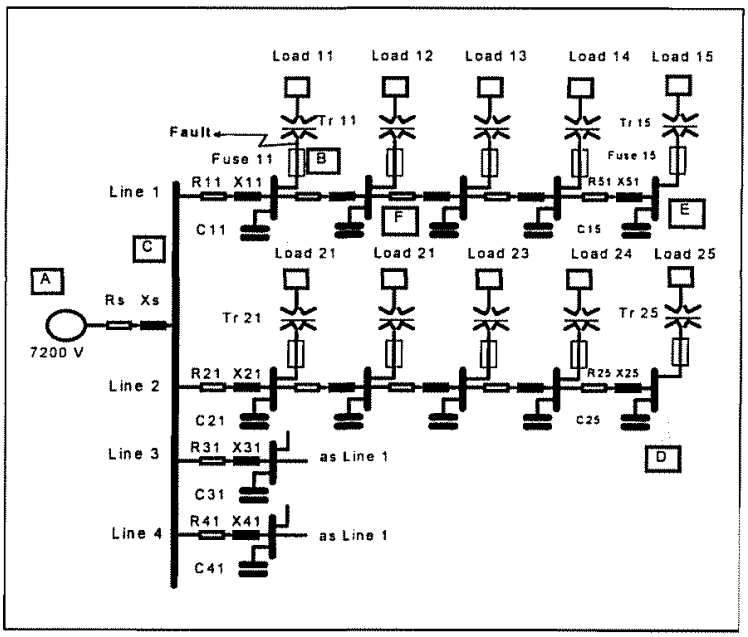

Figure 10. Power System Model used in EMTP Simulations

The distribution system model used in this analysis consisted of four lines (4x2.5 MVA) with five taps on each line as shown in Figure 10. Load was assumed to be 50% of rated load. A fault was initiated at Tap 11, location **B**. Simulations were run with the transformer at this location fused with both expulsion and CLF fuses. The melt I^2t and the fuse resistance characteristic described in the first section of this paper were used to simulate the operation of an 8.3 kV, 12 A CLF. Voltages were monitored at all system buses. Voltages at locations **A**, **B**, **C**, **D**, **E**, and **F** are presented and discussed in this paper. Figure 11 shows expulsion fuse current at location **B**. Figures 12 and 13 show expulsion system voltages at locations **A**, **B**, **C**, **D**, **E**, and **F** during the expulsion fuse's operation. Figure 14 shows CLF fuse current at location **B**. Figures 15 and 16 show system voltages at locations **A**, **B**, **C**, **D**, **E**, and **F** during the CLF fuse's operation.

Results Analysis

Figures 11 and 14 present expulsion and CLF fuse currents. Expulsion fuses must wait for a natural current zero before interrupting. Because of this, fault current duration depends on the system power factor and fault incidence angle. In this case the expulsion fuse carries current for 8.1 ms and lets through an I^2t of 97,000 A^2s. CLFs force a current zero, limiting both the current peak and its duration. In this case the CLF carries current for 2.5 ms and limits the let-through I^2t of 3,900 A^2s which is 25 times smaller than the expulsion fuse I^2t. This reduction in let-through I^2t better protects the faulted equipment, as well as all equipment on the source side of the fault, from overcurrent induced stresses.

Figures 12 and 15 compare the voltages at locations **A**, **B**, **C** and **D** for expulsion and CLF fuses respectively. Figure 12 shows that the voltage at fuse location **B** collapses to zero and stays at zero for 8.1 ms until the current is interrupted. At this point the system is subjected to a transient recovery voltage (TRV). The TRV frequency and amplitude factors depend of the system power factor and loading. Frequencies can range of kHz to tens of kHz and amplitude factor magnitudes ranging from 1.2 to 1.7 pu. Voltages at locations **C** and **D** decrease due to the fault current induced voltage drop across the source impedance. Figure 15 shows that the voltage at the CLF location collapses to zero for only 1.2 ms and then rises to an overvoltage of 1.85 times peak system voltage. This fuse induced overvoltage exceeds normal system peak voltage for about 1 ms. The fault is cleared after 2.5 ms total and the system voltage returns to normal. This overvoltage is lower downline from the fault location (locations **E** and F) and less than 1 pu of normal system peak voltage on other lines that tap off the same substation bus (locations **C** and **D**).

This analysis shows that for the same fault conditions, CLFs have significant advantages in supporting system voltage and in improving power quality when compared with expulsion fuses of the same rating.

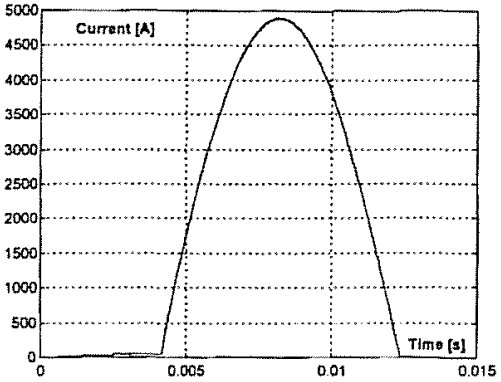

Figure 11. Expulsion Fuse Current during Operation

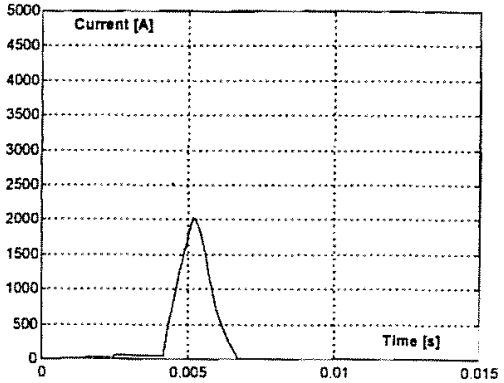

Figure 14. CLF Current during Operation

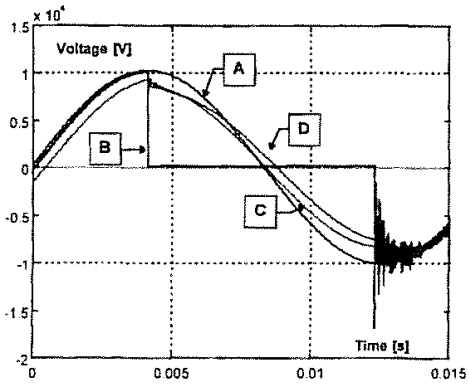

Figure 12. Voltages at Locations A, B, C and D due to Expulsion Fuse Operation

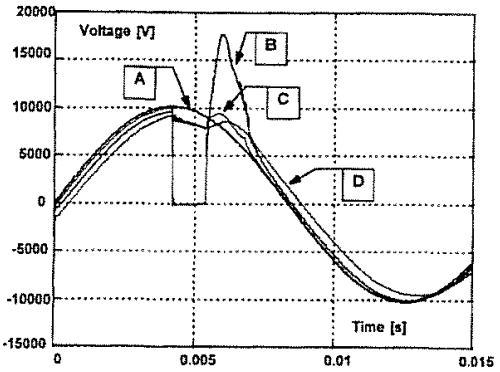

Figure 15. Voltages at Locations A, B, C and D due to CLF Fuse Operation

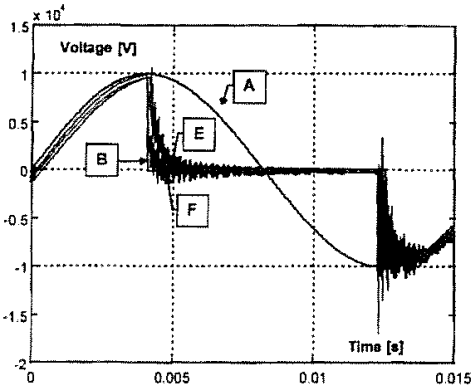

Figure 13. Voltages at Locations A, B, F and E due to Expulsion Fuse Operation

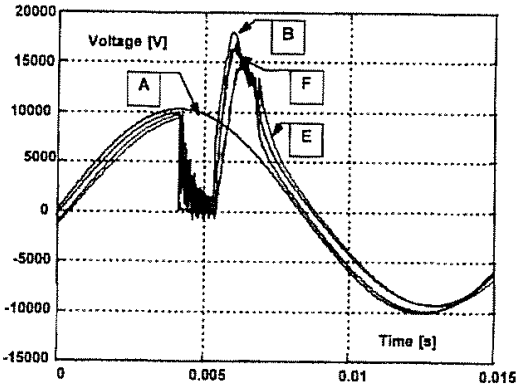

Figure 16. Voltages at Locations A, B, F and E due to CLF Fuse Operation

The simulated fault current interrupting characteristics of expulsion and CLF fuses are compared in Table 2.

Table 2. The Fault Current Interrupting Characteristics of Expulsion and CLF Fuses

	Expulsion Fuse	CLF Fuse	Comments
Let-through I^2t	97,000 A^2s	3,900 A^2s	Smaller I^2t reduces stress on all equipment from the fault location back to the source
Let-through current (Available current 3470 A_{rms})	4900 A_{pk}	2000 A_{pk}	As above
Fault duration	8.1 ms	2.5 ms	Shorter fault duration causes shorter voltage dips and reduces fault current flow duration
Overvoltages	1.2-1.7 p.u. depending of the system parameters	1.85 p.u. caused by the fuse arc voltage	Overvoltages occur in both cases
Duration of the voltage reduction	8.1 ms	1.2 ms	Longer voltage reduction can affect electronic equipment operation

SUMMARY and CONCLUSIONS

This paper presents three main subjects:

1. Current limiting fuse (CLF) modeling. Digital fuse models have been developed for use with the EMTP/ATP program. CLFs were modeled by representing them as non-linear resistances. The non-linear resistances were calculated using laboratory test results of actual CLF operations. The models were verified by simulating the laboratory tests using EMTP/ATP and comparing results. The models are convenient for simulating and analyzing CLF operations and their interaction with the distribution system.

2. Simulation of expulsion and CLF operation in distribution systems using the EMTP/ATP program. A typical 7.2 kV distribution system was modeled. The method can be extended to any distribution power system.

3. The analysis of CLF applications to improve distribution systems overcurrent protection and power quality. The results show that CLFs significantly improve power quality by supporting system voltage during faults. A CLF reduced the duration of the voltage dips to 1.2 ms followed by an overvoltage of 1.85 pu peak for customers near the fault location. The voltage dip when using an expulsion fuse is 8.1 ms in this case, but can be longer with other fault incidence angles. Also, when current is interrupted by an expulsion fuse, the system is subjected to a TRV of 1.2-1.7 pu. Customers on other lines out from the substation will not be significantly affected by the operation of either CLF or expulsion fuses. An additional advantage of CLF fuses is that they reduce fault let-through I^2t.

References

[1] J. Douglas,: "Solving Problems of Power Quality", EPRI Journal, December 1993.
[2] C. L. Schuck,: "Performance Criteria for Current-Limiting Power Fuses-I", AIEE Trans.Vol. 65, 1946
[3] E. W. Boehne,: "Performance Criteria for Current-Limiting Power Fuses-II", AIEE Trans.Vol. 65, 1946
[4] H. W. Mikulecky,: "Current Limiting Fuse Arc-Voltage Characteristics", IEEE Trans. on Power App. and Sys., Vol. PAS-87, No. 2, February 1968.
[5] S. B. Toniolo, G. Cantarella,: "Conditions of Maximum Arc Energy in Operation of Current-Limiting Fuses", IEEE Trans. on Power App. and Sys., Vol. PAS-88, No. 2, February 1969.
[6] W. R. Crooks, A. C. Westrom,: "Progress in Current Limiting Fuse Developments", Presentation to Edison Electric Inst., T&D Committee, St. Petersburg Beach, FL, January 18, 1980.
[7] T. Tanaka, H. Momoshima, N. Takaoka, I. Eguchi, A. Watanabe, C. Sekine,: "Metallographic Study of

Dual Type Current Limiting Fuse Element", 81 TD 677-4, IEEE PES T&D Conf., Minneapolis, MN, Sept. 1981.

[8] M. Dolegowski,: "Calculation of the Course of the Current and Voltage of a Current-Limiting Fuse", Int. Conf. on Electric Fuses and Their Applications, Liverpool, UK, April 1976.

[9] J. E. Daalder,: "The Arcing Voltage in High Voltage Fuses", Int. Conf. on Electric Fuses and Their Applications, Trondheim, Norway, June 1984.

[10] V. N. Narancic, G. Fecteau,: "Arc Energy and Critical Tests for HV Current-Limiting Fuses", Int. Conf. on Electric Fuses and Their Applications, Trondheim, Norway, June 1984.

[11] R. Wilkins,: "Generalized Short-Circuit Characteristics for H.R.C. Fuses", Proc. IEE, Vol. 122, No. 11, Nov. 1975.

[12] A. Hirose,: "Mathematical Analysis of Breaking Performance of Current-Limiting Fuses", Int. Conf. on Electric Fuses and Their Applications, Liverpool, UK, April 1976.

[13] R. Wilkins,: "Semiempirical Models of Arcing in Current-Limiting Fuses", 3rd Int. Symp. on Switching-Arc Phenomena, Lodtz, Poland, 1977, pp. 212-219.

[14] A. Wright,: "Analysis of High-Breaking-Capacity Fuselink Arcing Phenomena", Proc. IEE, Vol. 123, No. 3, March 1976.

[15] S. Ganalingam, R. Wilkins,: "Digital Simulation of Fuse Breaking Tests", IEE Proc., Vol. 127, Pt. C, No. 6, Nov. 1980.

[16] P.O. Leistad, H. Kongsjorden, J. Kulsetas,: "Simulation of Short Circuit Testing of High Voltage Fuses", Int. Conf. on Electric Fuses and Their Applications, Trondheim, Norway, June 1984, pp 220-226.

[17] A. Wright, P. G. Newbery,: ELECTRIC FUSES, 2nd Edition, IEE, London, UK, 1995

[18] A. Petit, G. St-Jean, G. Fecteau,: "Empirical Model of a Current-Limiting Fuse using EMTP", IEEE Transactions on Power Delivery, Vol. 4, No. 1, January 1989.

Biographies

Ljubomir Kojovic (SM' 1994) received his Dipl. Ing. degree from the University of Sarajevo, Yugoslavia, M. S. degree from the University of Belgrade, and Ph.D. degree from the University of Sarajevo, all in electrical engineering in 1972, 1977, and 1981, respectively. From 1972 to 1991 he was with the Energoinvest Company, Sarajevo, Yugoslavia. He was also an Assistant Professor at the University of Tuzla, Yugoslavia. In 1991 and 1992 he was a post doctorate research associate at Texas A&M University. Since 1993 he has been a Senior Staff Engineer for Cooper Power Systems at the Thomas A. Edison Technical Center. His name is included in the roster of experts for United Nations Development Organization (UNIDO). He is a registered Professional Engineer in the State of Wisconsin.

Stephen P. Hassler received his BSME from Michigan Technological University in 1966. He has worked for Cooper since 1969. This work includes the design and development of high voltage expulsion and current limiting fuses; the development of the electrical and mechanical functions of fuse housings and mountings, including mechanisms for automatic removal of blown fuses from the electrical circuit. He has been involved in the design and development of high voltage air break and load break switches and their operating mechanisms, SF_6-based power class circuit breakers and distribution class reclosers. He has also designed and developed cast resin supports for high voltage fuses and performed evaluation through instrumentation for the conducting of mechanical, load current, short circuit and dielectric tests. He is a member of IEEE.